# The role of calcium activated and voltage gated potassium channel BK, in glioblastoma multiforme membrane potential.

Thesis submitted to the University of Nottingham for the degree of Master of Research in Neuroscience

**Mathuscha Ratnasingham, BSc (Hons)**

Student number: 4325140

**School of Life Sciences**

**2022/23 Academic Year**

**September 2023**

Table of Contents

**Abstract**

Glioblastoma multiforme (GBM), is an aggressive brain tumour that accounts for nearly half of all glial brain tumours. Large conductance voltage and $Ca^{2+}$-activated potassium channels, BK, are overexpressed in GBM and are thought to play a role in their invasion and migration. Although changes in resting membrane potential modulate these processes, little is known about the origin of it in GBM and the role of BK. I have used cell-attached and whole-cell patch clamp in the glioblastoma cell lines, SF188 and GCE62 to investigate the role of BK in GMB resting membrane potential. Single channel BK currents were measured with cell-attached patch clamp. Pipettes contained 140 mM $K^+$. Currents were measured with holding potentials from 0 mV to -90 mV. The resting membrane potential of intact cells was estimated from the reversal potential of cell-attached single-channel BK current-voltage (I-V) plots. Resting membrane potential was then measured with current clamp immediately after forming the whole-cell configuration. In SF188s, at a pipette potential of 0 mV, BK was spontaneously active in 31 out of 71 patches. Cell-attached I-V analyses indicated voltage-dependent activation of gBK with a bimodal distribution of median slope-conductance of around 124 and 215 pS. Membrane potential estimated from the cell-attached I-V reversal potential, -35±0.18 mV was similar to that subsequently measured under whole-cell current clamp -35±0.18 mV ([$Ca^{2+}$] = 120 nM). With high [$Ca^{2+}$] pipette solution (2.5 mM), membrane potential was significantly hyperpolarized in whole-cell current clamp (-44 ± 17 mV) whereas the input resistance, 220 ± 173 MΩ; was similar to that with low pipette [$Ca^{2+}$]: 396 ± 173 MΩ. In 100% of cell-attached patches, BK activity was abolished by 10 µM paxilline and 200 µM quinine. With low pipette [$Ca^{2+}$] whole-cell membrane potential was unaffected by 200 µM quinine but was significantly hyperpolarised by 13 mV with 10 µM paxilline and 9 mV with 1 mM TEA. With low pipette [$Ca^{2+}$] whole-cell membrane potential was unaffected by $Cl^-$ free Hanks but was significantly depolarised by 8 mV with $K^+$ Hanks and hyperpolarised by 8 mV with $Na^+$ free Hanks. In GCE62's, at a pipette potential of 0 mV, BK was spontaneously active in 2 out of 30 patches. In whole cell current clamp there was no significant difference in the membrane potential and input resistance in the high [$Ca^{2+}$] pipette solution compared to low [$Ca^{2+}$] in the pipette solution. GBM SF188 exhibit spontaneous $K^+$ channel activity in cell-attached patches, with biophysical and pharmacological properties typical for BK. At low intracellular [$Ca^{2+}$] BK does not appear to be

responsible for the resting membrane potential. The reversal potential of BK in cell-attached patches appears to be an accurate non-invasive measure of the resting membrane potential of SF188 cells. The membrane potential seems to be predominated by potassium with a degree of sodium. Further studies are required to determine what underlies BK activation in cell-attached patches in SF188 and under what conditions is BK activated to contribute to membrane potential in this cell line.

## Introduction

### *Glioblastoma Multiforme*

Glial cells are one of the main components of the nervous system, making up about half the volume of the brain. There are several sub-types of glia such as astrocytes and oligodendrocytes, in the central nervous system and Schwann cells, enteric glial cells, and satellite cells in the peripheral nervous system. (Jessen, 2004). The functions of glial cells include guidance for neuronal migration in the developing brain, aid in the survival of neurones, synapse formation, myelination, control of synaptic function and finally homeostatic regulation of neurotransmitter and potassium ion concentrations (Allen and Lyons, 2018). There are several diseases associated with glial cells, such as multiple sclerosis, Type 1 Charcot-Marie-Tooth disease, and importantly malignant brain tumours, most of which arise from glial cells (Jessen, 2004).

Glioblastoma multiforme is an aggressive brain tumour that accounts for 42.5% of malignant primary and CNS brain tumours originating from glial cells (Kanderi & Gupta, 2022). It presents with a very poor prognosis and a low survival rate of 1 to 2 years from diagnosis, with a global incidence of 10 per 100,000 of the population. Gliomas can be classified as grades I to IV using the World Health Organisation (WHO) classification system, glioblastomas fall under the grade IV category, the most aggressive and malignant type (Hanif *et al.*, 2019, Vigneswaran *et al.*, 2015). Initial diagnosis of gliomas is conducted by MRI in conjunction with other imaging methods such as functional MRI, diffusion-weighted imaging, diffusion tensor imaging, proton magnetic resonance spectroscopy and positron emission tomography. This is followed by confirmation of diagnosis via surgical resections or biopsy samples (Alifieris & Trafalis, 2015, Gilard *et al.*, 2021) (Figure 1). Gliomas are extensively invasive and have uncontrolled proliferation and abnormal cell death. These characteristics make the treatment of the diseases incredibly difficult (Sherriff *et al.*, 2013). The primary treatment for glioblastoma is surgical resurrection during which maximal resurrection is attempted. This is followed by radiation and chemotherapy. Regardless of these aggressive treatments, survival time is only extended up to 3 years, with around 80% of patients still relapsing near the initial site of the tumour (Hanif *et al.*, 2019, Sherriff *et al.*, 2013, Silantyev *et al.*, 2019)

(Figure 2). To date, the only risk factors associated with glioblastoma are radiation and genetic syndromes (Hanif *et al.*, 2019). Migration and invasion of glioblastoma cells are the main reasons why eradication of the tumour is nearly impossible. The migration of gliomas involves the invasion of the brain parenchyma through narrow spaces. To fit into these narrow spaces, glioblastomas reduce their cell volume to about 30% of their original volume (Watkins & Sontheimer, 2011). This is attained by altering the osmotic equilibrium within the cell resulting in a release of cytoplasmic water, ultimately shrinking the cell. This process is mediated by ion channels which are responsible for controlling cell volume and intracellular calcium signals (Catacuzzeno *et al.*, 2015). In glioblastomas chloride and potassium channels are found to be the main channels which modulate the ionic gradient that is modified (Catacuzzeno *et al.*, 2015).

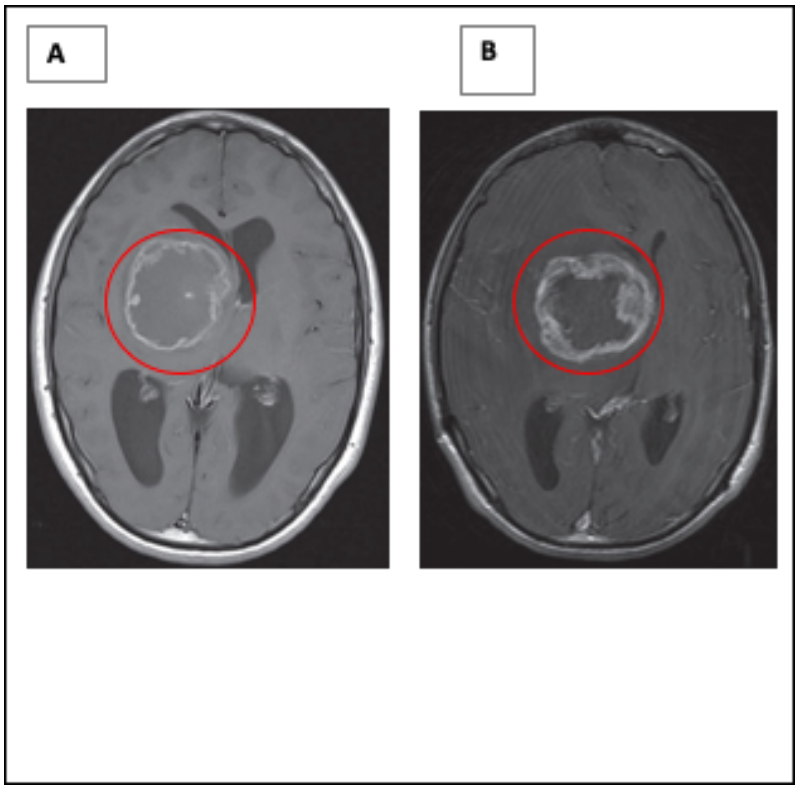


***Figure 1.***

MRI of a 17-year-old with a 4-cm glioblastoma. The patient presented with headaches, blurred vision, and upper left limb weakness. Red circles indicate the tumour. **A)** Initial MRI at the time of admission **B)** MRI scan following treatment with radiation and chemotherapy for 5 months. Scan indicates treatment had no effect on the reduction of the tumour (Tan & Tan, 2012).

*Image and data taken and adapted from Tan & Tan, 2012.*

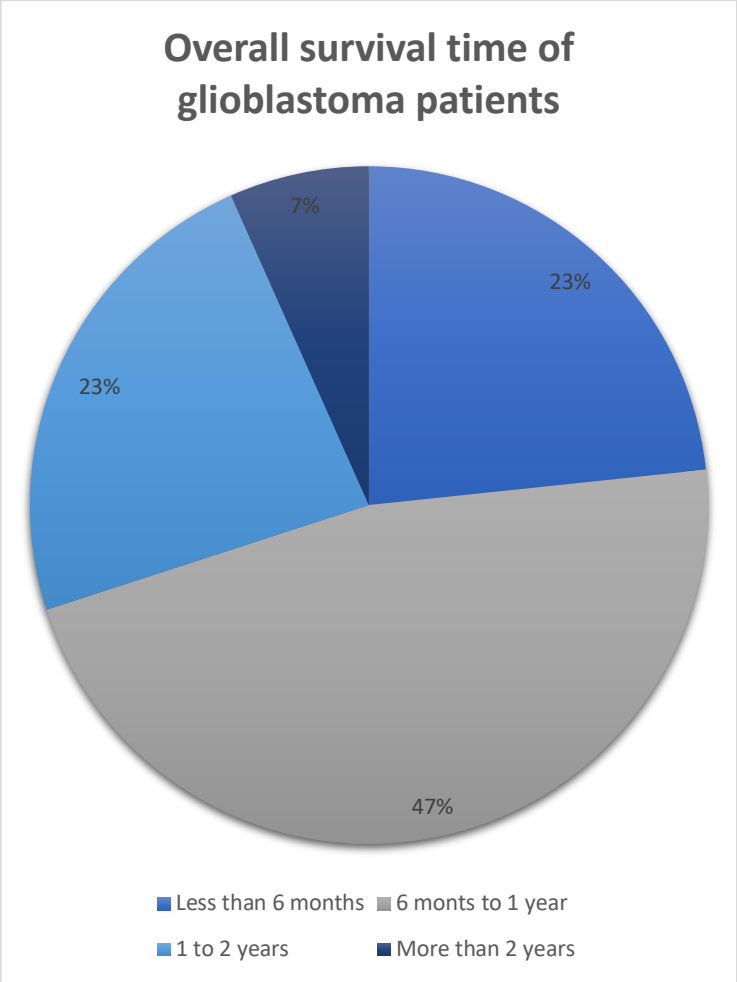


***Figure 2.***

Graph showing the overall survival time of 60 glioblastoma patients who were treated with chemoradiotherapy following their surgery. Data shows that 47% of patients survived up to 6 months to 1 year, with only 7% of patients surviving for more than 2 years. Quality of life was assessed using the European Organization for Research and Treatment of Cancer Core Quality-of-Life Questionnaire and it was reported that there was an improvement in their quality of life following radiotherapy, with patients reporting decreased pain and headaches (Mohammed *et al.*, 2022).

*Data obtained from the study conducted by Mohammed et al., 2022*

***Potassium Channels***

Potassium channels are found in most species, in both excitable and non-excitable cells and are vital in the control of the cell's membrane potential. Potassium channels are also involved in other cellular processes such as hormone secretion, epithelial function as well as damping excitatory signals (González et al., 2012). Potassium channels can be grouped into three main categories: the voltage-gated, the inwardly rectifying and the tandem pore domain. They have a tetrameric structure composed of a fourfold symmetric complex that is formed from a pore-forming domain. This complex surrounds the ion conducting pore (Choe, 2002, Ge *et al.*, 2014, Kuang *et al.*, 2015). Potassium channels are identified using the two transmembrane helices and the short loop which connects the two, known as the P loop. Potassium channels exhibit a high degree of selectivity as a result of the selectivity filter. This filter can be found at the narrowest part of the ion-permeation pathway. Although the gating mechanisms vary depending on the type of potassium channels, they

all have similar selectivity filter. (Choe, 2002, Ge *et al.*, 2014, Kuang *et al.*, 2015). The narrow selectivity filter (12 Å-long segment) contains carbonyl oxygen atoms on its walls, which are spaced in a way which balances the energy required to remove the hydration shell of the potassium ions (Bernèche & Roux, 2003, Bernèche & Roux, 2005). The oxygen atoms are unable to interact with sodium ions as they are energetically unfavourable, therefore it cannot dehydrate sodium the same way it dehydrates potassium. The filter allows the binding of four potassium ions at sites S1 to S4 (Figure 3) (Bernèche & Roux, 2003, Bernèche & Roux, 2005, Choe, 2002, Doyle *et al.*, 1998, Morais-Cabral *et* ., 2001).

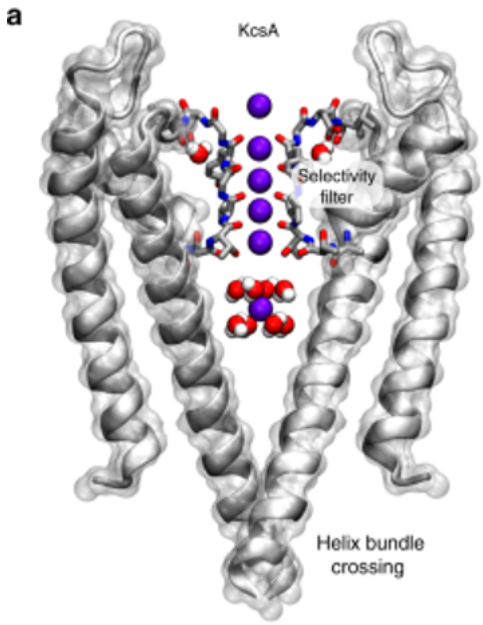


***Figure 3.***

Crystal structure of the KcsA potassium channel in its closed state. The image shows an example of the two transmembrane helices connected by a short P-loop. Only 2 of the 4 subunits are shown in the image. The selectivity filter is shown, this is responsible for the high degree of selectivity of potassium channels.

*Image taken from Kopec, Rothberg and de Groot, 2019.*

***Large conductance voltage and $Ca^{2+}$ - activated potassium channel (BK)***

Large conductance voltage and $Ca^{2+}$ - activated potassium channel (BK, KCNMA1, Slo/Slo1, Maxi-K, $K_{Ca}$ 1.1 and Slowpoke) referred to as BK hereafter, is a type of potassium channel that is activated by membrane depolarisation and binding of intracellular calcium and magnesium (Lee & Cui, 2010) (Table 1). Electrophysiology studies using patch clamp identified that the single-channel potassium conductance of BK ranges from 100 to 300 Pico siemens (pS) (Table 2) when the channel is open, this is significantly higher than the other types of $Ca^{2+}$ -activated potassium channel; small potassium channel (sk) and intermediate potassium channels (IK) have a much smaller conductance 4– 80 pS (Franciolini et al. 2001, Gong et al. 2001, Hirano et al., 2002, Sun et al. 2004).

| V.05 (mV) | at [$Ca^{2+}$] | Reference |
|---|---|---|
| -40 ± 3<br>122 ±53 | **50 µM**<br>0.5 µM | De Wet et al., 2006 |
| 150<br>65<br>12 | 0 µM<br>0.1 µM<br>1 µM | Ransom and Sontheimer, 2001 |
| 168.5 ±2.23<br>136.89 ± 0.9<br>39 ± 0.5<br>2.4 ± 0.7<br>-42 ± 0.6 | 0 µM<br>1 µM<br>10 µM<br>100 µM<br>1 mM | Zhang, Solaro and Lingle, 2001 |

***Table 1.***

Table showing the voltage for half-maximal activation (V0.5) of BK, at different concentrations of $Ca^{2+}$. A negative shift in the V0.5 is seen with increased [$Ca^{2+}$]. The data presented in the literature shows a calcium-dependent activation in BK channels.

| Cell Type | Slope Conductance (pS) | Reference |
|---|---|---|
| ***Xenopus* motor nerve terminals** | 120.7 ± 8.8 pS | Sun et al. 2004 |
| **Cholinergic presynaptic nerve terminal** | 210 ± 7 pS | Sun et al. 1999 |
| **Neonatal rat intra cardiac ganglion neurons** | 207 ± 19 pS | Franciolini et al. 2001 |
| **Cultured rat melanotrophs** | ~ 190 pS | Kehl and Wong 1996 |
| **Cerebrovascular smooth muscle cells** | 207 ± 10 pS | Wang and Mathers 1993 |
| **Cultured rat superior cervical ganglionic neurones** | ~ 200 pS | Smart 1987 |
| **Rat hippocampal neurons maintained in culture** | 220 pS | Wann and Richards 1994 |
| **Rat hippocampal CA1 pyramidal neurons** | 245.4 pS | Gong et al. 2001 |
| **Cultured human renal proximal tubule epithelial cells** | 300 pS | Hirano et al., 2002 |

***Table 2.***

Table showing the slope conductances of BK channels measured in a variety of different cells. When BK channels are open, they have a slope conductance ranging from 100 – 300 pS.

Structurally BK is similar to voltage gated potassium channels, containing four alpha subunits, coded by the Slo1 (KCNMA 1) gene that is found at the chromosomal 10q22.3 region in humans and chromosomal 14 regions in mouse and consists of 27 exons (Ge *et al.*, 2014). Mutation at these loci has been associated with epilepsy and paroxysmal dyskinesia (Du et al., 2005). The gene undergoes extensive pre-mRNA spicing which results in BK having many diverse functions. Alternative splicing of the stress-regulated exon (STREX) can give rise to differences in calcium and voltage sensitivity (Chen *et al.*, 2005, Saito *et al.*, 1997) as well as regulation via cellular signalling pathway (Chen *et al.*, 2005, Erxleben *et al.*, 2002, Tian *et al.*, 2001). Modified intracellular targeting has also been shown via SV1 insert (Zarei *et al.*, 2004). A review by Fodor & Aldrich, 2009 reports that consecutive exons amidst different species of the same phylum are conserved, whereas alternative exons are not conserved. When looking across phyla, they report that some regions seem more liable to alternative splicing in comparison to others.

BK channels consist of 7 transmembrane spanning regions S1-S4, a hallmark of the voltage-dependent potassium channel, with the addition of S0, an extracellular amino acid terminal and a large cytosolic C terminal domain. The S1-S4 domains contain the voltage sensors which are responsible for the voltage activation of BK sensor (Ge *et al.*, 2014, Lee & Cui, 2010). Similar to voltage gated potassium channels, the voltage sensing domain and the pore-gate domain are formed by S1- S4 and S5-S6. The S4 helix has a positively charged Arginine residue (Arg213) that acts as the primary voltage sensor (Ge *et al.*, 2014, Lee & Cui, 2010). This was determined by Ma *et al.*, 2006 who mutated the residues in the Slo1 gene and found only the S4 (Arg213) residue was able to give rise to gating charge. The pore and the selectivity filter of the channel are encoded by S5 and S6 (Ge *et al.*, 2014, Kim & Nimigean, 2016, Yuan *et al.*, 2010). The C terminus contains two regulatory cytosolic units (RCK1 And RCK2) intracellularly. Divalent cations such as calcium and magnesium can bind to the regulatory units with the calcium bowl present at the RCK2 terminal (Ge *et al.*, 2014). Binding of calcium increases the intracellular levels of calcium which in turn decreases the voltage at which the channel is activated at (Ge *et al.*, 2014, Li & Yan, 2016). Four alpha subunits and smaller regulatory beta (β*)* subunits are arranged to form a functional BK channel (Figure 4).

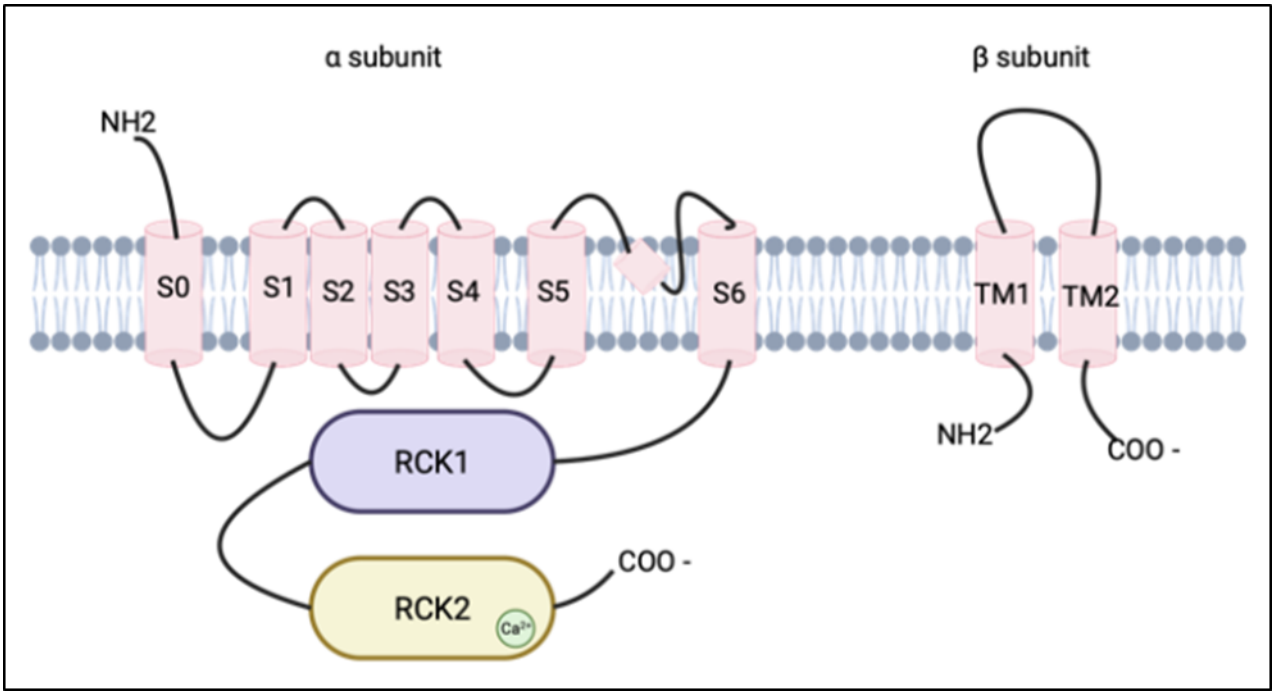


***Figure 4.***

Structure of the large conductance voltage and calcium activated potassium channel. The α subunit consists of the S0 segment, S1 – S4, the voltage sensing domain, S5 and S6 the pore gate domain, as well as RCK1 and RCK2 which are the cytosolic domain. RCK2 contains the calcium bowl which is responsible for calcium sensitivity. Four α subunits joined together to form a functional BK channel. The β subunit has two transmembrane subunits, expression of these are tissue specific.

*Image is created on BioRender.com.*

Four types of β subunits exist: β1- β4. A β1 subunit consists of two membrane spanning regions with intracellular N and C terminals. The β1 subunit is attached to the alpha subunit via the transmembrane region near the C terminus and interacts with the S0 region of the alpha subunit. β subunits are not needed to form a functioning BK channel; however, they slightly alter the BK channel activity (Ge *et al.*, 2014). They increase the voltage gating and calcium sensitivity gating and decrease threshold potential and inactivation kinetics (Ge *et al.*, 2014, Orio *et al.*, 2002). Sequence homology between β1- β2 and β2- β3 are closely related in comparison to β4. When β1 subunits are co-expressed with the alpha subunits an apparent increase in calcium sensitivity, a decrease in voltage sensitivity and slower deactivations are observed. (Cox & Aldrich, 2000, Orio & Latorre, 2005, Wallner *et al.*, 1995) The β1 subunit also regulates the interactions with toxins and other activators.

For example, co-expression of the β1 subunit with the alpha subunit increased the potency of the BK blocker tetrandrine (Dworetzky *et al.*, 1996). The β1 subunit is mostly expressed in smooth muscle cells (Behrens *et al.*, 2000). β2 subunits increase calcium sensitivity similarly to β1 but has no effect on voltage sensitivity. It also increases inactivation but slows down deactivation (Lee *et al.*, 2010, Orio & Latorre, 2005, Wallner *et al.*, 1995). Uebele *et al.*, 2000 reported that the coexpression of β3 subunits did not affect calcium sensitivity or voltage sensitivity. They also reported four subfamilies of the β3 subunits, β3a-d, that resulted from alternative splicing of a single gene. They found that β3a-c partially inactivated the current whereas β3d presented with an inward rectification. β2 and β3 are predominantly neuronally expressed (Behrens *et al.*, 2000). Both Brenner *et al.*, 2000*a* and Wang *et al.*, 2006 illustrated that the β4 subunit affected voltage sensitivity in a concentration dependent manner, in which at low concentrations there was a decrease of open channel probability, whereas, at a higher concentration, there was a higher open channel probability, suggesting that they are more voltage sensitive at a higher calcium concentration. β4 subunits are expressed mainly in the brain (Behrens *et al.*, 2000). Interestingly Zeng *et al.*, 2008 study reveals that the functional properties of β3 subunits vary between mammalian species with some B3 variants being primate-specific ion channel subunits.

BK is ubiquitously expressed in a myriad of cell types such as endocrine, smooth, and neuronal cells and is responsible for many physiological processes (Yuan *et al.*, 2010). As seen with voltage-gated potassium channels, an influx of potassium ions, results in hyperpolarisation of the cell membrane, however, a unique property of BK is that it is also sensitive to changes in intracellular calcium (Faber and Sah, 2003). However, it should be noted that the effect of calcium and voltage are independent of each other (Faber and Sah, 2003). This allows the channel to control the activity of excitable cells, by negative feedback regulation of calcium influx by coupling with voltage-gated calcium channels (Grunnet and Kaufmann, 2004, Hu et al., 2001, Yuan *et al.*, 2010). Upon BK channel activation, the membrane becomes hyperpolarised, which in turn closes voltage-dependant channels such as the potassium and calcium channels, this decreases the calcium influx into the cell (Grunnet and Kaufmann, 2004, Hu et al., 2001, Yuan *et al.*, 2010). Within the central nervous system, BK is responsible for many functions, including action potential shape, propagation, and frequency (Gu et al., 2007, Golding et al., 1999, Ly et al., 2010, Martinez-Espinosa et al., 2014, Pitts et al., 2006, Raffaelli et al., 2004) and release of neurotransmitters (Griguoli et al., 2016, Raffaelli et al., 2004).

BK also contributes to non-neuronal cells in the CNS, such as astrocytes, which are essential in the regulation of cerebral blood flow (Filosa et al., 2006, Price et al., 2002) and microglia cells in the hippocampus (Bordey & Spencer, 2003) and spinal cord (Hayashi *et al.*, 2011). BK also plays a critical role, outside of the CNS, it contributes to the regulation of blood pressure (Brenner *et al.*, 2000*b*, Sausbier *et al.*, 2005), urinary bladder function (Meredith *et al.*, 2004) as well as erectile function (Werner *et al.*, 2005) and cell proliferation (Wiecha *et al.*, 1998) and cell migration (Soroceanu *et al.*, 1999).

Several recent discoveries have shown that implications with BK channels play a role in neurological diseases. Zhang *et al.*, 2006, hypothesise that BK is implicated in schizophrenia due to the potassium conductance enhancing nature of the commonly used antipsychotics that are used to treat the disease. They also report that in the prefrontal cortex of schizophrenics presented with significantly lower levels of mRNA expression of the BK channel in comparison to the control. Correspondingly, in a study conducted by Laumonnier *et al.*, 2006, it was shown that a defect in the BK channel, leading to a decreased expression of BK can contribute to autism and mental retardation. Epilepsy has also been linked to mutations in the alpha subunit of BK channels (Du *et al.*, 2005) and the β3 subunit (Lorenz *et al.*, 2006). A study by Zhao *et al.*, 2020 found that upregulation of the β4 subunit in the anterior cingulate cortex may contribute to anxiety-like behaviour induced by neuropathic pain. Several studies have also demonstrated that deletion of the BK alpha results in movement disorders such as ryegrass staggers, cerebral ataxia and Purkinje cell dysfunction (Du *et al.*, 2005, Du *et al.*, 2020, Imlach *et al.*, 2008, Sausbier *et al.*, 2004). However, Imlach *et al.*, 2008 report that only deletion of the alpha subunit causes the syndrome, whereas upon deletion of β1 and β4, no effect was seen. Genetic deletion of BK subunits has also been shown to lead to hypertension (Brenner *et al.*, 2000*b*, Sausbier *et al.*, 2005). Typlt *et al.*, 2013 illustrate that BK plays a crucial role in learning but not memory storage. However, it should be noted that the correlation between changes in genetic markers and phenotype does not necessarily indicate causation, several other factors could result in the disease aside from BK. Furthermore, several of the studies mentioned were conducted on mouse models, hence it may not be a true reflection on what will happen in humans. This is specifically a cause for concern with regard to BK as it has previously been shown by Zeng *et al.*, 2008 that the B3 subunits vary amongst mammalian species.

***The role of BK in glioblastoma***

A subclass of BK, termed glioma BK (gBK) exists, this channel is a result of an alternative splice variant with a 34 amino acid exon at splicing site 2 of *hSlo,* the gene that is responsible for encoding the alpha subunit (Ge et al., 2012). gBK also exhibits a higher sensitivity to calcium at physiological intracellular calcium concentrations, V0.5 was 12 mV with 1 μM $[Ca^{2+}]_i$ in glioblastomas (Ransom and Sontheimer, 2001) in comparison to 35 mV with 1 μM $[Ca^{2+}]_i$ in human smooth muscle cells (Hurley, Preiksaitis and Sims, 1999). This increased sensitivity could be a result of the altered structure (Liu *et al.*, 2002, Ransom *et al.*, 2002). Several studies have demonstrated that there is an overexpression of BK in glioblastoma (Catacuzzeno *et al.*, 2015, Liu *et al.*, 2002, Ransom & Sontheimer, 2001, Rosa *et al.*, 2017, Weaver *et al.*, 2006). Liu *et al.*, 2002 looking at biopsies of glioblastoma patients have reported that not only is BK overexpressed there is also a positive correlation between the glioma malignancy grade and the BK channel expression. However, this finding is restricted to a small sample cohort of seven human biopsies and three glioblastoma cell lines. Furthermore, Liu *et al.*, 2002, fail to statically analyse the correlation, stating a "positive correlation" is observed. Even though these findings are inciteful, one cannot assume that the correlation is significant as well as the fact an observed correlation does not prove causation.

Across, the literature BK in glioblastoma is implicated in cell migration and proliferation. However, there are discrepancies in the role of BK in migration, invasion, and proliferation. The migration is a result of cell shrinkage from the electrochemical driving force exerted by the BK channel which results in the release of cytoplasmic water (Molenaar, 2011). Whilst certain evidence suggests that BK channel activation gives rise to the migration of glioma cells, others show evidence of inhibition of migration. Weaver *et al.*, 2006 provide evidence to suggest that inhibition of BK channels using the blockers, paxilline and iberiotoxin resulted in a reduction in migration of the glioma cells, they also reported that activation of the BK channel using NS1619, had no effect on enhancing migration. Similarly, Soroceanu *et al.*, 1999 found a dose-dependent inhibition of glioblastoma migration with the use of BK blocker tetraethylammonium chloride. Research by Wondergem *et al.*, 2008 and Wondergem & Bartley, 2009 illustrate that BK activation via methanol resulted in glioma migration. This process is facilitated by methanol activating the TRPM8 channel, which increases intracellular calcium, and as a result, BK channels are activated. They also provide evidence that

blocking the BK channels via paxilline and tetraethylammonium chloride inhibits migration. This suggests that BK plays an important role in the migration of glioma cells. Inhibition of glioblastoma migration via BK channel blocker paxilline has also been observed in induced migration such as hypoxia (Rosa *et al.*, 2018) and radiation (Edalat *et al.*, 2016, Steinle *et al.*, 2011). However, in contradiction, Bordey *et al.*, 2000 illustrated that activation of BK channels via muscarinic activation of acetylcholine receptors results in an inhibition of cell migration in glioma cell line, this was also corroborated by Kraft *et al.*, 2003, who also found activation of BK channels via phloretin, and acetylcholine led to inhibited migration of glioma cells. Interestingly they also reported that upon co-application with BK channel blockers, paxilline and iberiotoxin the effects of the BK activators were nullified. These contradictory results could be caused by the difference in migration modes used in the study, both, Bordey *et al.*, 2000 and Kraft *et al.*, 2003 used patch clamp and time-lapse microscopy to study migration which is not an accurate mimic of the extracellular environment of the brain. Whereas Weaver *et al.*, 2006 used a 3D migration system using a transwell insert with 8µm pore coated with a chemoattractant, which is more accurate due to the small pore size that mimics the narrow spaces tumour cells encounter during migration. Catacuzzeno *et al.*, 2015 suggest that the discrepancies across the literature are due to the difference in intracellular calcium concentration, they propose that in low concentrations of intracellular calcium, BK are not activated and therefore do not contribute to migration, however, once the concentration of intracellular calcium increases to an intermediate level, one which is not enough to activate BK channels but are efficient for preparing them for cyclic activation following intracellular calcium oscillations. Furthermore, they suggest that a prolonged high concentration of intracellular calcium would cause a steady activation of BK that would inhibit the migration of glioblastoma cells.

BK has been shown to have an effect on cell proliferation on other cell types such as Muller glial cells and astrocytoma cell lines, in which BK blockade results in inhibition of cell proliferation. This provides evidence for BK's critical role in cell proliferation of glioma cells (Basrai *et al.*, 2002, Bringmann *et al.*, 1999). Although there is extensive research on the role BK plays in migration, there is much less information about the role the channel plays in cell proliferation of glioblastoma, where the research available is inconsistent. Weaver *et al.*, 2004 discovered that inhibition of BK by the toxin iberiotoxin resulted in a dose and time-dependent decrease in cell growth, they found that the toxin inhibited cell growth by eradicating cells in the S phase of the cell cycles, resulting in cell death. They also observed that gBK channel expression depended on the growth factor.

Similarly, Weaver *et al.*, 2006 illustrated that in the presence of BK channel inhibitors, iberiotoxin and paxilline cell growth was inhibited. Conversely, Abdullaev *et al.*, 2010, found that BK does not play a role in cell proliferation using the BK channel blocker paxilline and penitrem A. They found that an inhibition in proliferation was only seen at supraphysiological concentrations of the blocker but at concentrations which were sufficient to inhibit the channel activity, no effect on cell proliferation was seen. The difference between the studies could be a result of the different blockers used in each study or the fact that the study by Abdullaev *et al.*, 2010 used a 10% growth factor for the cell lines. As discovered by Weaver *et al.*, 2004, the effect of the blocker was abolished when the cells were in 7% fetal calf serum. This same phenomenon may have resulted in Abdullaev *et al.*, 2010 observing no effect. A hypothesis of the role of BK is that activation of these growth factors would lead to activation of BK which in turn increases intracellular calcium levels and as a result cause membrane depolarisation (Weaver *et al.*, 2006).

***The Role of BK role in Other Cancers***

BK is not only implicated in glioblastomas, but several studies also indicate its expression in many different cancers and is involved in cell proliferation, migration, and invasion as well. For example, BK has been shown to be a promotor of hepatocellular carcinoma cell proliferation, migration, and invasion by He *et al.*, 2021 who also reported that blocking BK channels resulted in cells arresting at the G2 phase. Similarly, Li *et al.*, 2018 reported that overexpression or silencing of BK in endometrial cancer cells enhanced or inhibited proliferation and migration respectively. These findings were supported by pharmacological data as activators of the channel increased proliferation and migration in these cells. Corresponding results were seen in astrocytoma cells (Basrai *et al.*, 2002) and breast cancer cells (Mohr *et al.*, 2020, Schickling *et al.*, 2014)

***Significance of glutamate and calcium signalling in Glioblastoma Multiforme***

Glioblastoma is well known to express glutamate, it is released by glioma cells via the cysteine/glutamate antiporter, xCT. xCT is upregulated in glioma cells, whereas the glutamate reuptake transporter, glutamate transporter 1 (GluR1) is downregulated, leading to the accumulation of glutamate in the cytoplasm of the glioma cell (Corsi, Mescola and Alessandrini, 2019 and Lange, Hörnschemeyer and Kirschstein, 2021). High levels of glutamate eventually lead to

increased levels of intracellular $Ca^{2+}$. $Ca^{2+}$ signalling plays a vital role in glioblastoma proliferation and invasion (Pei et al., 2020). In the present study, I have used glutamate as a means to increase intracellular $Ca^{2+}$ to see if it can activate BK channels.

***Membrane Potential***

The membrane potential is fundamental in the physiology of a cell. An electrochemical gradient arises due to ion diffusion and electrogenic pumps (Alberts *et al.*, 2002, Wright, 2004)**.** There are three main functions of membrane potential: cellular functions such as such as movements of nutrients and water in and out of cells, as well as cell-to-cell signalling and osmotic homeostasis (Moorhouse, 2016). A resting membrane potential is defined as the membrane potential during a period in which the cell is not active, the potential is maintained at a steady and stable condition of around -80 to -60 mV (Alberts *et al.*, 2002). Both the ion concentration and the permeability of the ions determine the resting membrane potential. The ions which have a significant role in generating membrane potential are sodium, potassium, and chloride, of which potassium and chloride are present at a high concentration within the cell. As a result of the ion gradient a negative intracellular potential is created. The selective permeabilities lead to the diffusion of ions (Figure 5) (Ramahi & Ruff, 2014). There are two forces at work: a chemical and an opposing electrical force. Eventually, the ion flux either reaches equilibrium or steady state depending on the relative permeability. The sodium-potassium pump (Na-K pump) which is expressed ubiquitously maintains the ion gradients. The equilibrium reached by the ion can be quantitively expressed using the Nernst equation (Figure 6A), in which known values of internal and external ion concentration are used to calculate a theoretical value of the resting membrane potential for a single ion. However, the Nernst equation assumes that the cell is permeable only to one ion. This results in discrepancies between the calculated resting membrane potential and the true resting membrane potential due to the existence of other ion permeabilities (Alberts *et al.*, 2002, Chrysafides *et al.*, 2019, Ramahi & Ruff, 2014). Therefore, to account for multiple ions, we use the Goldman-Hodgkin-Katz equation (Figure 6B) to calculate the membrane potential. The equilibrium potential of both sodium is +65 mV and potassium is -90 mV; however, the resting membrane potential of cells is usually around -70 to -80 mV, this is due to potassium being much more permeable in comparison to sodium, resulting in the membrane potential being closer in value to the equilibrium potential of potassium. (Chrysafides *et al.*, 2019).

| Ions | Intracellular Concentration | Extracellular Concentration | Equilibrium Potential |
|---|---|---|---|
| **Sodium** | 15 mM | 145 mM | + 60.60 mV |
| **Potassium** | 150 mM | 4 mM | -96.81 mV |
| **Calcium** | 70 nM | 2 mM | + 137.04 mV |
| **Chloride** | 10 mM | 110 mM | -64.05 mV |

***Figure 5.***

Table of intracellular and extracellular concentrations of the different ions that contribute to the membrane potential. The Nernst equilibrium potential of each ion is also given.

A $$V_{eq.} = \frac{RT}{zF} \ln \frac{[X]_o}{[X]_i}$$

B $$Vm = 61.5 \log_{10} \frac{P_K[K^+]_o + P_{Na}[Na^+]_o}{P_K[K^+]_i + P_{Na}[Na^+]_i}$$

***Figure 6.***

A) Nernst equation used to calculate the equilibrium potential of a particular ion. *R* is the gas constant, *T* is the temperature, *F* is the Faraday constant, and *z* is the valence of the ion. $[X]_o$ is the extracellular concentration of the ion and $[X]_i$ is the intracellular concentration of the ion. B) Goldman-Hodgkin-Katz (GHK) equation that is used to calculate the membrane potential when two or more ions contribute to it as the Nernst potential no longer is applicable as an equilibrium is no longer reached. For sodium and potassium, RT/zF is equal to 61.5.

It should be noted that the resting membrane potential is not only vital in excitable cells, but it also plays an important role in non-excitable cells. Several studies have shown that the membrane potential is vital for a multitude of biological functions. These include circadian rhythm (Belle et al., 2009), contractility (Nelson and Quayle, 1995), proliferation (Cone & Cone, 1976, Nelson and Quayle, 1995), cell cycle (Amigorena et al., 1990, Neher and Sakmann, 1976), tissue patterning (Levin, 2014), cell differentiation (Chen *et al.*, 2019, Tsuchiya & Okada, 1982) as well as insulin secretion (Aguiliar-Bryan and Bryan, 1999, Lin et al., 2005).

***Membrane potential and cell proliferation and cell differentiation***

Dysregulation of normal cell proliferation and invasion in healthy individuals results in the development of tumours as well as growth and metastasis. Several recent studies have revealed a correlation as well as a functional relationship between membrane potential and cell proliferation and differentiation. Cone & Cone, 1976 demonstrate that upon depolarisation with depolarising agents, there was an increase in DNA synthesis and mitosis in CNS neurones. Sustained depolarisation results in an increase in intracellular sodium and a decrease in potassium ions. Similarly, Cone & Tongier, 1973 also found that the mitotic activity of Chinese hamster ovary cells could potentially be coupled to membrane potential, with a complete mitotic arrest seen at a membrane potential of -75 mV, which was reversed by bringing the membrane potential back to -10 mV.

Across the literature, several studies indicate a sustained depolarised membrane potential in a range of cancerous cells when compared to a hyperpolarised membrane potential in healthy cells (Table 3). From this data Binggeli & Weinstein, 1986 suggested that a threshold membrane potential exists, when the membrane potential crosses this supposed threshold, it promotes mitosis and subsequent DNA synthesis. The proposed mechanism for the promotion of mitosis and DNA synthesis by Binggeli & Weinstein, 1986 is cancer and normal proliferating cells have a much lower membrane potential than non-proliferating cells, this means that the threshold membrane potential can be crossed when cells undergo division, then normal proliferating cells repolarise above the threshold potential once growth ceases. However, Binggeli & Weinstein, 1986 hypothesised that the cancer cells are unable to repolarise and maintain a depolarised membrane potential, which promotes mitosis and DNA synthesis.

| Cancer Cell Type | Membrane Potential in comparison to healthy cells | Reference |
|---|---|---|
| Ehrlich Ascites tumour | Depolarised | Johnstone,1959 |
| Breast cancer | Depolarised | Marino *et al.,* 1994 |
| Cancerous fibroblasts and hepatocytes | Depolarised | Binggeli & Cameron, 1980 |
| Hepatocellular carcinoma cells | Depolarised | Stevenson *et al.,* 1989 |
| Adrenocortical tumour | Depolarised | J. R. Lymangrover *et al., 1975* |
| Fibrosarcoma | Depolarised | Biggeli & Weinstein, 1985 |
| Skin cancer | Depolarised | Melczer & Kiss, 1957 |
| Ovarian tumour | Depolarised | Berzingi *et al.*, 2016 |

***Table 3.***

Table of studies that demonstrate a depolarised membrane potential in cancerous cells in comparison to healthy cells.

These findings suggest that ion channels play a key role in tumour development as membrane potential itself is regulated by channels present on the cell membrane. Pharmacological blockers of several channels have been shown to affect the proliferation rate in a variety of cancer cell lines. One of the major channels which have been implicated in cell proliferation is potassium channels. However, in contradiction to the hypothesis suggested by Binggeli & Weinstein, 1986, the following studies indicate that blocking of the potassium channel, subsequently depolarising the membrane potential results in reduced proliferation. For example, Fraser *et al.*, 2000 demonstrated that blocking voltage-gated $K^+$ channels in prostate cancer cell lines using a variety of blockers, reduced proliferation by 8-15% in a dose-dependent manner. Similarly, Abdul & Hoosein, 2002 reported a 30-50% increase in proliferation in prostate cancer cell lines when exposed to potassium channel activators, however, they observed a subsequent decrease in proliferation with blockers of the same channel, followed by apoptosis following 4 hours of treatment. Decreased proliferation by inhibition of potassium channel was also seen in human melanoma cell lines by the blocker TEA (Nilius & Wohlrab, 1992), neuroblastoma cells, when treated with TEA, 4-aminopuridine and capsicum.(Rouzaire-Dubois & Dubois, 1991), malignant lymphocytes with the blockers quinidine, 4-

aminopyridine, barium and TEA (Wang *et al.*, 1992) as well as in MCF-7 breast cancer cell line with a range of potassium channel blockers TEA, 4-aminopuridine, quinidine, glibenclamide and linogliride (Wonderlin *et al.*, 1995). The cell division cycle plays a major role in cell proliferation and ion channels aid this process by means of regulating the membrane potential. Specifically, the $G_1$/S phase is thought to be a key player. Studies such as that by Weaver *et al.*, 2004 have demonstrated that upon blocking potassium channels using iberiotoxin in glioma cell lines, cells arrest in the S phase of the cell cycle. Similarly, Woodfork *et al.*, 1995 reported the arrest of human breast cancer cells at the $G_1$ phase when treated with potassium channel blockers quinidine, glibenclamide, and linogliride. In the same breast cancer cell line, Wonderlin *et al.*, 1995 showed that hyperpolarisation of the membrane potentials drives cell passage from the $G_1$ phase to the S phase.

Furthermore, membrane potential is also seen to play a role in cell differentiation. Modulation of the membrane potential has been linked to the differentiation pathway. Sundelacruz *et al.*, 2008 modulated the membrane potential using ouabain; which is a $Na^+/K^+$ ATPase pump inhibitor. This allowed them to inhibit the transmembrane potential, they then depolarised the cell with high extracellular potassium and found this inhibited osteogenic and adipogenic differentiation of mesenchymal stem cells, suggesting that hyperpolarisation is necessary for the differentiation of those cells. In accordance with this Konig *et al.*, 2004 report that when hyperpolarisation is blocked using blockers of the inward rectifier potassium channel, differentiation of human myoblasts is suppressed. Konig *et al.*, 2004 suggest that hyperpolarisation triggers transcription factors that result in differentiation of human myoblasts. Finally, Sempou *et al.*, 2022 show that deletion of the KCNH6 gene, which is a voltage gated potassium channel protein coding gene, in pluripotent embryonic cells results in membrane depolarisation followed by the cell remaining at the pluripotent stage as opposed to germ layer differentiation in the embryo. Their results suggest that the membrane potential is important in regulating the intracellular calcium levels and subsequently the mTOR pathway that is responsible for the differentiation of pluripotent embryonic cells. These studies indicate that hyperpolarisation is a key modulator in the differentiation process in a range of different cell types and most cases the membrane potential is modulated by potassium channels.

***Measuring Membrane potential***

The most common method to measure membrane potentials is patch clamping or intracellular recordings. Both techniques use two microelectrodes, one functions as the ground electrode and the other is the recording electrode. Both electrodes are connected to the voltmeter. The recording electrode is made up of a glass tube and a silver wire coated with AgCl. In patch clamping the glass tube is filled with an intracellular buffer, whereas in intracellular recordings it is with KCL. Whereas the reference electrode is placed in the extracellular solution. In patch-clamping the recording electrode is attached to the cell for a giga-seal and in intracellular recording it is inserted into the cell (Figure 7) (Khadria, 2022). However, there are also other non-optical and optical methods available such as microelectrode assays, fluorescent bioelectricity reporters, and calcium-sensitive fluorescent dyes (Adams & Levin, 2012 Khadria, 2022, Meister *et al.*, 1994, Wilson & Chused, 1985). A detailed review of all techniques available to measure membrane potential can be found in the review by Khadria, 2022. In the present study I have chosen to use a patch clamp, this allowed us to make high-resolution current recordings to measure as well as study single channel activity, allowing us to measure both membrane potential as well as study BK channel activity. One of the biggest advantages of patch clamp recordings is that there is less damage to the cell in comparison to intracellular recordings. The cell attached patch clamp method allows measurements to be made without rupturing the membrane (Figure 7B). When a direct comparison was made between whole cell patch clamp and intracellular recordings by Li, Soffe and Roberts, 2004 depolarisation and a 20-40% drop in input resistance were reported as a result of damage from the intracellular recording method. Furthermore, the patch clamp method also allowed us to modulate the pipette solution.

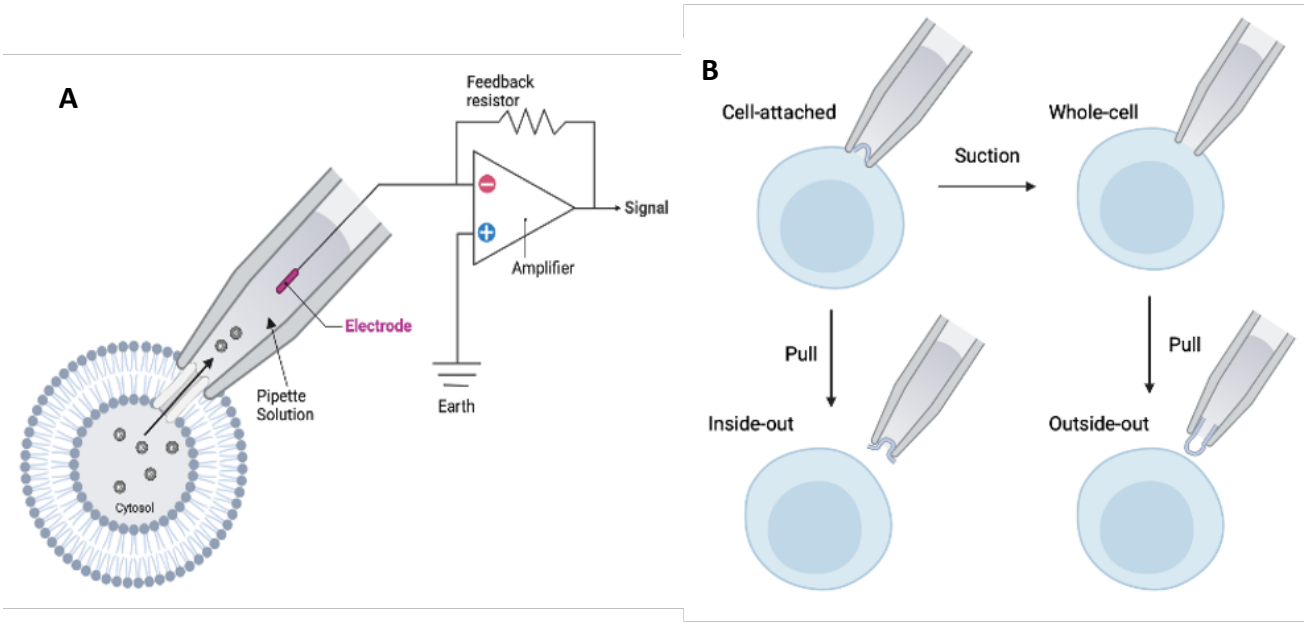


***Figure 7.***

Overview of the patch clamp technique. **A)** Standard set-up of patch clamp. The micropipette forms a high-resistance gigaohm seal on the cell membrane using suction. Two recording techniques are utilised; voltage clamp which clamps the membrane potential at a fixed voltage and measures the current, and current clamp in which current is injected into the cell and the membrane potential is measured. **B)** The different patch clamp configurations. *Cell-attached*: achieved by applying suction to form a high resistance seal, with the membrane still attached. This allows recordings of single channel activity *Whole cell*: is achieved by applying a stronger suction which ruptures the membrane, allowing access to the cytosolic space. *Inside out*: Pulling the micropipette from the cell attached configuration gives rise to the inside out. This allows manipulation of the conditions the intracellular surface of the cell membrane is exposed to. *Outside out*: Pulling the microelectrode from the whole cell configuration results in outside out.

*(Hill & Stephens, 2020) Image created with BioRender.com*

***SF188***

SF188 is a commercially purchased patient-derived glioblastoma cell line, derived from the frontal lobe tumour of an 8-year-old male. It has several characteristics such as tumour cell morphology and growth kinetics, proliferates as adherent monolayers and expresses glial markers that make it a reliable model for studying glioblastoma multiforme (Bax *et al.*, 2009, Rutka *et al.*, 1987). SF188's have been utilised in multiple studies looking into glioblastoma migration and invasion (Aretz *et al.*,

2022, Cockle *et al.*, 2015, Cockle *et al.*, 2017, Egbivwie *et al.*, 2019), proliferation (Andrade *et al.*, 2016, Grossman *et al.*, 2012, Nguyen *et al.*, 2017) signalling pathway studies (Al-Saffar *et al.*, 2014, Haas-Kogan *et al.*, 1998, Nguyen *et al.*, 2017), mutation studies (Bjerke *et al.*, 2013, Chen *et al.*, 2020, Fang *et al.*, 2018, Rakotomalala *et al.*, 2021), cell viability (Hu *et al.*, 2019) as well as cell cycle studies (Qin *et al.*, 2022). Although no studies have utilised patch clamping to investigate the electrophysiology and biophysics of SF188's, unlike cell lines such as the human glioblastoma U87 and U251 cells which have been used in electrophysiology studies (Brandalise et al., 2023, Catacuzzeno et al., 2011).

***Aims and hypothesis***

The range of evidence presented by these authors accentuates the importance of BK in migration and invasion in glioblastoma cells and provides a potential pharmacological target for therapeutic agents. Researching ion channels as potential therapeutic targets is important as around 13% of drugs used for treatments such as cardiovascular and neurological disorders whose primary therapeutic targets are ion channels (Overington *et al.*, 2006). However, future on the impact of gBK knockout could provide additional evidence needed to fill the gap in this field. From the evidence presented here, it is clear that intracellular calcium dynamics play a crucial role in cell migration and cell growth. BK channels have been a key regulator of membrane potential, which in turn affects calcium influx. However, the effect that BK has on glioblastoma membrane potential has been relatively unexplored, investigating this will allow us to further understand its role in the pathogenesis of this disease. In this present study, I intend to examine the role of the large conductance voltage and $Ca^{2+}$ - activated potassium channel, BK on membrane potential in glioblastomas, with a specific focus on the SF188 paediatric glioblastoma cell line. Using a single-channel patch clamp I investigated the amplitude of the channel opening at different membrane potentials. I also used cell attached whole cell recordings to measure the reversal potential of BK in glioblastomas. I also used blockers and activators of BK to investigate if BK had a direct effect on the membrane potential. Furthermore, investigation using $Ca^{2+}$ imaging could provide us with further insight into calcium activity in SF188s.

## Methods

*All materials are sourced from Sigma Aldrich, Gillingham, UK unless stated otherwise.*

### *Cell culture*

*Culturing cell lines*

2 cell lines and human-derived astrocytes were used. SF188 were cultured in Dulbecco's modified Eagle's medium (DMEM)/F12 (Gibco) (Branter et al., 2022) and GCE62 was cultured in Dulbecco's modified Eagle's medium (DMEM). Both media were supplemented with 10% (v/v) foetal bovine serum (HyClone), 10IU/ml penicillin and 100 µg/ml streptomycin. SF188 had a further addition of 1% (v/v) L-Glutamine in its media.

SF188 and GCE62's were incubated in a humidified incubator at 37 °C with a 5% $CO_2$ atmosphere. To ensure completely sterile environments, cells were handled individually in a biohazard hood with laminar air flow that was wiped with 70% ethanol, which decreased the chance of contamination. Cells were checked microscopically daily and left in the incubator to grow until 80-90% confluency in Nunc 75 $cm^2$ flasks (Fisher, Loughborough, UK). To passage the cells, the old media was pipetted out and discarded to remove the non-adherent cells. This left the live cells adhered to the bottom of the flask, the cell's monolayer was washed in 5 ml of phosphate-buffered solution (Thermosphere Scientific) without $Mg^{2+}$ or $Ca^{2+}$. Then 3 ml of 0.5 mg/ml trypsin-EDTA (Sigma-PAA, UK) was added the flask was then incubated for 3-5 minutes to detach the cells by disrupting the monolayer. The flask was viewed under the microscope the see if cells had detached, if cells remained attached, they were removed by 'sharp knocking' of the flask against the palm or further incubation. The trypsin was then inactivated by adding 7 ml of complete media. The suspension of cells was then pipetted and transferred to a 15 ml conical tube and centrifuged at 300 xg for 4 minutes to form a cell pellet. The supernatant was removed, and the pellet was re-suspended in 8 ml of media for the SF188s and 10 ml of media for the GCE62'S to create a 1:8 and 1:10 spilt ratio respectively. 1 ml of the cell suspension was then transferred into a new flask containing 9 ml of media and was then incubated in the above conditions to grow up to 80-90% confluency. Human astrocytes (ScienCell™, Cat. No. 1800) were cultured in an astrocyte medium

containing 2% FBS, 1% astrocyte growth supplement and 1% Pen./Strep(v/v, ScienCell™) and were seeded at a density of 5000 cells/$cm^2$ onto flasks coated in 2 µg/cm2 Poly-L Lysine (ScienCell™).

SF188 is a well-established cell line that has a recognised STR profile (Bady et al., 2012), it is derived from a right frontal lobe glioblastoma multiforme of an 8-year-old male (Merck, Germany). GCE62 is an in-house tumour that is derived from a sample core tumour region of a teenage patient. The GCE62 was collected by Mr Stuart Smith, Neurosurgical Department, Queens Medical Centre, Nottingham during a routine surgical resection. Human derived astrocytes acquired from the cerebral cortex were used as an automatically matched control for human glioblastoma cells.

| Cell Line | Origin | Donor Age | Sex | Brain Region | Histology | Culture Media | Split Ratio | Doubling Time |
|---|---|---|---|---|---|---|---|---|
| **SF188** | Merck, Germany | 8 | Male | Right frontal lobe tumour | Glioblastoma multiforme – pediatric high-grade glioma | DMEM F12 (Gibco™), 10% FBS (Hyclone™), 1% PenStrep (Sigma-Aldrich), 1% L-Glutamine (Sigma-Aldrich), | 1:8 | 26 hours |
| **GCE62** | Patient derived by Mr Stuart Smith, Neurosurgical unit, Queens Medical Centre, Nottingham | 19 | Male | Right temporal lobe | Glioblastoma multiforme (WHO 2021, paediatric high-grade glioma) | DMEM (Gibco™), 10% FBS (Hyclone™), 1% PenStrep (Sigma-Aldrich) | 1:10 | 36 hours |
| **Human Astrocyte** | ScienCell™, California (1800) | - | - | - | Cerebral cortex astrocytes | Astrocyte media (ScienCell™), 1% Astrocyte Growth Serum 1% (ScienCell™), | 1:4 | 50 hours, increasing with passage number. Astrocytes senesce after 14 |

***Table 4.***

Cell lines with associated patient information and media, doubling time and split ratio of cell lines used.

*Plating for experimental work*

Cells were seeded onto Nunc 35 mm Petri dishes (Fisher, Loughborough, UK) for patch clamp experiments. They were seeded depending on the day that the experiments were carried out (Table 5). For calcium imaging cells were seeded onto Size 0 22 mm glass cover slides, and placed in 6 well plates containing 3ml of media.

***Table 5.***

Seedings of SF188s and GCE62s per day for patch clamp experiments, amount of cell suspension added to the dishes depended on the total number of cells in each cell suspension. The total number of cells in the flask was calculated using a haemocytometer.

*Cell counting*

Cells were manually counted using a Neubauer haemocytometer to determine the amount of cell suspension needed for the specific seeding density. After the supernatant was removed following centrifugation, 8ml of media was used to resuspend the cell pellet. The cell suspension was then applied to the haemocytometer and the number of cells was counted under a x10 objective lens. Cells to the left and top of the square were included in the count. Cell number was calculated according to the following formula:

$$\textit{The number of cells per millimetre}^3 = \textit{number of cells counter per square millimetre x 10 x 1000}$$

$$\textit{Total cell number= cell concentration x volume of cell suspension}$$

*Cell revival*

To revive cells from liquid nitrogen tanks, they are removed and rapidly thawed in a 37 °c water bath for ~1 minute or until visibly defrosted. They are then seeded into T25 flasks containing 5 ml of media and left in the incubator at 37 °C at 5% CO2 atmosphere for 24 hours. Following this, cells were checked under the microscope to ensure cells had adhered, then the media was changed to remove any traces of DMSO. They were placed back in the incubator for another 24 hours. They were then passaged as mentioned above.

*Cell storage*

Once cells were at 80-90% confluency, the growth medium was pipetted out and discarded and washed with 5 ml of phosphate buffered solution, then 3 ml of 0.5 mg/ml trypsin-EDTA was added and incubated for 3 minutes. Cells were then centrifuged at 300 xg for 4 minutes, the supernatant was removed then the cell pellet was resuspended in 3 ml of freezing medium, made up of 10% vol/vol DMSO and 90% FBS. 1 ml of the cell suspension was then transferred to cryovials to form a concentration of 1 x $10^7$ cells/mL, which were stored at -80°C freezer for 24 hours and then moved to the nitrogen tank for long term storage.

***Electrophysiology***

*Patch clamp preparations*

Pipettes were pulled from Harvard GC150TF-15 thin-walled borosilicate glass capillaries (Harvard Apparatus, Cambridge, UK) using a PC-10 Dual-Stage Glass Micropipette Puller (Narishige International, London, UK) and the tips were coated in sticky wax (Kerr Dental, Peterborough, UK) to reduce electrical capacitance and improve noise. Prior to experiments, pipettes were fire polished using an MF-900 microforge (Narishige) to a resistance between 3-5 MΩ. The bubble number of the pipette was checked using ethanol, and a bubble number of 6-7 was utilised. Pipettes were filled with either an internal solution of high calcium (in mM): 140 KCl, 1.2 $MgCl_2$, 2.6 $CaCl_2$, and 10 HEPES (pH 7.4 with NaOH; 2.6 mM free [$Ca^{2+}$]) or low calcium (in mM): 130 K Gluconate, 10 NaCl, 3 EGTA, 10 HEPES, 1 $CaCl_2$ and 2 $MgCl_2$ (pH 7.4 with KOH; <35 nM free [$Ca^{2+}$]).

*Cell attached patch clamp*

Cell-attached patch clamp experiments were performed to investigate the properties of the ion channels that affect membrane potential. Recordings were made for 1 minute from a holding potential of 0 mV to -90 mV, decreasing in 10 mV increments each time. A median of 5 individual amplitude determinations was calculated. Current-voltage graphs were plotted using the amplitude determination, which allowed calculations of the slope conductance and reversal potential of the channel. Currents above 5 pA were classified as BK. For cell-attached patch clamp experiments cells

were bathed in solutions depending on the experiment carried out. A standard HEPES-buffered Hanks bath solution contained 137 NaCl, 4.2 $NaHCO_3$, 1.2 $NaH_2$ $PO_4$, 5.6 KCl, 1.2 $MgCl_2$, 2.6 $CaCl_2$, 10 HEPES (pH 7.4 with NaOH) supplemented with 10 mM glucose, unless stated otherwise.

*Whole-cell patch clamp*

Whole cell recordings were made using either the high calcium or low calcium pipette solution and Hanks solution in the bath. Voltage-gated currents were elicited by a voltage step protocol, from a holding potential of -60 mV, with the membrane potential increased by 10 mV increments at a frequency of 0.1 Hz and step duration of 240 ms. Currents were filtered at 5 kHz.

Membrane currents were recorded with an Axopatch 1D patch clamp amplifier (Axon Instruments, Molecular Devices), and a Digidata 1440A low-noise digitizer controlled by PClamp 10.6 software (Molecular Devices, Sunnyvale, CA, USA). Currents were filtered by an 8-pole Bessel filter at 2 kHz and digitized at 5 kHz. Membrane potential was referenced to an Ag/AgCL agar bridge reference electrode in the bath. Currents were zeroed with the pipette in the bath, no correction has been made for junction potentials All electrophysiology experiments were performed at 25 °C, 30 °C or 35 °C as indicated.

*Patch clamp analysis*

Single-channel current data were analysed with half-amplitude threshold techniques as implemented in PClamp Ver. 10.6. Single-channel current amplitudes were measured with cursors. NPo was calculated as the fraction of time channels were active. Open channel dwell time was estimated as the arithmetic average from all single-level openings. Whole cell input resistance was calculated using the inverse of the gradient of the current-voltage graph for the cell using PClamp Ver. 10.6.

To confirm I was observing BK, known activators and blockers of the channels were used in both cell attached and whole cell experiments. Preparations of these drugs are given below.

***Calcium imaging***

The concentration of intracellular calcium was monitored using Fluo 4-AM using standard epiflourescent imaging protocol as described by Bentley et al., 2014. Imaging was carried out by seeding SF188 cells onto 22 mm size glass cover slides sterilised using ethanol, transferred to 6 well plates and allowing 48 hours for cells to settle. Determination of calcium concentrations was carried out on cells loaded with 1 µM Fluo-4 AM (Thermo Fisher, Loughborough, UK) fluorescent dye, diluted in Hanks, for 40 minutes in the dark at room temperature (20 – 25 °C). To monitor changes in intracellular $Ca^{2+}$, cells are continuously illuminated at an excitation wavelength of 450-490 nm with the lowest light intensity that gives a detectable fluorescent signal without photobleaching. The emitted light is filtered at 515-565 nm and the signal is detected using an x20 Zeiss PlanNeofluar objective lens Images were captured at 1 Hz with a Coolsnap HQ2 camera (Photometrics, Tucson, AZ, USA) with a Zeiss XBO 75 xenon short-arc lamp (Zeiss, Oberkochen, Germany). Recordings were recorded with Imaging Workbench ver. 6.0 software (INDEC Biosystems, Los Altos, CA, USA).

Regions of interest were drawn around cells corrected for background fluorescence by subtraction, and the average fluorescence intensity was calculated. ROIs were from both single cells and cell clusters. For each experimental group, samples were pooled from multiple visual fields from at least 4 different preparations. Initially, the cells were washed by perfusing Hanks at for 4 minutes before carrying out treatments, cells were continually perfused at 32 °C. The experimental set-up is summarised in Figure 8. To calibrate $[Ca^{2+}]_i$, fluorescence changes were calibrated by a one-point method that involved permeabilization of the cells with Triton X-100 (0.00125 - 0 0.1% vol/vol) with the maximum fluorescence value observed taken as Fmax. To calculate $[Ca^{2+}]_i$ the following equation was used:

$$[Ca^{2+}]_i = K_d X \frac{F}{Fmax - F}$$

Where F is the background corrected fluorescence, and Kd is the dissociation constant of Fluo-4 (345 nM, Molecular Probes).

*Calcium analysis*

Imaging analysis was carried out using Origin 6.1 software with custom scripts written in Labtalk (Originlab, Northampton, MA, USA). Raw fluorescent trace was extracted from each ROI and analysed in Origin 6.1 to calculate the steady states and peaks. Data was calibrated and only cells in which $[Ca^{2+}]_i$ was stable were used. Furthermore, if the majority of cells responded to glutamate in a group, those who did not respond were excluded.

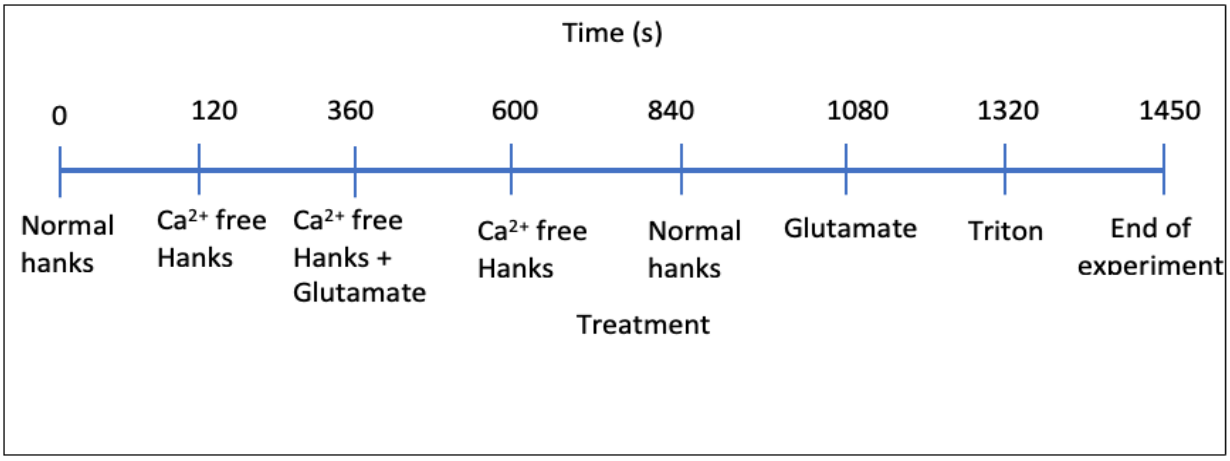


***Figure 8.***

Summary of the experiment protocol. Initially, cells were perfused with normal Hanks for two minutes, followed by perfusion with $Ca^{2+}$ free Hanks. Glutamate with $Ca^{2+}$ was then perfused for 4 minutes. This was then washed with $Ca^{2+}$ free Hanks, followed by normal Hanks. Glutamate was then perfused for 4 minutes. Finally, triton was perfused as the calibration treatment. Experiments were done at 0.1, 1, 10 and 100 mM.

***Preparation of solutions and drugs***

*Hanks* (in mM) 137 NaCl, 4.2 $NaHCO_3$, 1.2 $NaH_2PO_4$, 5.6 KCl, 1.2 $MgCl_2$, 2.6 $CaCl_2$, 10 HEPES (pH 7.4 with NaOH). *Na free Hanks* (in mM) 92 NaCl, 4.2 $NaHCO_3$, 1.2 $NaH_2PO_4$, 45 n-methyl-d-glucamine, 1.2 $MgCl_2$, 2.6 $CaCl_2$, 10 HEPES (pH 7.4 with HCL). *Cl free Hanks* (in mM) 137 Na gluconate, 4.2 $NaHCO_3$, 1.2 $NaH_2PO_4$, 5.6 KCl, 1.2 $MgCl_2$, 2.6 $CaCl_2$, 10 HEPES (pH 7.4 with NaOH). *K Hanks* (in mM)

92 NaCl, 4.2 $NaHCO_3$, 1.2 $NaH_2$ PO4, 50.6 KCl, 1.2 $MgCl_2$, 2.6 $CaCl_2$, 10 HEPES (pH 7.4 with NaOH). *Ca free Hanks* (in mM) 137 NaCl, 4.2 $NaHCO_3$, 1.2 $NaH_2$ $PO_4$, 5.6 KCl, 3.8 $MgCl_2$, 10 HEPES (pH 7.4 with NaOH).

*TEA* 1 mM: 33 mg in 100 ml of Hanks, *Paxilline* - 1 µM: 5 mg in 11.5 ml of DMSO, *Quinine* - 200 µM: 10 mg into 2.5 ml of water to create 10 mM stock, then 1 ml of stock into 50 ml of Hanks. *Isopimeric acid* - 20 µM 10 mg into 3.3 ml of DMSO to create 10 mM stock then 100 µl of stock to 50 ml Hanks. *Glutamate* – in 50 ml Hanks for: 0.1 mM add 0.73 mg, 1 mM add 73.56 mg, 10 mM add 73.56 g and 1M add 735 g. *Triton* - 0.02%: add 100 µl of 10% to 50 ml of Hanks.

***Statistics***

All statistical analysis was carried out using PRISM 9 software (GraphPad Software Inc., San Diego, CA), normality of data sets was determined by D'Agostino & Pearsotest. A combination of box and whisker and bar graphs were used to represent results, which are expressed as means ± SEM., with *n* representing the number of values represented. Tests used are detailed in the text where a $p < 0.05$ was deemed statistically significant, *$p \leq 0.05$, **$p \leq 0.01$, ***$p \leq 0.001$, **** $p \leq 0.0001$.

## ***Results***

### *SF188 Electrophysiology Characterisation*

To determine the channel's identity and biophysics in SF188's, a cell-attached single channel patch clamp was used. Figure 9A shows a representative single channel linear current-voltage curve of BK in high calcium pipette solution. Figure 9B shows representative BK activity in a high calcium pipette solution. Single channel analysis revealed BK was spontaneously active in 31 out of 71 patches. Figure 9C shows that the open probability of BK channels was voltage-dependent across the range of holding potential tested, suggesting the channel is voltage activated. Figure 9D shows the frequency distribution of slope conductance from 27 patches which revealed a bimodal distribution of single channel amplitude in SF188's with midpoints of around 124 and 215 pS. A bimodal distribution is indicative of two channels being active: in this instance BK and an unidentified $K^+$ permeable ion channel.

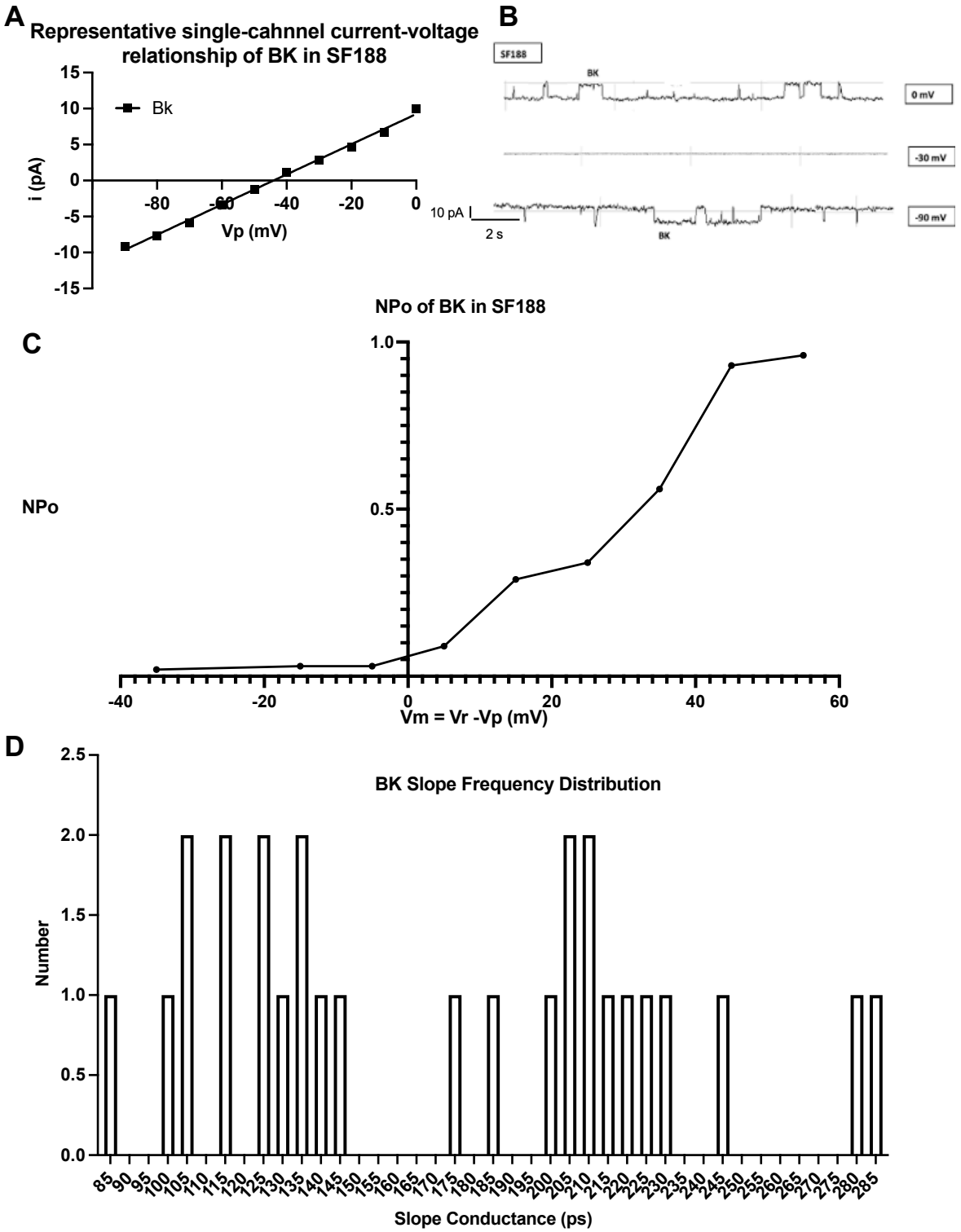


***Figure 9.*** BK are spontaneously active in SF188's. **A)** Representative single-channel current (i) voltage (Vp) relationship BK channel measured on a SF188 cell. Each point is the median of 5 individual amplitude determinations. A solid line is fit by linear regression. In this case, the slope conductance and reversal potential are 210 pS and -44.06 mV. **B)** Representative activity of BK in an SF188 cell in high calcium pipette solution. Downward flickers are characteristic of the BK channel.

Vertical bars represent amplitude and horizontal bars represent time **C)** Open probability (NPo) of BK channel plotted against membrane potential (Vm) in a SF188 cell. Membrane potential = reversal potential (Vr) – holding potential (Vp). Voltage dependency of the channel is seen. **D)** Frequency distribution of slope conductance from 27 patches. Bimodal distribution with midpoints of around 124 and 215 pS. A bimodal distribution is indicative of two channels being active: in this instance BK and an unidentified $K^+$ permeable ion channel. Data is mean. *N* = 27

***Membrane Potential***

Membrane potential was determined using two different methods. Cell attached current-voltage curve was used to calculate the reversal potential of the cell followed by the whole cell current clamp. Figure 10 A-B shows a current activated by a voltage step going from -120 mV in 10 mV increments. A shift in the current-voltage relationship with high [$Ca^{2+}$] pipette solution reversing at a more negative potential is seen. Figure 10C shows a linear current-voltage curve of a whole cell recording measured in a low [$Ca^{2+}$] pipette versus a low [$Ca^{2+}$] pipette. A negative shift in membrane potential with the high [$Ca^{2+}$] pipette solution is seen. High [$Ca^{2+}$] in the whole-cell pipette solution was also associated with a linear current-voltage relationship (n=38, p=0.0020, Fisher's exact test) (not shown). Figure 10D shows that in the whole cell, the current clamp membrane potential was significantly different ( -46.42 ± 16.77 mV, p=0.001, unpaired t-test) when measured with high [$Ca^{2+}$] pipette solution, which was 16.8 mV more negative than that measured with low [$Ca^{2+}$] (-29.65 ± 16.77 mV). Figure 10E shows that in the whole cell, the input resistance showed no significant difference 220 ± 172.8 MΩ (n=8, p=0.1568, unpaired t-test) in high [$Ca^{2+}$] pipette solution compared to low [$Ca^{2+}$] in the pipette solution 396 ± 172.8 MΩ (n=28). Although in this particular cohort of experiments, the input resistance is high, compared to those cells presented in Figure 14C, there was no notable difference in the cell capacitance, access resistance or membrane potential between these cells. The reason for a lower channel density is unknown.

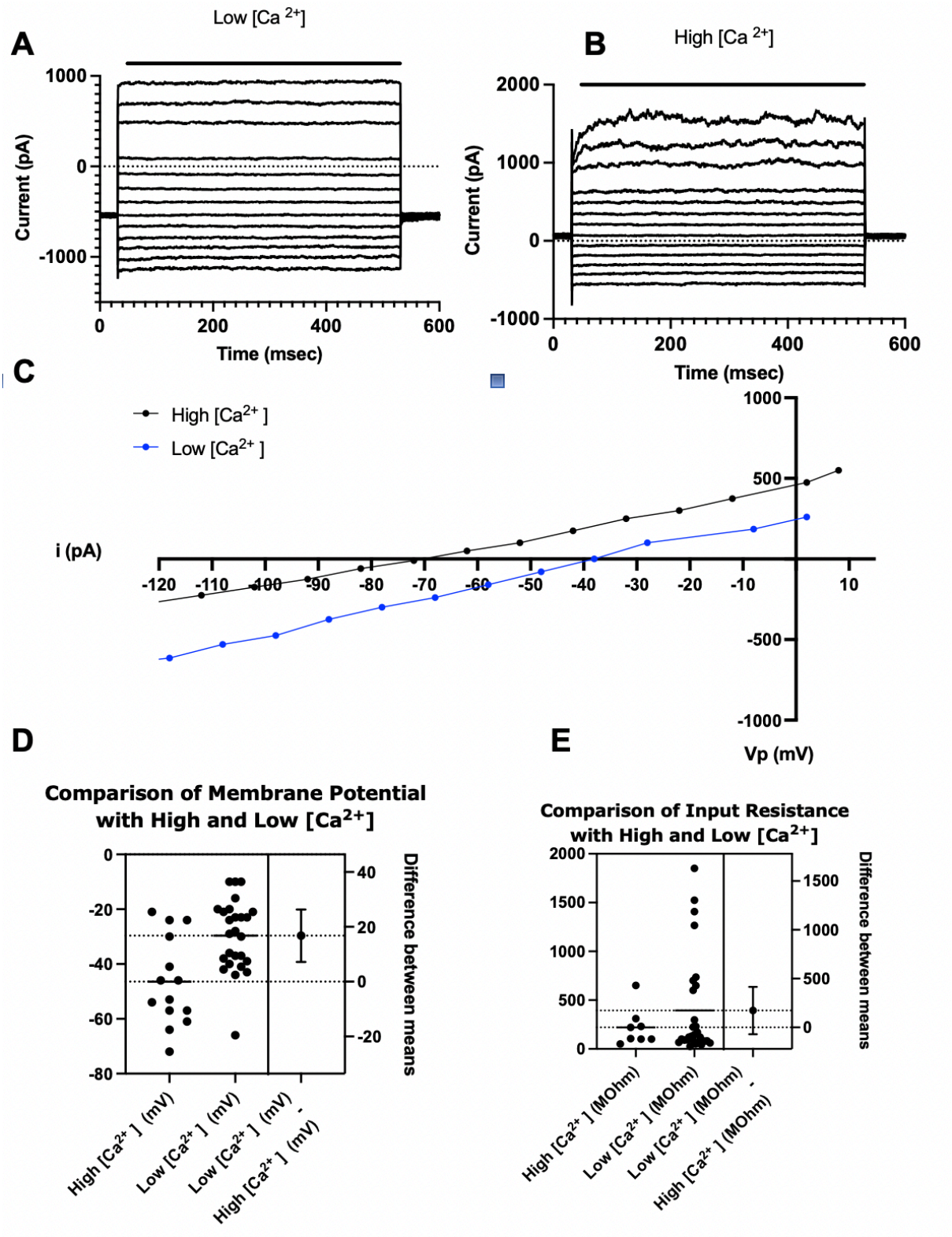


***Figure 10.*** High [$Ca^{2+}$] pipette solution caused hyperpolarisation of membrane potential by 16.8 mV, which is consistent with a cell that expresses BK. **A-B)** Current activated by voltage step going from -120 mV in 10 mV increments, for the period indicated by the black line. Note the shift in the

current-voltage relationship with high [$Ca^{2+}$] pipette solution reversing at a more negative potential. **C)** Representative comparison of whole-cell current (i) voltage (Vp)relationship of two different cells with high and low [$Ca^{2+}$ ] in the pipette solution. **D)** Comparison of membrane potential measured with current clamp from different cells with high and low [$Ca^{2+}$ ] in the pipette solution. High [$Ca^{2+}$] pipette solution was significantly different (p=0.001, unpaired t-test). **E)** Comparison of input resistance measured from different cells with high and low [$Ca^{2+}$ ] in the pipette solution. No significant difference (p=0.1568, unpaired t-test ) was seen. Data is shown as mean. *N* = 8-28.

Figure 11A shows a representative single channel current-voltage relationship, the reversal potential was used as an estimate of membrane potential. Figure 11B shows the comparison of the membrane potential estimated from the reversal potential of the cell attached current-voltage relationship -34.9±2.37 mV (n=21) and that measured from whole cell current clamp -35.09±2.35 mV (n=45) ([$Ca^{2+}$] = 1mM) was similar (p=0.732, Paired t-test).

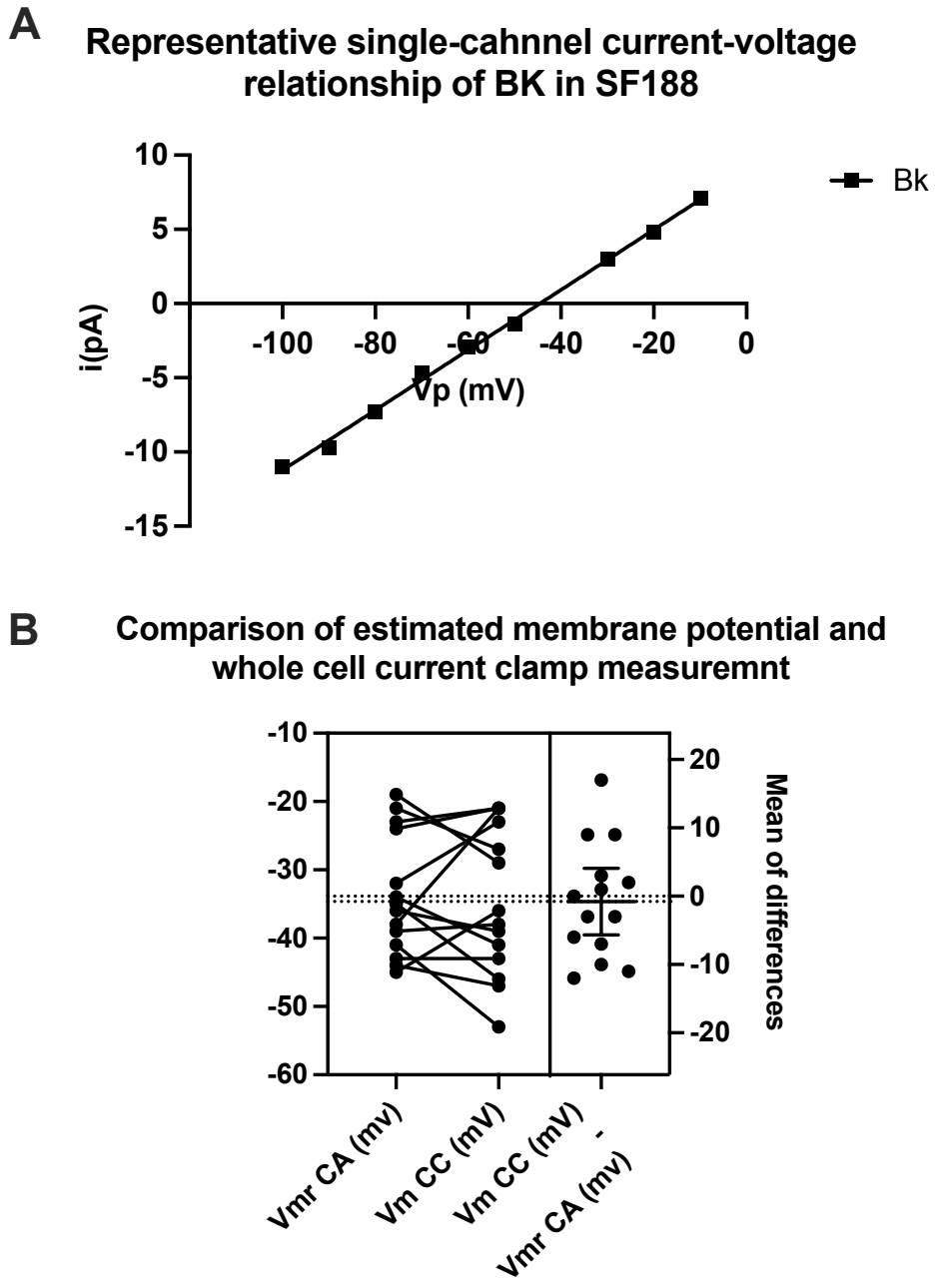


***Figure 11*** Comparison of membrane potential estimated from cell attached reversal potential and whole cell current clamp in SF188. **A)** Representative single-channel current (i) voltage (Vp) relationship of BK channel measured on an SF188 cell. Each point is the median of 5 individual amplitude determinations. A solid line is fit by linear regression. In this case, the reversal

membrane potential is -44.5 mV, and the slope conductance is 206 pS **B)** Paired t-test shows no significant difference (p=0.732) between the estimated membrane potential (Vmr CA) and that of the subsequent whole cell current clamp measurement (Vm CC). Data is shown as mean. *N* = 14

***Effect of different drugs on BK channel activity in SF188***

Channels were modulated using known blockers and activators of BK to determine the effect it had on channel activity, which allowed us to determine if the channels were indeed BK.

In experiments using 1 µM of paxilline (Wei et al., 2015), 4 out of 11 patches initially had inward currents > 5 pA at Vp = 0 indicative of BK. In 100% of patches that expressed BK, 1 µM paxilline abolished BK channel activity following its perfusion (Figure 12 A-B). In experiments using 200 µM of Quinine, 4 out of 10 patches had inward currents > 5 pA at Vp = 0 indicative of BK. In 100% of patches that expressed BK, 200 µM quinine (Mancilla and Rojas, 1990) abolished BK channel activity following perfusion (Figure 12 C-D). In experiments using 20 µM of Isopimeric acid an agonist of BK (Henney et al., 2009), 8 out of 9 patches initially had inward currents > 5 pA at Vp = 0 indicative of BK (Figure 12 E-F). 20 µM of Isopimeric acid did not affect BK channel activity as no significant effect was seen in the slope conductance before and after perfusion of the drug (n=5, p=0.9452, paired t-test) (not shown). Due to the absence of channels at the different voltages, I could not see the effect on NPo. However, the reversal potential hyperpolarised by 22.69mV following perfusion of 20 µM of Isopimeric acid (n=5, p=0.0313, paired t-test) (Figure 12 G-H). Experiments were performed in low [$Ca^{2+}$] pipette solution.

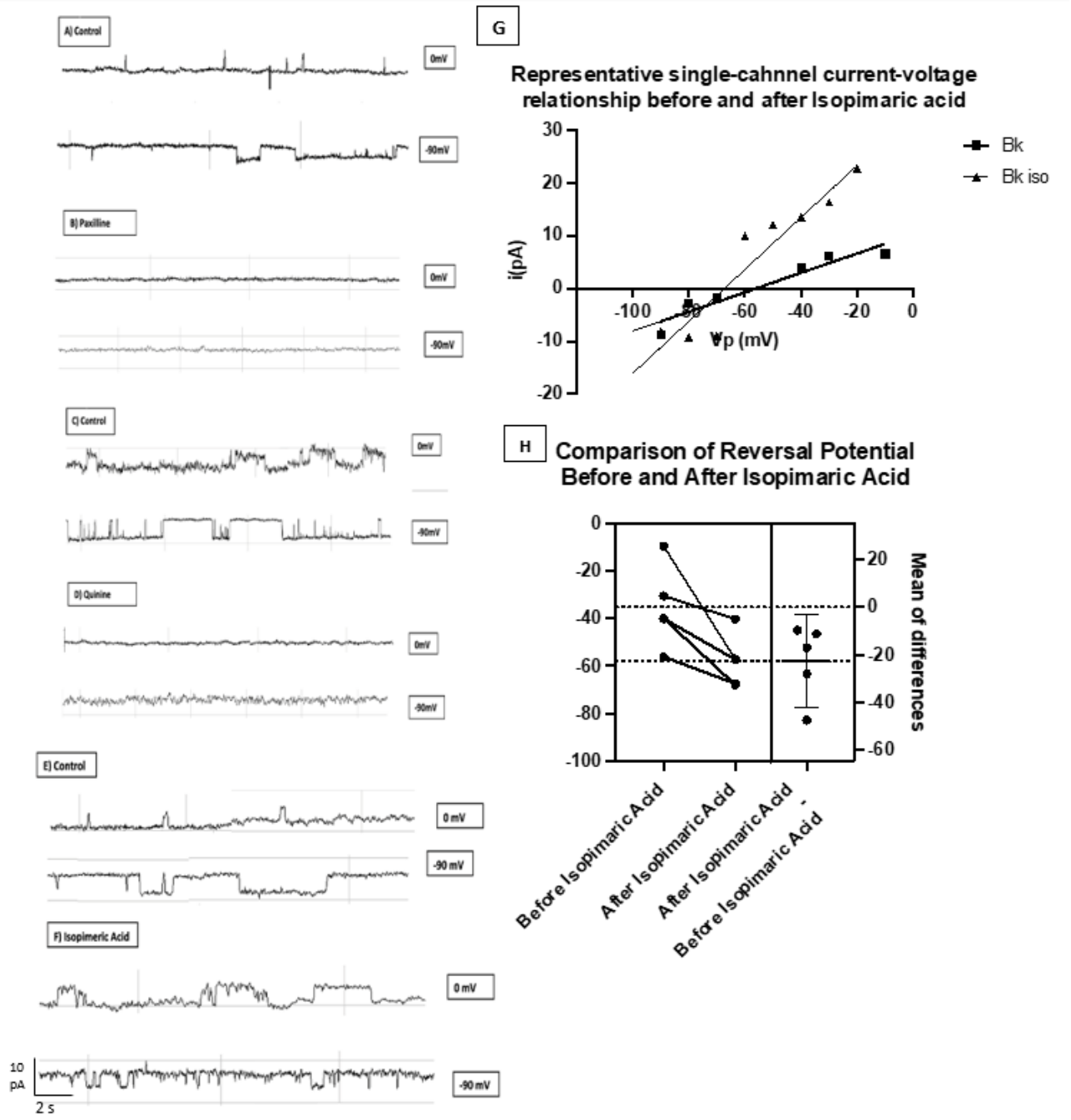


***Figure 12.*** Representative single channel activity of BK channel measured on SF188 cells under different BK channel blockers and activator at different holding potential as indicated. **A-B)** Perfusion of 1 µM paxilline abolishes all channel activity of the same cell measured across a holding potential of 0 mV to -90 mV**. C-D)** Perfusion of 200 µM quinine abolishes all channel activity of the same cell measured across a holding potential of 0 mV to -90 mV. **E-F)** Perfusion of 20 µM Isopimeric acid shows no effect on BK channel activity of the same cell measured across a holding potential of 0 mV to -90 mV. Experiments were performed in low [$Ca^{2+}$] pipette solution**. G)** Representative single-channel current (i) voltage (Vp) relationship of BK channel measured before

and after perfusion of Isopimeric acid on an SF188 cell. **H)** Paired t-test shows a significant difference (p=0. 0313) between the reversal potential before and after perfusion with Isopimeric acid. Data is shown as mean. *N* = 5.

***Effect of different drugs on membrane potential in SF188***

The effect of modulation of BK channels on membrane potential was assessed using the same blockers and activators.

Since paxilline blocked BK activity, I could not then see any shift in a cell attached resting membrane potential, therefore the initial BK cell-attached reversal potential and the subsequent post paxilline whole cell current clamp value was used. As Figure 13A shows, a comparison between membrane potential measured via the reversal potential and that on subsequent current clamp after going whole cell in the presence of paxilline appears to depolarise the membrane potential, but this was not significant (p= 0.0594, n=3, paired t-test), hence I performed experiments where paxilline was perfused in whole cell to see its effect. Figure 13B shows in whole cell patches 1 µM paxilline significantly depolarized membrane potential by 13 mV (p= 0.0178, n=7, paired t-test). However as seen in Figure 13C no effect of the drug was seen on the input resistance (p=0.2823, n=6, paired t-test). Experiments were performed in low [$Ca^{2+}$] pipette solution.

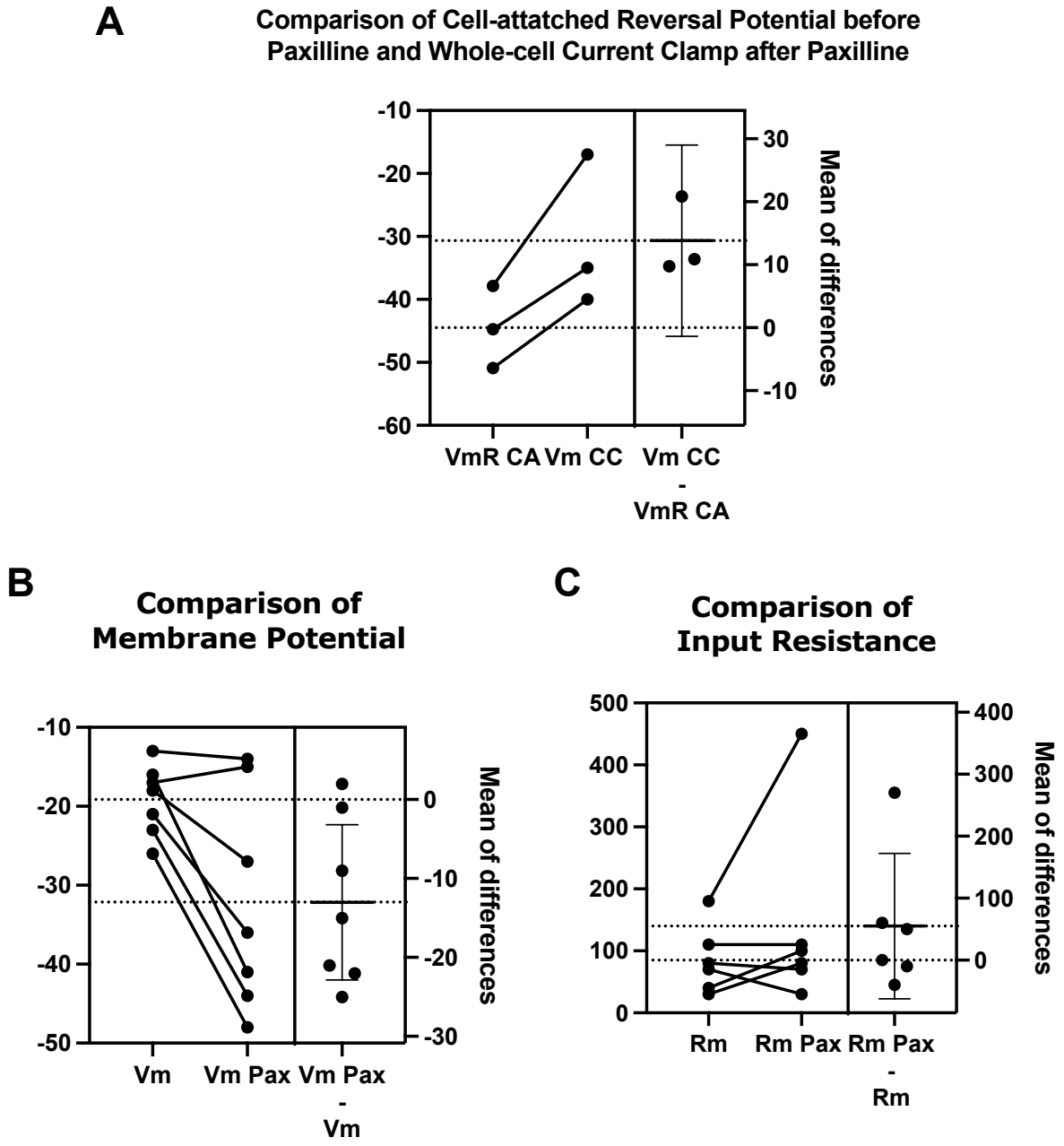


***Figure 13.*** Effect of 1 µM Paxilline on the membrane potential and input resistance before and after perfusion **A)** Comparison of cell attached reversal potential (VmR CA) before paxilline and the whole cell current clamp (Vm CC) after 1µM paxilline (p= 0.0594, n=3, paired t-test) **B)** Comparison of whole cell current clamp (Vm) before and after 1µM paxilline perfusion (Vm Pax). Paxilline caused hyperpolarization of the cell membrane potential by 13 mV. (p= 0.0178, n=7, paired t-test). **C)** Comparison of the whole cell input resistance before (Rm) and after 1 µM paxilline perfusion (Rm Pax). No significant effect is seen (p=0.2823, n=6, paired t-test). Data is shown as mean. *N* = 3-7. Experiments were performed in low [$Ca^{2+}$] pipette solution**.**

Figure 12 C-D shows that 200 µM quinine blocked BK activity, so I could not see the shift in a cell attached resting membrane potential, therefore the cell-attached reversal potential and the whole cell current clamp value were compared. Figure 14A shows that 200 µM of Quinine, had no significant effect on membrane potential ($p= 0.6541$, $n=4$, paired t-test). I then performed experiments where quinine was perfused in the whole cell to see its effect. Figure 14 B-C shows that in whole cell patches, the membrane potential and input resistance showed no significant effect ($p=0.2709$, $n=6$, paired t-test and $p=0.9521$, $n=6$, paired t-test) before and after perfusing with quinine.

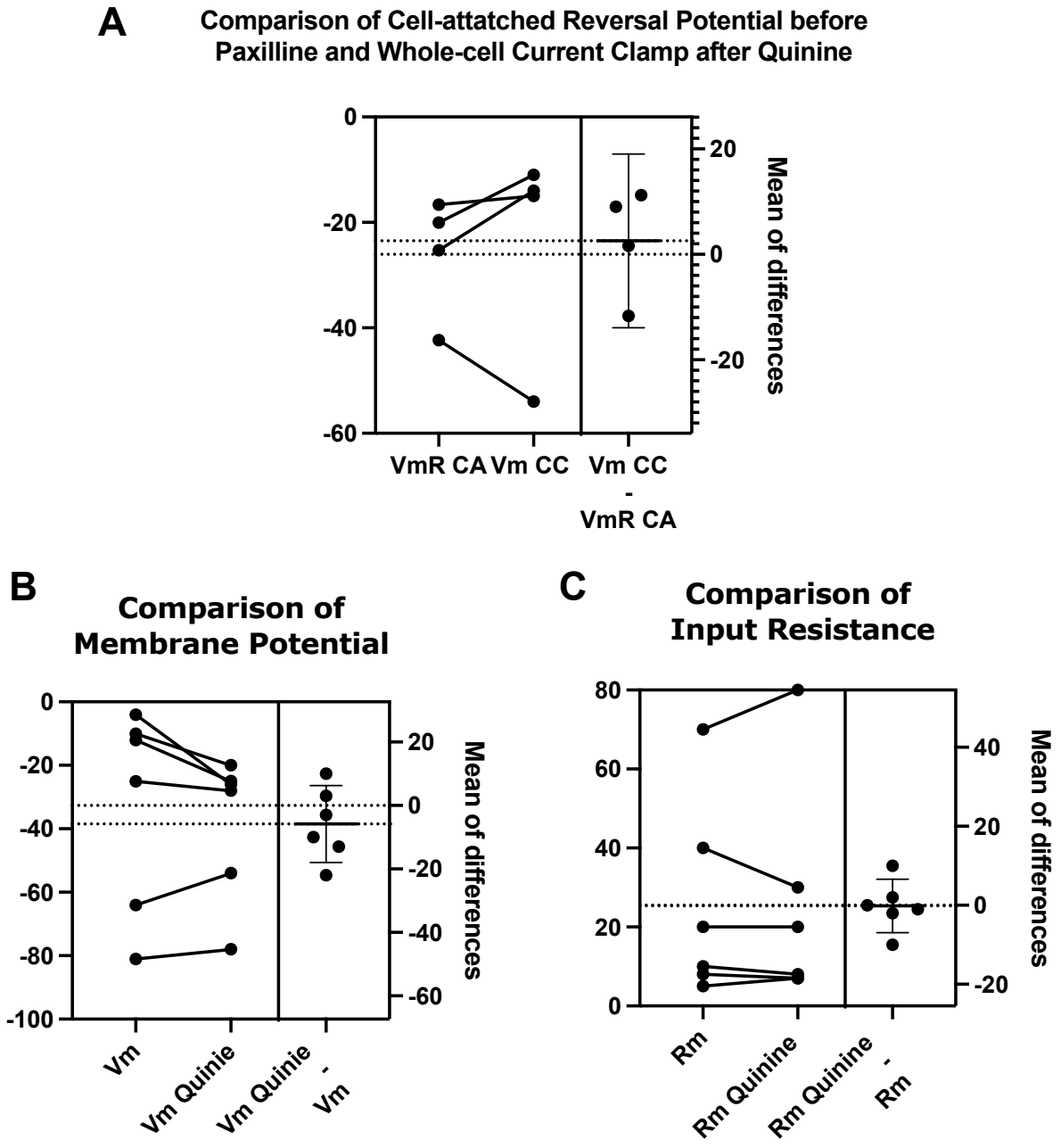


***Figure 14.*** Effect of 200 µM Quinine on the membrane potential and input resistance before and after perfusion **A)** Comparison of cell attached reversal potential (VmR CA) before quinine and the whole cell current clamp (Vm CC) after 200 µM quinine (p= 0. 6541, n=3, paired t-test) **B)** Comparison of whole cell current clamp (Vm) before and after 1µM quinine perfusion (Vm Pax). No significant effect is seen (p=0.2709, n=6, paired t-test). **C)** Comparison of the whole cell input resistance before (Rm) and after 200 µM quinine perfusion (Rm Pax). No significant effect is seen (p=0.9521, n=6, paired t-test). Data is shown as mean. *N* = 3-6. Experiments were performed in low [$Ca^{2+}$] pipette solution**.**

As shown in Figure 12 E-G, Isopimeric acid sustained BK activity, I compared the shift in cell attached resting membrane potential, using the cell-attached reversal potential. Figure 15 A shows that in cell attached patches, 20 µM of Isopimeric acid, had no significant effect on the resting membrane potential (p= 0. 1475, n=8, paired t-test) before and after perfusing with Isopimeric acid. Figure 15B shows no significant difference (p= 0.1211, n=8, paired t-test) was seen between the cell attached reversal potential and whole cell current clamp after perfusion of Isopimeric acid. Using one sample t-test, all 10 voltages were tested (0 mV - -90 mV) none gave a significant change in the mean amplitude difference from before and after perfusion of 20 µM of Isopimeric acid, suggesting it does not affect membrane potential.

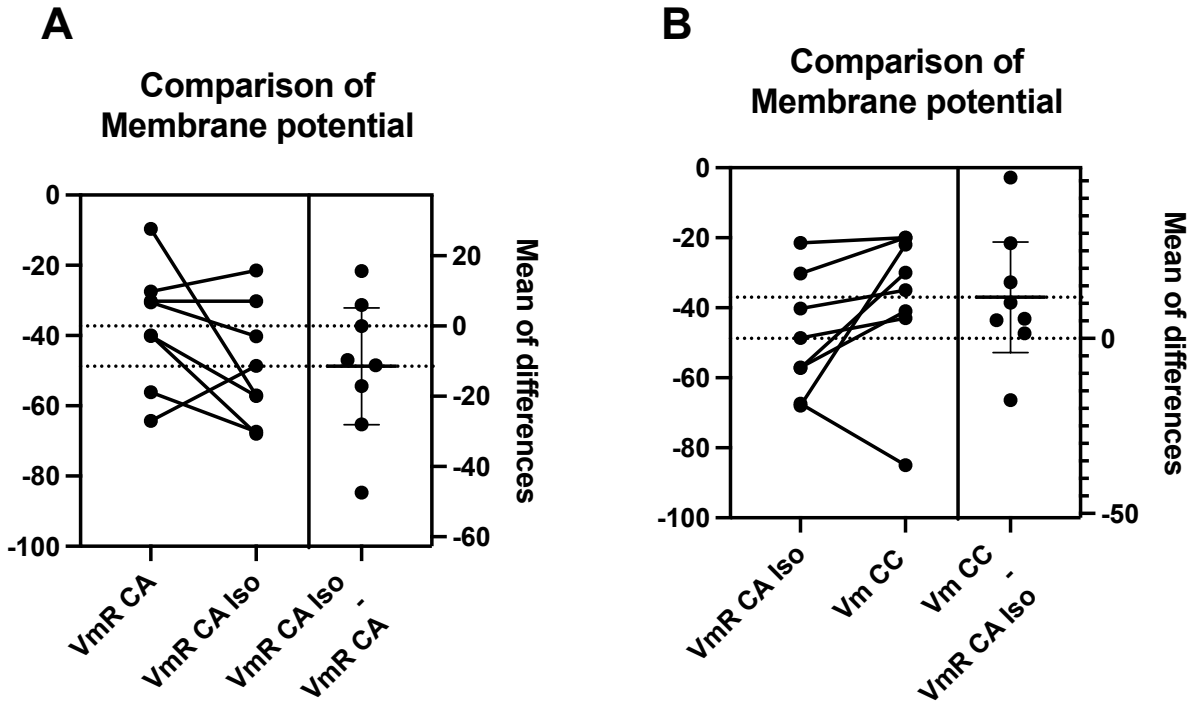


***Figure 15.*** Effect of 20 µM of Isopimeric acid on the membrane potential and input resistance before and after perfusion. **A)** Comparison of cell attached reversal potential before (VmR CA) and after (VmR CA Iso) 20 µM Isopimeric acid. No significant effect was seen (p= 0. 1475, n=8, paired t-test). **B)** Comparison of cell attached reversal potential (VmR CA Iso) and whole cell current clamp (Vm CC) after 20 µM Isopimeric acid. No significant effect is seen (p= 0.1211, n=8, paired t-test). Data is shown as mean. *N* =6. Experiments were performed in low [$Ca^{2+}$] pipette solution**.**

Figure 16 shows that in the whole cell, 1 mM TEA (Soroceanu, Manning and Sontheimer, 1999) showed a significant decrease by 9 mV (p=0. 0249, n= 16, paired t-test) in the membrane following

perfusing with 1 mM TEA. The input resistance showed a significant difference (p=0. 0135, n=16, Wilcoxon test) following perfusion with TEA.

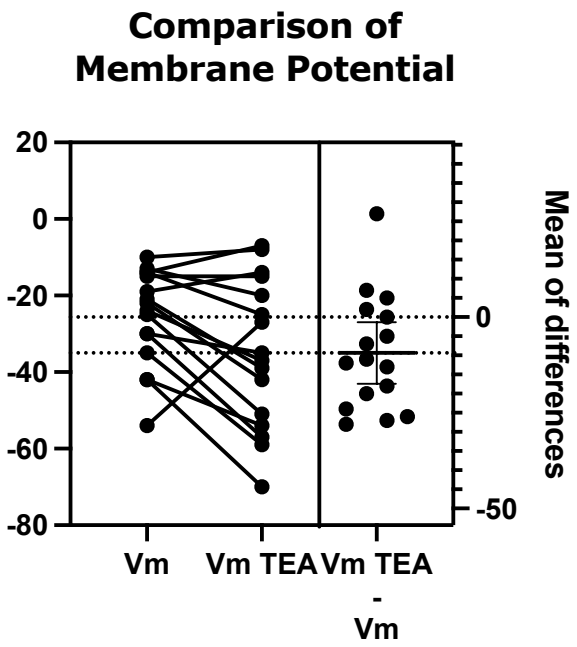


***Figure 16.*** Comparison of whole cell current clamp before (Vm) and after (Vm TEA) 1mM of TEA. A significant decrease by 9mV is seen (p=0. 0249, n= 16, paired t-test). Data is shown as mean. *N* =16. Experiments were performed in low [$Ca^{2+}$] pipette solution**.**

I performed control experiments to observe if perfusing had any effect on membrane potential and input resistance. Figure 17A shows that in cell attached control patches, no significant difference was seen in the resting membrane potential (p= 0. 6275, n=8, paired t-test) before and after perfusing with control Hanks. In Figure 17B no significant difference (p= 0. 1227, n=8, paired t-test) was seen between the cell attached reversal potential and whole cell current clamp after perfusion of Hanks. Figure 17 C-D shows that in whole cell patches, the membrane potential showed a significant effect (p=0.0067, n=7, paired t-test) before and after perfusing with Hanks. The membrane potential was 9 mv higher after perfusing with Hanks. The input resistance showed no significant effect (p=0.1996, n=7, paired t-test) following perfusion.

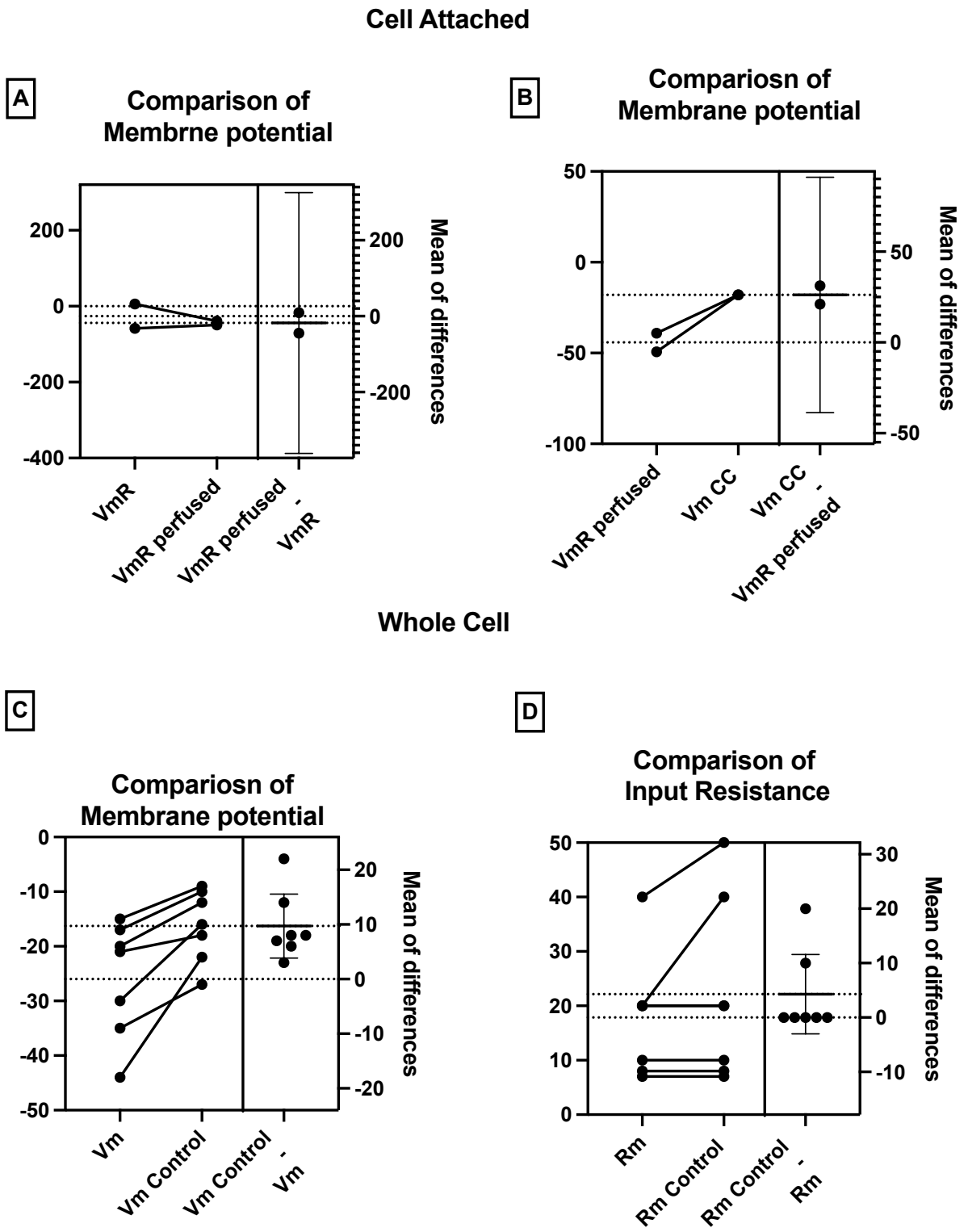


***Figure 17.*** Control experiments using vehicle Hanks on the membrane potential and input resistance before and after perfusion. **A)** Comparison of cell attached reversal potential of BK before (VmR) and after (VmR perfused) control Hanks. No significant effect was seen (p= 0. 6275, n=8, paired t-test). **B)** Comparison of cell attached reversal potential (VmR perfused) and whole cell

current clamp (Vm CC) after perfusion of control Hanks. No significant effect was seen (p= 0. 1227, n=8, paired t-test). **C)** Whole cell membrane potential before (Vm) and after (Vm Control) perusing with control Hanks. A significant effect was seen (p=0.0067, n=7, paired t-test). **D)** Whole cell input resistance before (Rm) and after (Rm Control) perusing with control Hanks. No significant effect was seen (p=0.1996, n=7, paired t-test). Data is shown as mean. *N* =6. Experiments were performed in low [$Ca^{2+}$] pipette solution**.**

Figure 18A shows the comparison of whole cell membrane potential using one-way ANOVA showed no significant effect in the difference between the membrane potential before and after perfusion of control (n=8) 200 µM Quinine (p=0.9870, n=6), 1 mM TEA (p=0.9936, n=16) and 1 µM Paxilline (p=0.7188, n=7). Figure 18B shows the comparison of whole cell reversal potential using one-way ANOVA showed no significant effect in the difference between the membrane potential before and after perfusion in control (n=8) and 200 µM Quinine (p=0. 9947, n=6), 1 mM TEA (p=0. 5186, n=16) and 1 µM Paxilline (p=0. 9992, n=7).

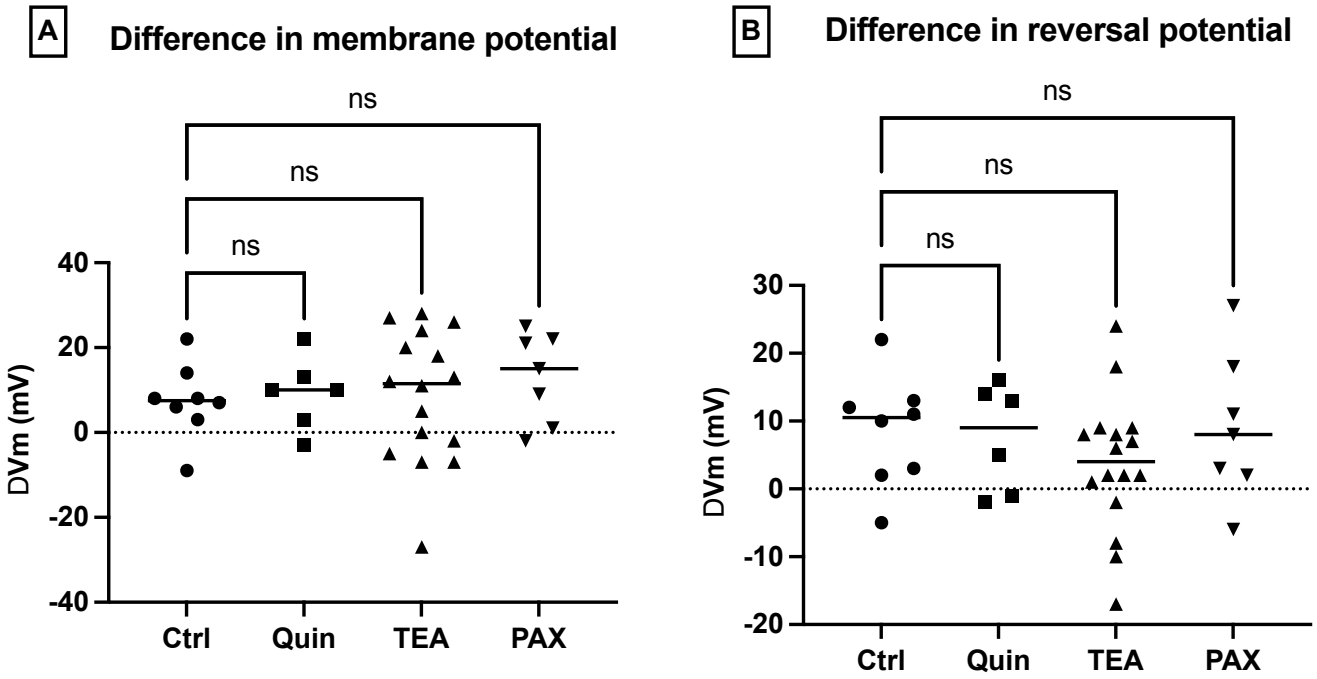


***Figure 18.*** Effect of blockers and activators of BK on membrane potential and reversal potential. **A)** Comparison of the difference in whole cell membrane potential measured with current clamp before and after perfusing with control (Ctrl), Quinine (Quin), TEA and Paxilline (PAX). No Significant differences were seen with 200 µM Quinine (p=0.9870, n=6), 1 mM TEA (p=0.9936, n=16) and 1 µM Paxilline (p=0.7188, n=7). **B)** Comparison of the difference in whole cell reversal potential before

and after perfusing with perfusing with control (Ctrl), Quinine (Quin), TEA and Paxilline (PAX). No Significant differences were seen with 200 µM Quinine (p=0. 9947, n=6), 1 mM TEA (p=0. 5186, n=16) and 1 µM Paxilline (p=0. 9992, n=7). Data is shown as mean. *N* =6-16. Experiments were performed in low [$Ca^{2+}$] pipette solution. All Statistical tests were by One-way ANOVA.

***Effect of different ions on membrane potential in SF188***

To investigate the ionic dependency of membrane potential, cell attached and whole cell patch clamp experiments were conducted with different ion compositions of Hanks. Experiments were conducted in the same manner as the drugs, with the Hanks being perfused for 2 minutes.
In cell attached patches in which $[K^+]_o$ was elevated to 50 mM by substitution of bath $Na^{+,}$ 5 out of 8 patches had inward currents > 5 pA at Vp = 0 indicative of BK. In Figure 19A no significant effect was seen on the resting membrane potential (p= 0.0648, n=4, paired t-test). Figure 19B shows that in whole cell, in which $[K^+]_o$ was elevated to 50 mM by substitution of bath $Na^+$, showed an 8 mV significant depolarization (p=0. 0016, n= 3, paired t-test). Figure 19C shows that the input resistance showed no significant difference (p=0. 7418, n=3, paired t-test) following perfusion with $K^+$ elevated Hanks.

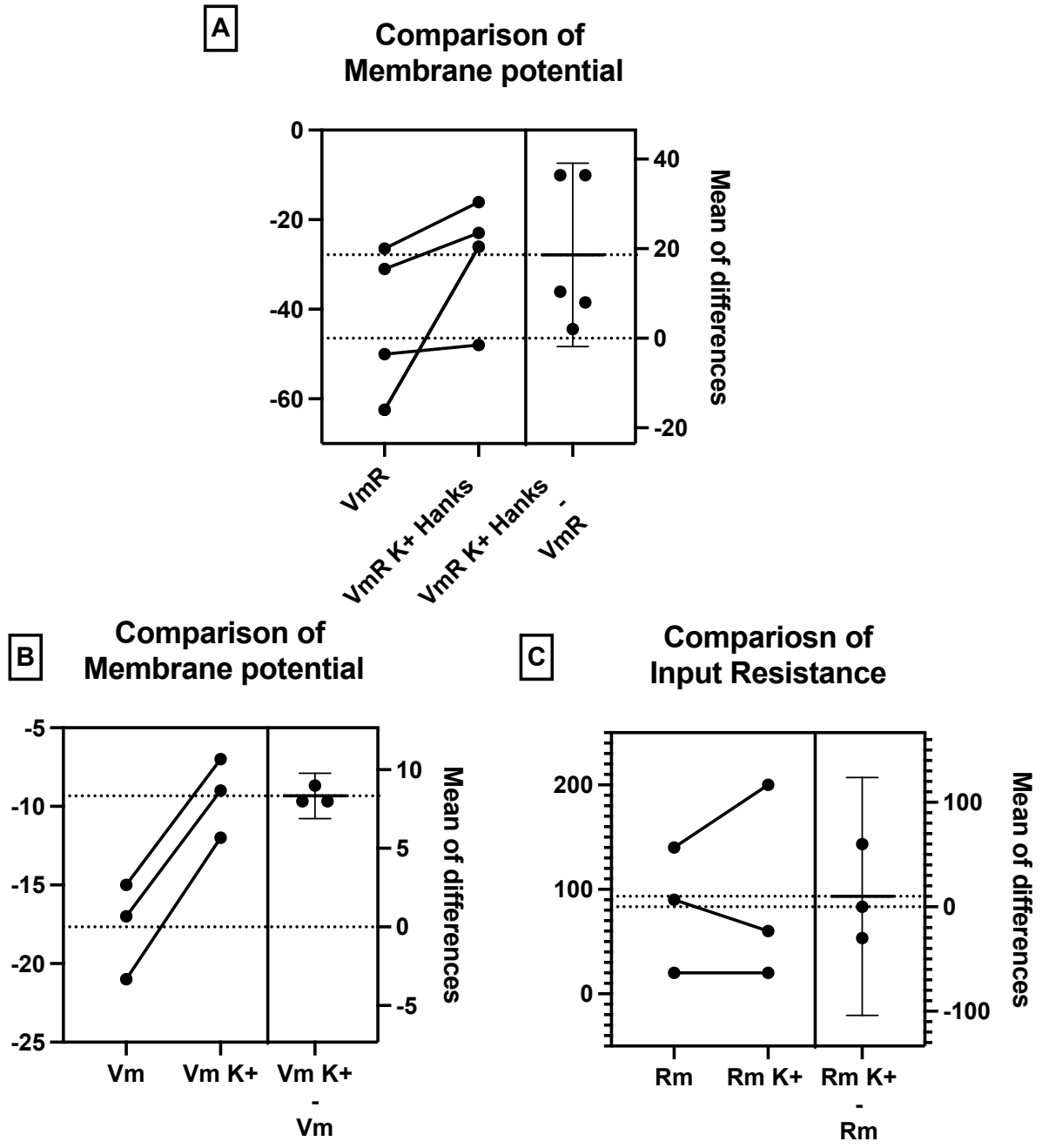


***Figure 19.*** Effect of $K^+$ Hanks, in which $[K^+]_o$ was elevated to 50 mM by substitution of bath $Na^+$ on the membrane potential and input resistance before and after perfusion. **A)** Comparison of cell attached reversal potential before (VmR) and after (VmR $K^+$ Hanks) $K^+$ elevated Hanks perfusion. No significant effect was seen (p= 0.0648, n=4, paired t-test). **B)** Comparison of whole cell current clamp before (Vm) and after (Vm $K^+$) $K^+$ elevated Hanks perfusion. An 8 mV significant depolarization was seen (p=0. 0016, n= 3, paired t-test) **C)** Comparison of the whole cell input resistance before (Rm) and after (Rm $K^+$) $K^+$ elevated Hanks perfusion. No significant difference was seen (p=0. 7418, n=3, paired t-test) Data is shown as mean. *N* = 3-4. Experiments were performed in low $[Ca^{2+}]$ pipette solution**.**

In cell attached patches in which $[Cl^-]_o$ was decreased to 8 mM by substitution of bath $Cl^-$ with $Na^+$ gluconate, out of 7 patches 3 had large inward currents > 5 pA at Vp=0 indicative of BK. Figure 20A shows that in cell attached patches, no significant effect was seen on the resting membrane potential (p= 0.068, n=2, paired t-test) before and after perfusing with $Cl^-$ free Hanks. Figure 20B shows that in whole cell patches, in which $[Cl^-]_o$ was decreased to 8 mM by substitution of bath $Cl^-$ with $Na^+$ gluconate $Cl^-$ Hanks showed no significant difference (p=0. 0610, n= 4, paired t-test) in the membrane potential before and after perfusing with $Cl^-$ free Hanks. Figure 20C shows that the input resistance showed no significant difference (p=0. 4950, n=4, paired t-test) following perfusion with $Cl^-$ free Hanks.

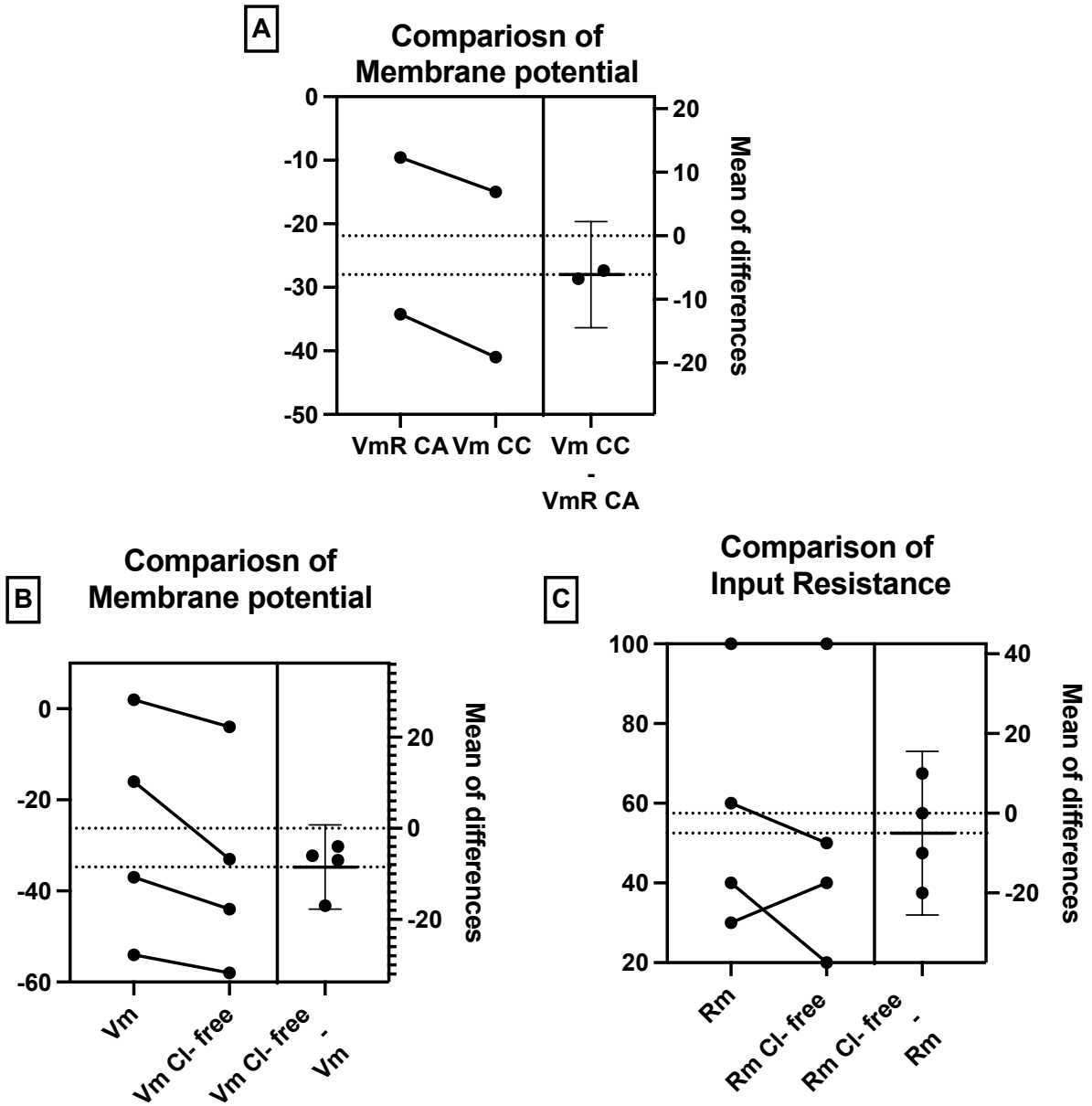


***Figure 20.*** Effect of $Cl^-$ free Hanks in which $[Cl^-]_o$ was decreased to 8 mM by substitution of bath $Cl^-$ with $Na^+$ gluconate, on the membrane potential and input resistance before and after perfusion. **A)** Comparison of cell attached reversal potential before (VmR CA) and whole cell current clamp after (Vm CC) $Cl^-$ free Hanks perfusion. No significant effect was seen (p= 0.068, n=2, paired t-test). **B)** Comparison of whole cell current clamp (Vm) before and after (Vm $C^{l-}$ free) $Cl^-$ free Hanks perfusion. No significant effect was seen (p=0. 0610, n= 4, paired t-test). **C)** Comparison of the whole cell input resistance before and after $Cl^-$ free Hanks perfusion. No significant effect was seen (p=0. 4950, n=4, paired t-test). Data is shown as mean. *N* = 2-4. Experiments were performed in low $[Ca^{2+}]$ pipette solution**.**

In cell attached patches perfused with $Na^+$ free Hanks, patches in which $[Na^+]_o$ was decreased to 100 mM by substitution of bath $Na^+$, out of 12 patches 2 had large inward currents > 5 pA at Vp = 0 indicative of BK. Figure 21A shows that in cell attached patches, in which $[Na^+]_o$ was decreased to 100 mM by substitution of bath $Na^+$, no significant effect was seen in the resting membrane potential (p= 0. 1890, n=2, paired t-test) before and after perfusing with $Na^+$ free Hanks. Figure 21B shows that in whole cell patches, $Na^+$ free Hanks showed significant hyperpolarisation by 8 mV (p=0. 0054, n= 10, paired t-test) in the membrane potential before and after perfusing with $Na^+$ free Hanks. Figure 21 C shows that the input resistance showed no significant difference (p=0. 9239, n=4, paired t-test) following perfusion with $Na^+$ free Hanks.

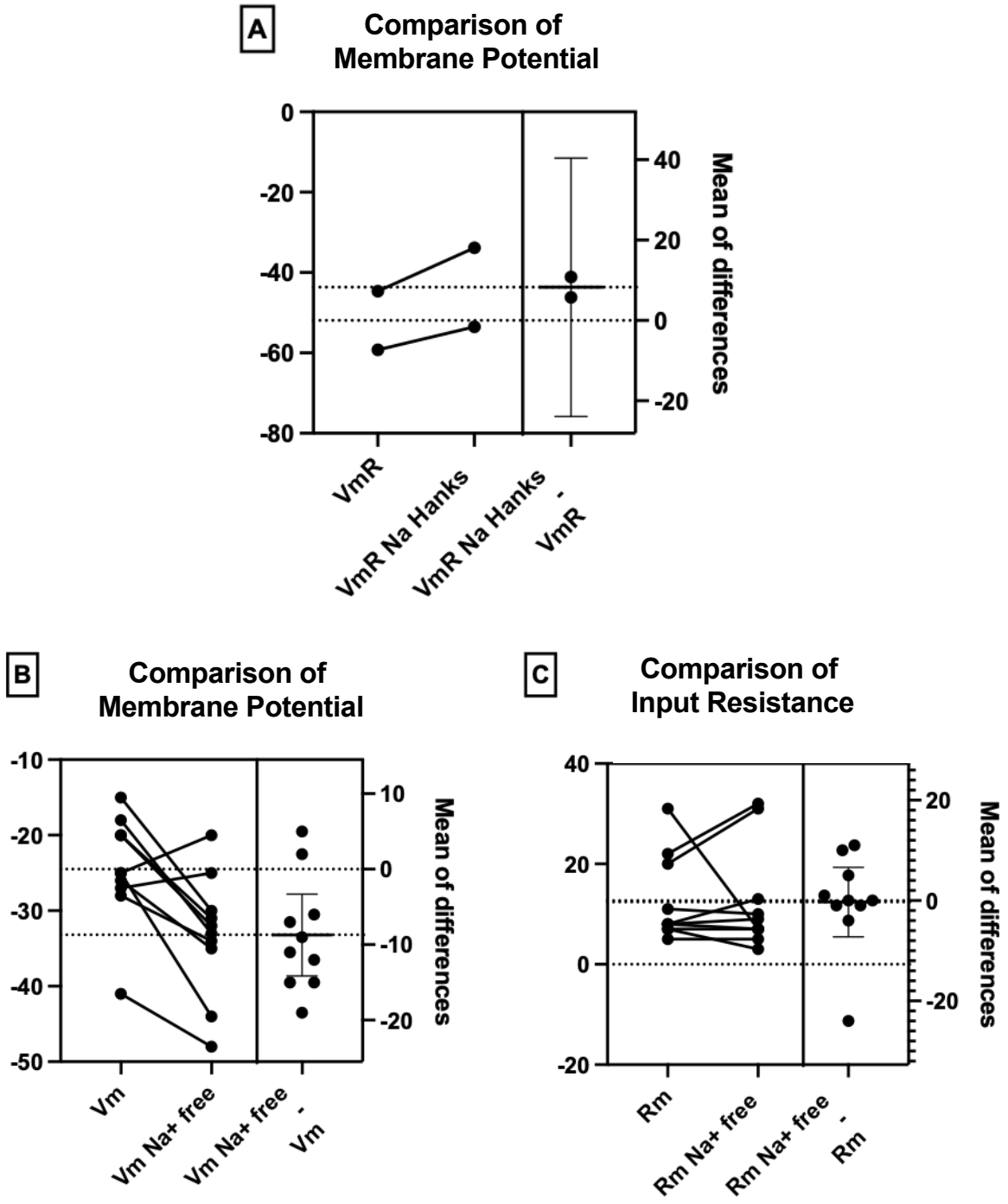


***Figure 21.*** Effect of $Na^+$ free Hanks on the membrane potential and input resistance before and after perfusion. **A)** Comparison of cell attached reversal potential before (VmR) and (VmR $Na^+$ Hanks) after $Na^+$ free Hanks perfusion. No significant effect was seen. (p= 0. 1890, n=2, paired t-test) **B)** Comparison of whole cell current clamp before (Vm) and after (Vm $Na^+$ free) $Na^+$ free Hanks perfusion. Ssignificant hyperpolarisation by 8 mV was seen (p=0. 0054, n= 10, paired t-test) **C)** Comparison of the whole cell input resistance before (Rm) and after (Rm $Na^+$ free) $Na^+$ free Hanks

perfusion. No significant difference was seen (p=0. 9239, n=4, paired t-test) Data is shown as mean. *N* = 2-10. Experiments were performed in low [$Ca^{2+}$] pipette solution**.**

Figure 22A shows the comparison of whole cell membrane potential measured with current clamp using one-way ANOVA showed no significant effect in the difference between the membrane potential before and after perfusion in control (n=8) high $K^+$ (p=0.0714 n=4), $Cl^-$free (p=0.9916, n=3) and low $Na^+$ Hanks (p=0.9720, n=10). Figure 22B shows the comparison of whole cell reversal potential using one-way ANOVA showed a significant effect in the difference between the membrane potential before and after perfusion in control (n=8) and high $K^+$ Hanks (p=0.0248, n=4) but no significant difference between control and $Cl^-$ free Hanks (p=0.9996, n=3 and low $Na^+$ Hanks (p=0.9995, n=10).

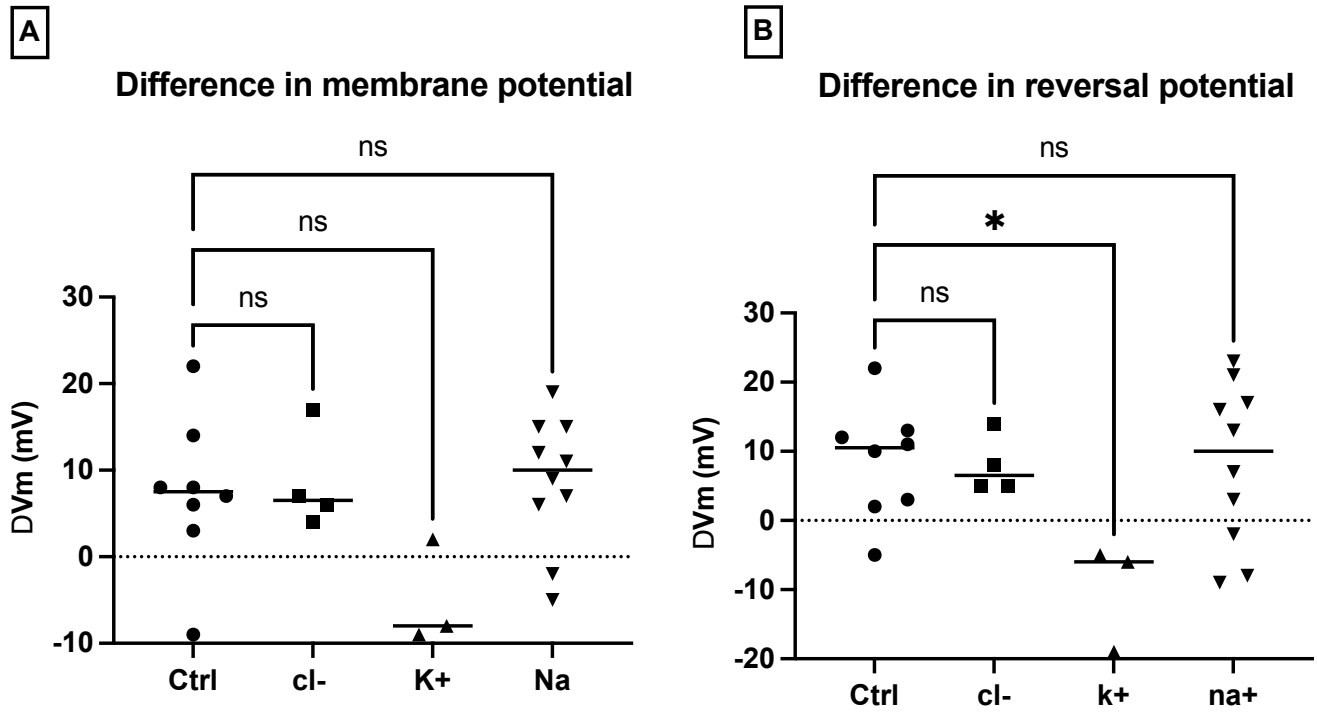


***Figure 22.*** Effect of different Hanks on membrane potential and reversal potential. **A)** Comparison of the difference in whole cell membrane potential measured with current clamp before and after perfusing with control (Ctrl), $Cl^-$ free Hanks ($Cl^-$), High $K^+$ Hanks ($K^+$) and low $Na^+$ Hanks ($Na^+$).No significant differences were seen with control (n=8) high $K^+$ (p=0.0714 n=4), $Cl^-$ free (p=0.9916, n=3) and low $Na^+$ Hanks (p=0.9720, n=10). **B)** Comparison of the difference in whole cell reversal potential before and after perfusing with control (Ctrl), $Cl^-$ free Hanks ($Cl^-$), High $K^+$ Hanks ($K^+$) and low $Na^+$ Hanks ($Na^+$). A significant difference was seen in the difference between the membrane

potential before and after perfusion in control and high $K^+$ Hanks (p=0.0248, n=4) but no significant difference between control and $C^{l-}$ free Hanks (p=0.9996, n=3 and low $Na^+$ Hanks (p=0.9995, n=10) was seen. Data is shown as mean. *N* =4-10. Experiments were performed in low [$Ca^{2+}$] pipette solution**.** All Statistical tests were by One-way ANOVA.

***GCE62***

To determine the channel's identity and biophysics in GCE62's, cell-attached single channel patch clamp was used. Figure 23A shows a representative single channel current-voltage relationship of BK in high calcium pipette solution. Figure 23B shows representative BK activity in a high calcium pipette solution. Single channel analysis revealed BK was spontaneously active in 2 out of 30 patches.

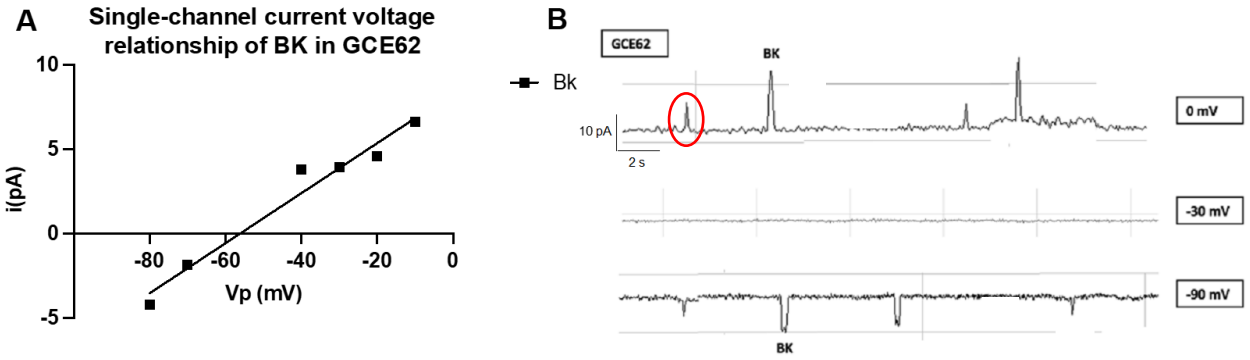


***Figure 23.*** BK is spontaneously active in GCE62's. **A)** Representative single-channel current-voltage relationship of BK channel measured on a GCE62 cell. Each point is the median of 5 individual amplitude determinations. A solid line is fit by linear regression. In this case, the slope of BK is 148 pS and Vmr is -56.27 mV. **B)** Representative activity of BK in a GCE62 cell in high calcium pipette solution. Downward flickers are characteristic of BK channel openings. Note: The red circle indicates an unidentified $K^+$ permeable channel.

Figure 24A shows that in whole cell, the membrane potential showed no significant difference -47 ± 5.6.8 mV (n=5, p=0.5426, unpaired t-test) in high [$Ca^{2+}$] pipette solution compared to low [$Ca^{2+}$] in the pipette solution -41.38 ± 5.6 mV (n=5). Figure 24B shows that in whole cell, the input resistance

showed no significant difference 168 ± 16.3 MΩ (n=4, p=0.8628, unpaired t-test) in high [$Ca^{2+}$] pipette solution compared to low [$Ca^{2+}$] in the pipette solution 184 ± 16.3 MΩ (n=8).

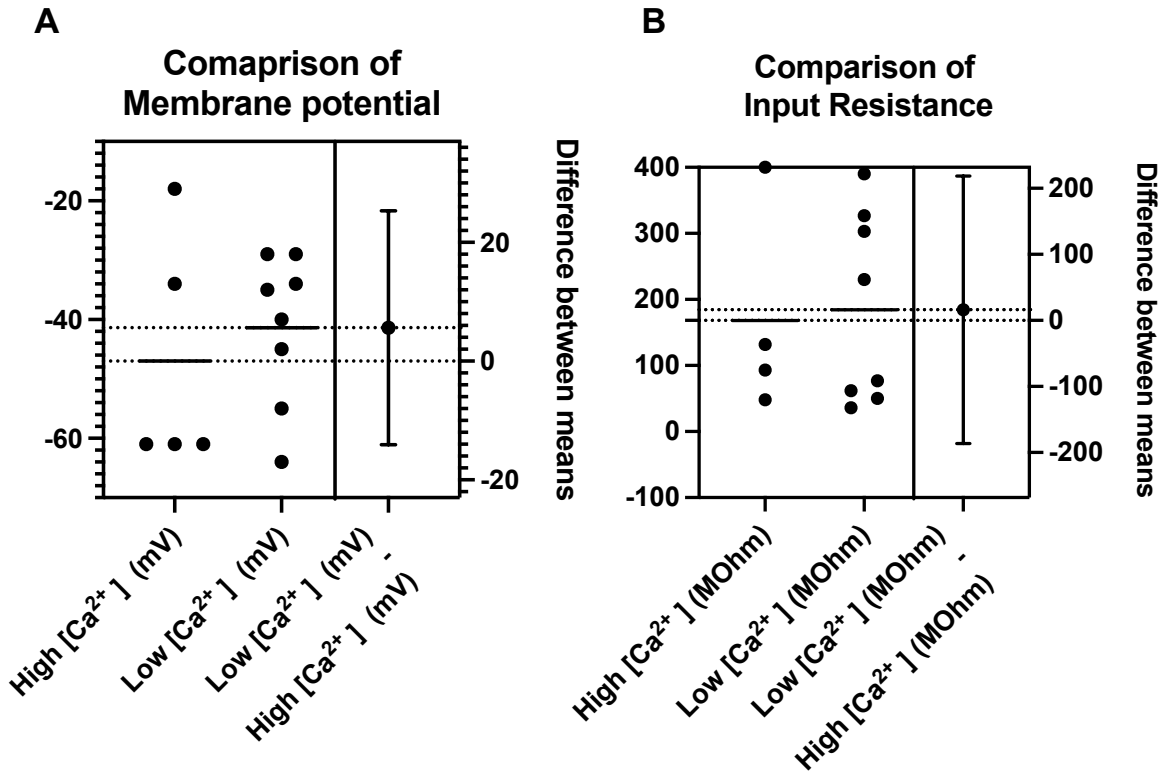


***Figure 24***. Whole cell membrane potential and input resistance in high [$Ca^{2+}$] and low [$Ca^{2+}$] pipette solution in GCE62's. **A)** Comparison of membrane potential measured from the current clamp in different cells with high and low [$Ca^{2+}$] in the pipette solution. No significant difference was seen -47 ± 5.6.8 mV (n=5, p=0.5426, unpaired t-test) **B)** Comparison of input resistance measured from different cells with high and low [$Ca^{2+}$] in the pipette solution. No significant difference was seen 168 ± 16.3 MΩ (n=4, p=0.8628, unpaired t-test). Data is shown as mean. *N* = 4-8

Figure 25 shows no significant difference (p=0.0926, unpaired t-test) was seen between the membrane potential measured from the current clamp of SF188 (n= 45, -35.09 ± -8.45 mV) and GCE62 (n= 13, -43.54 ± -8.45 mV).

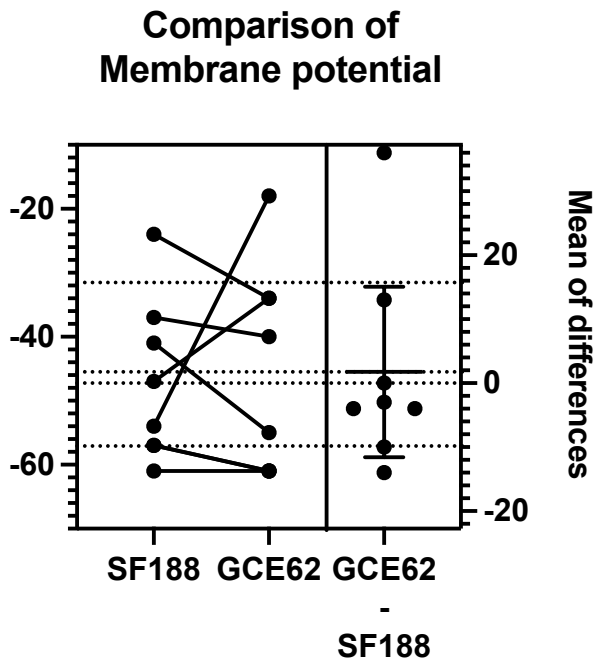


***Figure 25***. Comparison of membrane potential measured from the current clamp of SF188 and GCE62. Paired t-test shows no significant difference between SF188 (n= 45, -35.09 ± -8.45 mV) and GCE62 (n= 13, -43.54 ± -8.45 mV). Data is shown as mean. was seen *N* = 13-45

***Calcium Imaging***

To measure intracellular calcium levels in SF188's, I used Fluo-4 imaging to under different conditions to measure the cells response. Initially, cells were continuously perfused with Hanks solution, followed by $Ca^{2+}$ free Hanks, $Ca^{2+}$ free Hanks and glutamate, $Ca^{2+}$ free Hanks, wash, Glutamate then Triton (Figure 8). Concentrations of 100 nM, 1 mM, 10 mM and 100 mM glutamate were used, only cells which elicited a glutamate response ≥ 10% of the basal value were selected for analysis, and the steady state and peaks were analysed. Figure 26A shows a representative image of SF188 cells loaded with the dye. Figure 26B shows trace details of 5 representative cells responding to 10 mM glutamate. Out of the 5, 3 responded under $Ca^{2+}$ -free glutamate and all responded to glutamate. From the 73 cells in total, 18 cells responded to $Ca^{2+}$-free glutamate and 100% of cells responded to glutamate.

Analysis showed a significant effect between peaks of $Ca^{2+}$ free and $Ca^{2+}$ free 100 nM glutamate (p= 0.0202, n=38, Friedman test), $Ca^{2+}$ free 100 nM glutamate and 100 nM glutamate (p= 0.0116, n=38, Friedman test) (Figure 27A), $Ca^{2+}$ free and $Ca^{2+}$ free 1 mM glutamate (p= 0.0020, n=131, Friedman test), wash and 1 mM glutamate (p= <0.0001, n=131, Friedman test)and $Ca^{2+}$ free 1 mM glutamate and 1 mM glutamate (p= <0.0001, n=131, Friedman test) (Figure 27B), although these statistics

suggests a significant effect, the effect seen is a decrease in intracellular calcium following glutamate perfusion, which is the opposite of expected.

10 mM data was parsed: cells which did not respond to glutamate were excluded, both data sets were analysed (Figure 27 C-D), which revealed a significant difference in the peaks between wash and 10 mM glutamate (p= <0.0001, n=125, Friedman test) (Figure 27D), whereas the parsed data revealed a significant difference between peaks of $Ca^{2+}$ free and $Ca^{2+}$ free 10 mM glutamate (p= 0.0078, n=86, Friedman test), wash and 10 mM glutamate (p= <0.0001, n=86, Friedman test) and $Ca^{2+}$ free 10 mM glutamate and 10 mM glutamate (p= 0.0001, n=86, Friedman test) (Figure 27D). Finally, Figure 27E shows a significant difference between peaks of wash and 100 mM glutamate (p= 0.0008, n=116, Friedman test).

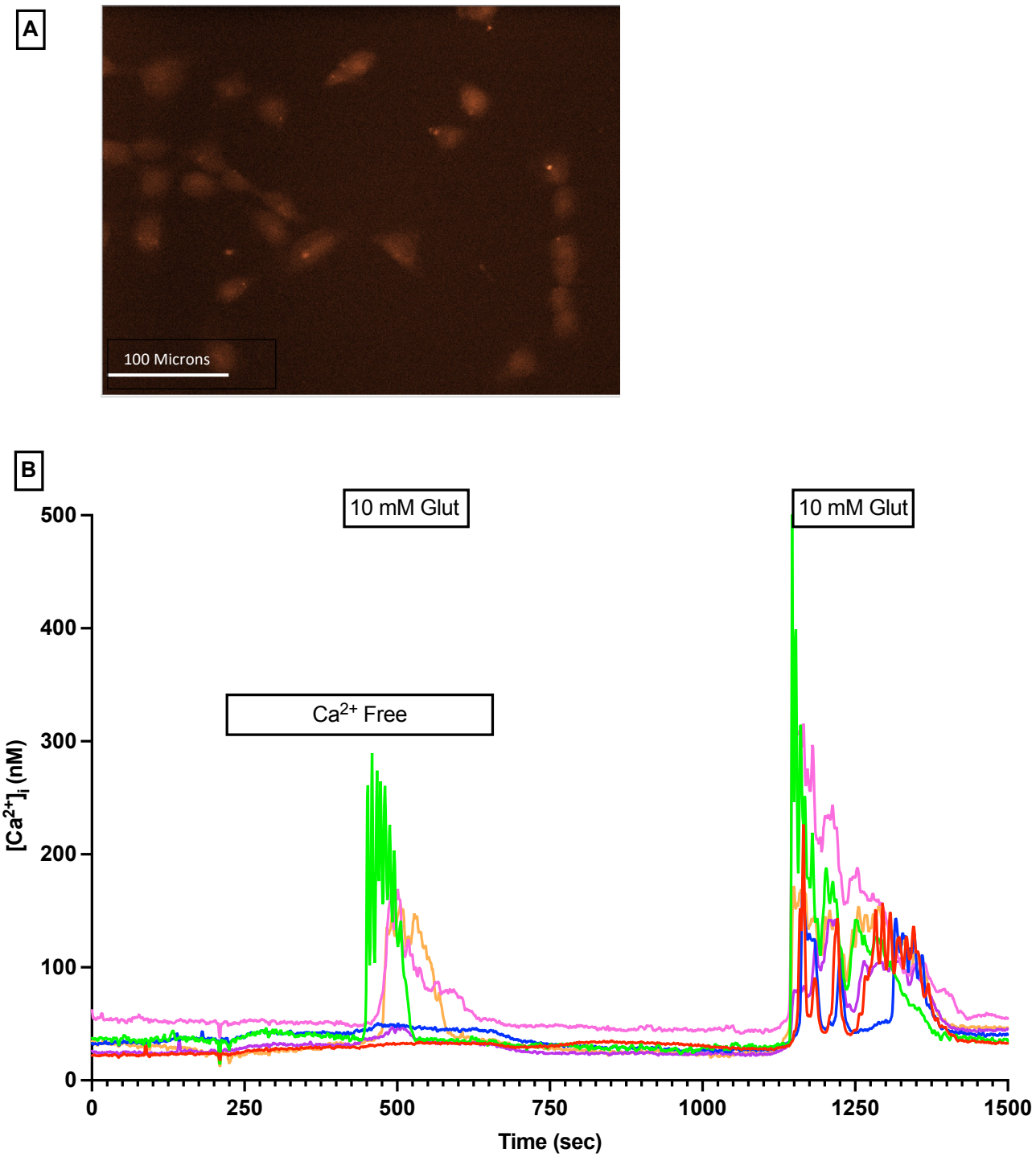


***Figure 26.*** Calcium imaging in SF188 cells. **A)** Representative image of SF188 cells stained with Fluo-4 AM dye. Cells were loaded for 40 minutes at room temperature. Cells are continuously illuminated at an excitation wavelength of 450-490 nm with the lowest light intensity that gives a detectable fluorescent signal without photobleaching. The emitted light is filtered at 515-565 nm. **B)** Representative recording of intracellular $Ca^{2+}$ for 5 SF188 cells in response to 10 mM glutamate in the absence and presence of extracellular $Ca^{2+}$. Out of the 5, 3 responded under $Ca^{2+}$-free glutamate and all responded to glutamate.

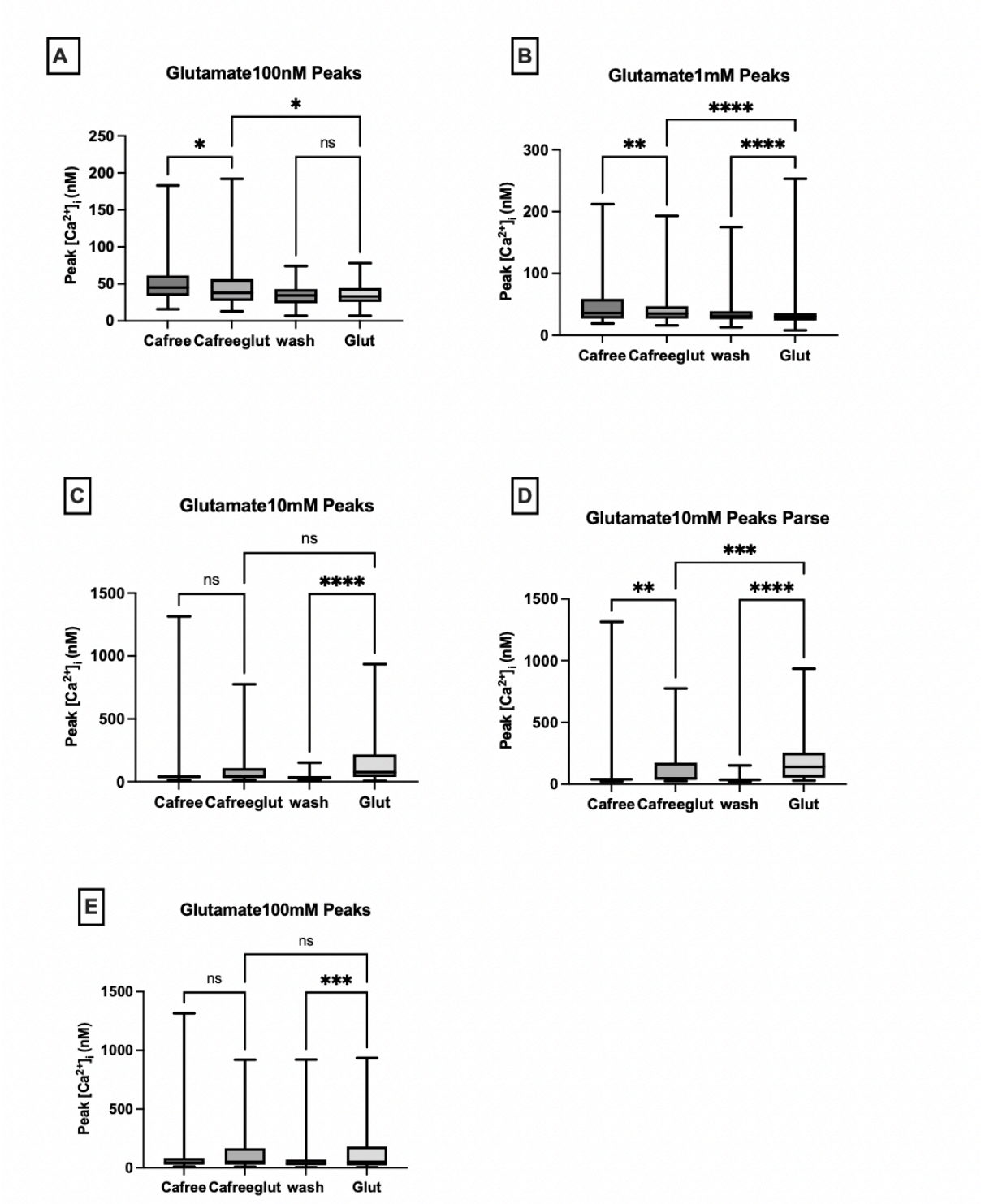


***Figure 27***. Effect of different concentrations of glutamate on calcium response in SF188 cells. **A)** Peaks of calcium response to 100 nM $Ca^{2+}$ -free glutamate and 100 nM glutamate **B)** Peaks of calcium response to 1 mM $Ca^{2+}$ -free glutamate and 1 mM glutamate **C)** Peaks of calcium response to 10 mM $Ca^{2+}$ -free glutamate and 10 mM glutamate. **D)** Parse data of 10 mM glutamate peaks, cells which did not respond were excluded peaks of calcium response to 10 mM $Ca^{2+}$ -free glutamate and 10 mM glutamate. **E)** Peaks of calcium response to 100 mM $Ca^{2+}$ -free glutamate and

10 mM glutamate. Absolute [Ca $^{2+}$ ]$_i$ is reported as an absolute peak from baseline. Data is shown as mean± SEM. *N* = 38-131. All Statistical tests were by Friedmans the *s indicates significance. *p ≤ 0.05, **p ≤ 0.01, ***p ≤ 0.001, **** p ≤ 0.0001.

Finally, Figure 28 shows one-way ANOVA comparing the intracellular calcium response of the different concentrations of glutamate. This revealed a significant difference between 100 nM and 1 mM (p= <0.0001) 100 nM and 10 mM (p= <0.0001), 100 nM and 100 mM (p= <0.0001), 1 nM and 10 mM (p= <0.0001), 1 mM and 100 mM (p= <0.0001) and 10 mM and 100 mM (p= 0.0005) Results also indicate, as concentration of glutamate increases, the concentration of intracellular calcium also increases.

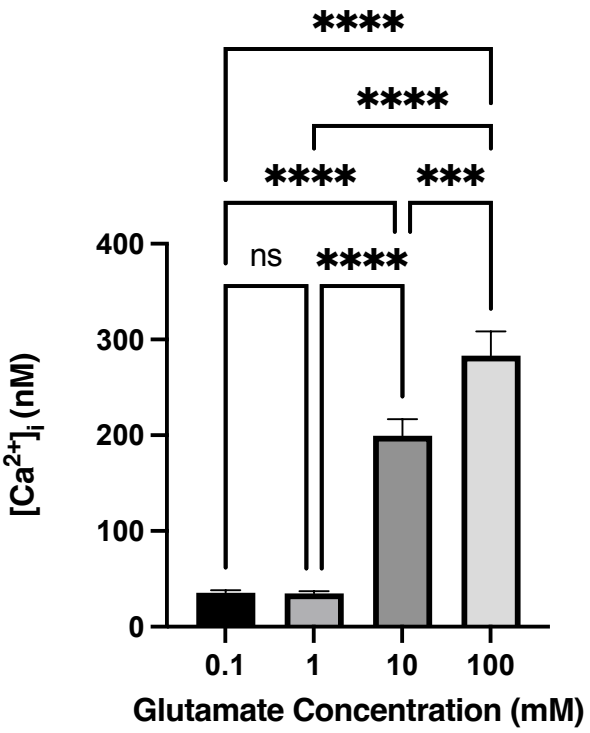


***Figure 28***. Comparison of peak calcium response to different concentrations of Glutamate in the presence of bath $Ca^{2+}$. Data is shown as mean± SEM. *N* = 269. Statistical test was by One-way ANOVA.

***Discussion***

***Identification of the BK channel***

From cell attached electrophysiology I have demonstrated the existence of a channel with properties characteristic of BK in SF188 and GCE62 cells. This was identified by the slope conductance observed in these cells, these were calculated using the slope of the linear current-voltage curve. Using the frequency distribution of 27 patches, I identified two slope conductance of around 124 to 215 pS, this electrophysiological profile is consistent with the expected conductance of 100-300 pS in BK (Lee and Cui 2010). Similar BK slope conductance's in the range of 200 – 250 pS were also found in cholinergic presynaptic nerve terminal (210 ± 7 pS) (Sun et al. 1999, neonatal rat intracardiac ganglion neurons (207 ± 19 pS ) (Franciolini et al. 2001), cultured rat melanotrophs, (~ 190 pS) (Kehl and Wong 1996),

cerebrovascular smooth muscle cells (207 ± 10 pS) (Wang and Mathers 1993), cultured rat superior cervical ganglionic neurones (~ 200 pS ) (Smart 1987), rat hippocampal neurons maintained in culture (220 pS) (Wann and Richards 1994) and rat hippocampal CA1 pyramidal neurons (245.4 pS) (Gong et al. 2001) in 140 – 150 mM of potassium in the pipette solution, which is similar to that used in this study. This is in accordance with Sun et al. 2004, who reported a BK slope conductance of 120.7 ± 8.8 pS in inside out patches in *Xenopus* motor nerve terminals. In cell-attached patches, they report a slope conductance of 78.3 ± 6.2 pS, however, they suggest that the lower value could be a result of internal $Na^+$, partially blocking cell-attached channels.

The identity of BK was also confirmed using pharmacology, I found that 1 µM paxilline and 200 µM Quinine completely abolished BK activity following perfusion. No channels were present during experiments with TEA, its effect on blocking the channel could not be observed. The effect of 20 µM Isopimeric acid on BK channel activity could not be quantified due to the absence of channels at different voltages, hence I could not see the effect on NPo. Paxilline is a widely used inhibitor, that is highly selective for BK channels ($IC_{50}$ = 2-50 nM) (Dorte Strøbæk et al., 1996, Wulff and Zhorov, 2008, Yu et al., 2016). In human glioblastoma cell lines, DBTRG (Wondergem and Bartley 2009) and U251 MG (Abdullaev et al. 2010), 2 µM of paxilline was shown to abolish whole cell BK currents. Although quinine is a non-selective potassium channel blocker, in the review on BK blockers by Yu et al., 2016, quinine is characterised to have BK channel blocking properties. Several studies have demonstrated its capability of blocking BK channels; 50µm of quinine blocked single channel BK activity in an open channel block manner in neonatal rat intra cardiac ganglion neurons (Franciolini et al. 2001). Furthermore, Bokvist et al. 1990 reported that in pancreatic beta cells, 20 µM did not decrease channel amplitude but instead decreased channel openings in rat pancreatic beta cells, however in this study a ten-fold increase in concatenation of 200 µm completely abolished channels. Although in the present study, I couldn't see the effect of TEA on BK channel activity due to the absence of channels, TEA is a well-known blocker of potassium channels, with capabilities of blocking BK in a voltage-dependant manner ($IC_{50}$ = 250 µM) (Ransom, Liu and Sontheimer, 2002, Yu et al., 2016). A range of concentrations of TEA has been demonstrated to block BK channels; 50 and 200 µM in neonatal rat intra cardiac ganglion neurons (Franciolini et al. 2001), 1 mM in guinea-pig urinary bladder myocytes (Herrera and Nelson 2002) and 10 mM in the glioblastoma cell line D54 MG (Ransom et al. 2002). Moreover, I used a BK channel activator, Isopimeric acid at a concentration of 20 µM to see its effect on BK activity. Isopimeric is highly selective for BK with an

$EC_{50}$ of 7.8 µM (Wu et al., 2014b). Although I could not see the effect of Isopimeric acid on BK channel activity in the present study, others such as Henney et al. 2009 saw that 10 µM of Isopimeric acid increased BK channel activity by 34% in human osteoblasts. Henney et al. 2009, also reported BK being blocked by paxilline and TEA. My results compared to the data available in the literature, allow us to confirm the identity of the channel as BK.

The existence of BK is well established in glioblastoma, quantitative RT-PCR has revealed the existence of BK in glioma cell lines U251 MG and U87 MG as well as a primary glioblastoma sample. The functionality of BK cells was also confirmed using whole cell electrophysiology. (Abdullaev et al. 2010). Immunoblotting revealed that BK channel expression is upregulated in glioblastoma cell lines U251 MG and D54 MG with a correlation between BK channel expression and glioblastoma malignancy grade (Liu et al. 2002). Edalat et al. 2016 examined the glioma cell line T98G and U-87MG-Katushka. The experiments performed were conducted in a similar manner to the present study. From single channel recordings, they report a depolarisation dependant increase in the open probability of the channel, which is a typical characteristic of BK channels, this is in accordance with what was observed in the present study. We observed a voltage-dependent open probability, as the membrane potential depolarised, an increase in the probability of open channels was seen. Edalat et al. 2016 also found in whole cell recordings, large outward currents were abolished by paxilline. This differs from the findings presented here. In the present study, paxilline did not block whole cell current but rather increased it, however, BK currents were abolished in cell attached patches. A possible explanation for this might be that in my study, BK seems prevalent and activated by the act of cell attached patching, seemingly by the stretch or suction of the pipette, however in whole-cell patches, BK makes a very little contribution, hence paxilline did not block the whole cell currents in our study. The electrophysiology data from U251 glioma cell lines presented by Hoa et al. 2007 are in accordance with those reported in my study, BK was present in single channel studies with a slope conductance of 150 pS. In combination, the electrophysiology, pharmacology data and the voltage-dependant open probability in this study are consistent with those across the literature, in both glioblastoma cell lines and other cell lines.

Furthermore, a smaller unidentified $K^+$ permeable channel was seen in the present study, in both SF188s and GCE62s. The channel had a slope conductance ranging from 80 – 100 pS and was attributed to being $K^+$ permeable as it reversed in a similar manner to BK in the single channel

studies (Ko et al., 2007). However further investigations are required to validate the identity of the channel.

***Predicting the membrane potential using cell attached I-V***

Using the cell-attached single channel data I was able to predict the membrane potential of the SF188 cells, by creating a current-voltage curve and using the reversal potential. This method of measuring membrane potential provides an alternative method which does not compromise the cell membrane integrity and prevents the development of leak and cell dialysis in which the pipette solution alters the ionic composition of the cytoplasm (Cota, 1986, Smith, Ashcroft and Rorsman, 1990). The estimations were based on the assumption that the currents were potassium selective and that the potassium concentration (140mM) was equal between the pipette and cytoplasm. The assumption of the currents being potassium selective is supported by several studies on BK channels in other cell models support this idea. For example, Findlay 1984 observed large outwards currents which they had identified as BK in cell-attached and excised inside out patches in acinar cells. When these were exposed to ion gradient which were quasi-physiological and they replaced the potassium in the pipette solution with rubidium, the currents were abolished, and considering no chloride gradient was observed they were able to conclude that the channel is highly selective for potassium. Similar methods were used by Gallacher and Morris 1986 in acinar cells. The potassium in the pipette was replaced with sodium they also showed it is selective to potassium. They observed rectification at negative membrane potential in the current-voltage relationship of cell-attached potassium currents. Had they been selective for sodium, a linear relationship would have been observed. They also found that the extrapolated reversal potential was -90 mV.

If we assume that in my experiment the intracellular concentration of potassium in the cytoplasm was similar to that of the potassium concentration in the pipette, we can assume that the potassium current should reverse direction when the patch has a potential of zero, at this point the pipette holding potential would theoretically be equivalent and opposite to that of the cell's resting membrane potential. Using this approach, I was able to estimate a mean resting potential of -34.9 ± 2.37 mV from 21 cell attached patches. In comparison, the measured whole cell current clamp value of the cells was -35.09 ± 2.35 mV. I found no significant difference between the two methods of measuring membrane potential. This is promising as it shows the reversal potential of BK in cell

attached patches appears to be an accurate non-invasive measure of the resting membrane potential of SF188 cells.

A similar approach was also reported by Verheugen et al. 1995 who found that in human T lymphocytes, the reversal potential of cell attached potassium currents was an accurate quantitative measure for membrane potential with a high $K^+$ pipette solution. However, slightly different results were observed by Fricker et al. 1999, in cell attached experiments of CA1 pyramidal cells and interneurons of rat hippocampal slices. Similar to the present experiment they used the reversal potential of potassium currents to estimate membrane potential. However, in their experiments, the cell attached membrane potential was 13 mV more hyperpolarised than the whole cell membrane potential. A hyperpolarised membrane potential in cell attached compared to whole cell was also reported by Verheugen et al. 1999, who applied the same method in interneurons in hippocampal brain slices as well as Tyzio et al. 2003 in CA3 hippocampal pyramidal cells. These authors suggest that the difference in membrane potential is likely to be related to the existence of the Donnan junction potential. This is a phenomenon that occurs as a result of the difference in Galvani potential that occurs as a result of the Donnan equilibrium in which the distributions of ion species differed between two ionic solutions that have been separated by a semi-permeable membrane, which in this case is the cell membrane. The act of going whole cell causes direct contact between the cytoplasm and the pipette solution causing a Donnan junction potential between the cytoplasm and pipette solution. This results in the whole cell membrane potential to be depolarised (Gokturk et al. 2022, Verheugen et al. 1999). However, Verheugen et al. 1999 found that after 20 minutes of going whole cell, the potassium current shifted by about -15 mV, which was the initial difference between the cell attached membrane potential and the whole cell membrane potential. All three authors concluded that if you consider the junction potential, the cell attached method is accurate at non-invasively measuring membrane potential.

***Effect of BK on membrane potential***

I then explored the role of BK on membrane potential in standard whole cell. When measured with a high calcium pipette solution (2.6 mM), the membrane potential was 16.8 mV more negative in comparison to low calcium (<35 nM). High calcium in the pipette increases BK activity which in turn increases the permeability of potassium ions leading to hyperpolarisation of the membrane

potential in SF188 cells. Hyperpolarisation of the membrane by BK activation has been observed in other cells which have BK. For example in airway smooth muscles, 8,9 and 14,15 epoxyeicosatrienoic acid hyperpolarised the membrane potential by -12 ± 3,5 mV and -16 ± 3 mV respectively, by activation of BK channels (Benoit et al., 2001). Similarly, hyperpolarisation of the membrane potential in neuroblastomas was also reported by Park et al., 2010, however, the degree of hyperpolarisation was not stated. I found that there was no effect on the input resistance. When BK channels are active in a cell, they should cause a decrease in input resistance like that observed by Whitt, Montgomery, and Meredith, 2016 and Meredith et al., 2006. Although my results suggest a decrease, it is not significant.

Given that the channels were active in cell-attached patches, I wanted to explore how BK would affect the membrane potential. For cell attached experiments I used the reversal potential of cell attached current voltage before perfusing with BK selective drugs and compared it to the current clamp value after BK was blocked. In SF188's the cell attached data suggests that the BK activator Isopimeric acid had no effect on the membrane potential in cell attached and whole cell, which could be due to the fact that BK maybe already maximally activated, such that Isopimeric acid had no further effect. Paxilline depolarised the membrane potential however this was not significant. In whole cell, paxilline caused a hyperpolarisation by 13 mV. This is somewhat surprising as my results indicated that paxilline caused depolarisation in cell attached. It is possible that the membrane potential could shift due to cell dialysis (Cota, 1986, Smith, Ashcroft and Rorsman, 1990). The input resistance showed no changes following perfusion of any of the drugs. Kryshtal', Nesin and Shuba, 2007 showed that membrane potential is not controlled by BK in smooth muscle cells as 1 mM paxilline did not affect membrane potential when measured with the amphotericin B perforated patch-clamp technique. Quinine had no effect on the membrane potential in cell attached and whole cell even though it blocked Bk; evidence that suggests perhaps that BK is not involved in the control of membrane potential as I initially thought where the effect of high calcium in whole cell is an ionic effect as mentioned earlier. I found that the concentration of TEA hyperpolarised the whole cell membrane potential by 9 mV, which was in contradiction to that observed by Jospin et al., 2002 who reported that the concentration of TEA depolarised membrane potential in body wall muscle cells from *Caenorhabditis elegans.* My analysis showed significant changes in the membrane potential and input resistance suggesting that perfusion with concentration TEA blocked basal potassium permeability. A possible explanation for this could be that using 200 µM of quinine only

knocks out 75% of the channel and therefore we do not see an effect on the membrane potential. However, 1 mM of TEA would knock out 90% of the channels only then does it affect the membrane potential. It seems possible that there is some type of voltage-gated dependency. When only 75% of the channel is blocked, the membrane depolarises but it is sufficient enough to activate the voltage-gated potassium channel, therefore it prevents the membrane potential from depolarising further. However, when 90% of the channel is blocked, the depolarisation is insufficient to stop the membrane potential from changing. In this case, the blocker is almost acting like a potassium buffer. When comparing the drug perfused membrane potential to the control, I saw no effect in both the membrane potential and input resistance. My results indicate that although BK channels are active in cell attached patches, they are not required for membrane potential or contribute to input resistance in whole cell, and they make very little contribution to the potassium permeability and membrane potential. There are several possible explanations for this result, there could be the possibility of losing the channel whist going whole cell. Another possibility is that the channels are activated by a second messenger modulator such as cAMP and cGMP-dependant protein kinases (Kyle et al., 2013, Nara et al., 1998, Zhou et al., 1996), protein kinase C (Zhou et al., 2012) which is lost by pipette dialysis in whole cell. The channel could also be activated by membrane stretch as seen by Mobasher et al., 2010 who found BK channels in chondrocytes, these channels had a conductance of 288 pS and channels were inhibited by TEA.

***Ion responsible for membrane potential***

The roles of other ions in membrane potential were explored, if BK channels were present, I performed cell attached experiments, whereas if they were not present, I performed whole cell experiments. To determine the relative contributions of different ionic moieties on membrane potential, it was compared at different ions bath solutions. In summary, the elevation of extracellular potassium by 45 mM from 5 mM to 50 mM of depolarised the membrane potential, removal of 137 mM extracellular sodium hyperpolarised by 8mv and finally removal of 45 mM extracellular chloride had not effect, however, these are not significant. When compared to the control, potassium showed a significant difference in the reversal potential. This suggests that the membrane seems to be dominated by potassium with a degree of sodium. My findings are somewhat limited by the lack of power in my study which could explain why I was unable to detect statistically significant results. Furthermore, there is a possible role of calcium ions in membrane

potential. As mentioned previously, in whole cell experiments with, a high calcium pipette solution (2.6 mM), the membrane potential was 16.8 mV more negative in comparison to low calcium ( <35 nM). This suggests there is a possibility of the membrane potential being permeable to calcium ions as well.

Using the known internal and external ion concentrations and mean membrane potential values (Table 6) I was able to get an estimate of the relative ion permeabilities. This was done using the Goldman-Hodgkin-Katz equation (Figure 6B) on the Nernst/Goldman simulator from the website. Under the assumption that there are three major contributing ionic species, and the pumps have no contribution to the membrane potential, I estimated a potassium permeability of 25 and a sodium permeability of 9. My results indicate that in glioblastoma SF188, potassium permeability is 2 and a half fold more than that of sodium. Thi**s seems** to be consistent with other research which found that membrane potential is highly selective for potassium (Gallacher and Morris, 1986, Lara, Acevedo and Onetti, 1999, Smart, 1987 Wang and Mathers, 1993 and Wann and Richards, 1994).

| | **Potassium** | **Sodium** | **Chloride** |
|---|---|---|---|
| **Ion Permeability** | 25 | 9 | 0 |
| **Internal concentration (mM)** | 135 | 10 | 16 |
| **External Concentration (mM)** | 50 | 100 | 8 |
| **Mean Membrane Potential (mV)** | -15 | -30.3 | -34.8 |

***Table 6.***

Table of the parameters I used to model and estimate the ion permeability using the Goldman-Hodgkin-Katz equation on the Nernst/Goldman simulator from the website**.** Mean membrane potential was calculated from whole cell current clamp data. The membrane potential that was estimated by the simulator matched the values we saw in our experiments.

The removal of chloride from the bath solution would cause chloride efflux from the cell which should have depolarised the membrane potential, but that is not what I saw. A possible explanation for this could be that in order to remove chloride, I substituted with sodium gluconate. Gluconate is permissible through the chloride channel, which would allow gluconate permeability (M. Hallani, Lynch and Barry, 1998). Chloride channels in glioma cells have previously been demonstrated to have gluconate permeability (Olsen et al., 2003). Another explanation could be that the gluconate buffers extracellular calcium and a subsequent effect is seen on membrane potential. This was observed by Akaniro-Ejim and Smith, 2021, who found a decrease in intracellular calcium as a result of reducing chloride by substituting with gluconate in mouse white fat adipocytes. Similar results of gluconate buffering calcium were also reported by Woehler, Lin and Neher, 2014. The chelate effect of gluconate could provide an explanation as to why my results indicate that the removal of chloride causes hyperpolarisation of the membrane potential, providing evidence that there may be some passive calcium permeability in these cells.

***Calcium Imaging***

Surprisingly, in my study, the intracellular calcium was very low, around 60nM or smaller compared to the values found in the literature. For example, Weaver, Liu and Sontheimer, 2004 found the resting calcium levels in glioma cells to be around 118 nM, using Fura-2 $Ca^{2+}$ imaging. Similarly, other studies report resting calcium levels in glioma cell lines to be around 100-200 nM (Verkhratsky, Orkand and Kettenmann, 1998). The addition of glutamate in glial cells causes an increase in intracellular calcium (Parpura and Haydon, 2000). I found that 10 mM and 100 mM glutamate caused an increase in intracellular calcium, in both the absence and presence of extracellular calcium. My results indicate glutamate caused a significantly higher increase in intracellular calcium levels with the presence of extracellular calcium. Glutamate acts on metabotropic and ionotropic receptors such as mGluR5 and AMPA on gliomas (Oh et al., 2012, Pei et al., 2020) which causes a subsequent increase in intracellular calcium. This increase can be a subsequent result of an extracellular influx of calcium via the activation of calcium permeable channels or a release from internal calcium stores such as the mitochondria (Leclerc et al., 2016). Increased intracellular calcium can also behave as a secondary messenger in various pathways. This increase in calcium signalling can result in glioma proliferation invasion and migration (Pei et al., 2020). In the literature, following activation of the channel, a tenfold increase in intracellular

calcium ions can be observed, this increase in calcium was a result of the influx of calcium from the external environment or release from the intracellular stores (Kuhn et al., 2009).

One of the possible reasons for the difference in basal calcium values could be the dye used in the experiments. I used Fluo-4, which is a low affinity calcium probe with a Kd of 345 nM, whereas Weaver, Liu and Sontheimer, 2004, used Fura-2 which is higher with a Kd of 140 nM. It could be possible that glioblastomas require a higher affinity calcium probe, glutamate in glioblastomas induces an increase in intracellular calcium, this response can be transient and as a result of influx from extracellular stores or released from intracellular stores. A higher affinity probe will be able to detect these changes with a higher sensitivity and provide a more quantitative measure. (Corsi, Mescola and Alessandrini, 2019, Lock, Parker and Smith, 2015). The multidrug resistance properties of cancer cells could be an alternative explanation for the lower values observed. The multidrug resistance is when there is a lower sensitivity to chemotherapeutic drugs as well as many other drugs with no specified structural homology or target, which results in reduced drug influx or increased drug efflux. This resistance is most commonly thought to be a result of the expression of P-glycoprotein. A higher expression of the glycoprotein has been linked to a higher degree of drug resistance (Gerlach et al., 1986, Simon and Schindler, 1994). In glioblastomas, a 90% expression of p-glycoprotein in primary and a 60% expression in secondary are found (Tews et al., 2000). Interestingly Abe et al., 1998 observed that both P-glycoprotein and multidrug resistance protein expression increased in glioblastoma cells following chemotherapy. This would mean that the Fluo-4AM dye is not completely taken up by the cell or only taken into the vesicles of the cell. Under normal conditions, once the dye permeates through the cell membrane, is esterified by the cell, forming the acidic form of the dye. This acid does not diffuse out of the cell which means it can bind to the free calcium ions in the cell (Kuhn et al., 2009). However, due to the drug-resistive property of glioma cells, it is possible that the dye is esterified and then discarded by the cell or is only taken up by the vesicles of the cell. Therefore, the calcium values recorded will not be the true intracellular calcium values. Another explanation could be that the glutamate is buffering intracellular calcium by acting on voltage-gated chloride channels as seen by Akaniro-Ejim and Smith, 2021. I also found several significant responses; however, these are misleading as the calcium levels decrease following the addition of glutamate.

***Limits***

The main issue I faced in my study was the dialysis that occurred as a result of going whole cell (Hooper et al., 2015). This could have potentially affected the membrane potential measured. An additional uncontrolled factor is the possibility that substituting the chloride with gluconate caused gluconate permeability or calcium buffering causing subsequent effects in the chloride channels as mentioned previously. Furthermore, this study is limited by the possible effect of temperature on the physiology whilst carrying out patch clamp experiments. Most of my experiments were conducted at 25 °C. However, Harberts et al., 2020 observed that the resting membrane potential increased by around 7mV at 37 °C compared to room temperature in T-Lymphocytes and stem cell-derived neurones. Moreover, the passage number of the cells could affect the physiology and properties of the cell, this has been seen by several different authors in a range of cell types (Cantor et al., 2022 and Gloy et al., 1994). Interestingly Ahring et al., 1997 observed that in HEK239 cells which were stably expressing high levels of transfected BK were no longer stable in passages over 50. This could explain the non-significant data seen in my study as the SF188 cells were passaged up to 53. Another possible limit of my research is that was conducted on BK channels in glioma cell lines SF188 and GCE62. Li et al., 2008 have shown that several established glioma cell lines show a difference between the genomic, transcriptome and functional pathway levels between the cell lines and primary glioma samples. Hence caution should be taken when translating data from glioma cell lines to human samples. In spite of its limitations, the study certainly adds to our understanding of the with biophysical and pharmacological properties of BK.

***Further experiments***

Further, consider for this work would involve q-PCR and western blots to quantify mRNA levels and protein expression of BK in SF188 cells, which would provide further information on the presence and quantity of BK channels expressed in SF188 cells. Other considerations would involve further investigations into what activates BK channels in SF188s using cell-attached patch clamp experiments as well as pharmacological experiments to determine what controls membrane potential in SF188s. Furthermore, repeating my calcium imaging studies using an x63 lens would let us know if the dye is taken up by vesicles. Finally, the calcium imaging experiments should be repeated using ATP rather than glutamate, as ATP can stimulate the release of glutamate and

increase in intracellular calcium in glioblastomas (Hartmmann and Verkhratsky, 1998, Strongg et al., 2018).

***Conclusion***

To summarise, in conclusion, I have shown that glioblastoma SF188 exhibits spontaneous $K^+$ channel activity in cell attached patches, with biophysical and pharmacological properties typical for BK. At low intracellular calcium concentrations, BK does not appear to be responsible for the resting membrane potential. Furthermore, the reversal potential of BK in cell attached patches appears to be an accurate non-invasive measure of the resting membrane potential of SF188 cells. The hyperpolarization of membrane potential that is seen on the elevation of calcium is indicative of BK activation. However pharmacologically, BK does not seem to be responsible for membrane potential. The membrane potential seems to be predominated by potassium with a degree of sodium, with potassium permeability being 2 and a half fold more than sodium. Further studies are required to determine what underlies BK activation in cell attached patches on SF188 and under what conditions is BK activated to contribute to membrane potential in this cell line.

**References**

Abdul Kadir, L., Stacey, M. and Barrett-Jolley, R. (2018). Emerging Roles of the Membrane Potential: Action Beyond the Action Potential. *Frontiers in Physiology*, [online] 9. doi:https://doi.org/10.3389/fphys.2018.01661.

Abdul, M. and Hoosein, N. (2002). Expression and activity of potassium ion channels in human prostate cancer. *Cancer Letters*, [online] 186(1), pp.99–105. doi:https://doi.org/10.1016/s0304-3835(02)00348-8.

Abdullaev, I.F., Rudkouskaya, A., Mongin, A.A. and Kuo, Y.-H. (2010). Calcium-Activated Potassium Channels BK and IK1 Are Functionally Expressed in Human Gliomas but Do Not Regulate Cell Proliferation. *PLoS ONE*, [online] 5(8), p.e12304. doi:https://doi.org/10.1371/journal.pone.0012304.

Abe, T., Mori, T., Wakabayashi, Y., Nakagawa, M., Cole, S.P., Koike, K., Kuwano, M. and Hori, S. (1998). Expression of multidrug resistance protein gene in patients with glioma after chemotherapy. *Journal of Neuro-Oncology*, [online] 40(1), pp.11–18. doi:https://doi.org/10.1023/a:1005954406809.

Adams, D.S. and Levin, M. (2012). General Principles for Measuring Resting Membrane Potential and Ion Concentration Using Fluorescent Bioelectricity Reporters. *Cold Spring Harbor Protocols*, [online] 2012(4), pp.pdb.top067710–pdb.top067710. doi:https://doi.org/10.1101/pdb.top067710.

Aguilar-Bryan, L. and Bryan, J. (1999). Molecular Biology of Adenosine Triphosphate-Sensitive Potassium Channels*. *Endocrine Reviews*, [online] 20(2), pp.101–135. doi:https://doi.org/10.1210/edrv.20.2.0361.

Ahring, P.K., Strøbæk, D., Christophersen, P., Olesen, S.-P. and Johansen, T.E. (1997). Stable expression of the human large-conductance Ca2+-activated K+ channel α- and β-subunits in HEK293 cells. *FEBS Letters*, [online] 415(1), pp.67–70. doi:https://doi.org/10.1016/S0014-5793(97)01096-X.

Akaniro-Ejim, N.E. and Smith, P.A. (2021). Intracellular Ca2+ in Mouse White Fat Adipocytes: Effects of Extracellular Anions, Growth Hormone, and Their Interaction with Ca2+ Influx. *Bioelectricity*, 3(4), pp.282–291. doi:https://doi.org/10.1089/bioe.2021.0020.

Al-Saffar, N.M.S., Marshall, L.V., Jackson, L.E., Balarajah, G., Eykyn, T.R., Agliano, A., Clarke, P.A., Jones, C., Workman, P., Pearson, A.D.J. and Leach, M.O. (2014). Lactate and Choline Metabolites Detected In Vitro by Nuclear Magnetic Resonance Spectroscopy Are Potential Metabolic Biomarkers for PI3K Inhibition in Pediatric Glioblastoma. *PLoS ONE*, [online] 9(8), p.e103835. doi:https://doi.org/10.1371/journal.pone.0103835.

Alberts, B., Johnson, A., Lewis, J., Raff, M., Roberts, K. and Walter, P. (2002). Ion Channels and the Electrical Properties of Membranes. *Molecular Biology of the Cell. 4th edition*. [online] Available at: https://www.ncbi.nlm.nih.gov/books/NBK26910/ [Accessed 22 Dec. 2022].

Alifieris, C. and Trafalis, D.T. (2015). Glioblastoma multiforme: Pathogenesis and treatment. *Pharmacology & Therapeutics*, [online] 152, pp.63–82. doi:https://doi.org/10.1016/j.pharmthera.2015.05.005.

Allen, N.J. and Lyons, D.A. (2018). Glia as architects of central nervous system formation and function. *Science*, [online] 362(6411), pp.181–185. doi:https://doi.org/10.1126/science.aat0473.

Amigorena, S., Choquet, D., Teillaud, J.L., Korn, H. and Fridman, W.H. (1990). Ion channel blockers inhibit B cell activation at a precise stage of the G1 phase of the cell cycle. Possible involvement of K+ channels. *Journal of Immunology (Baltimore, Md.: 1950)*, [online] 144(6), pp.2038–2045. Available at: https://pubmed.ncbi.nlm.nih.gov/2313087/ [Accessed 27 Dec. 2022].

Andrade, P.V. de, Andrade, A.F., Paula Queiroz, R.G. de, Scrideli, C.A., Tone, L.G. and Valera, E.T. (2016). The histone deacetylase inhibitor PCI-24781 as a putative radiosensitizer in pediatric glioblastoma cell lines. *Cancer Cell International*, [online] 16(1). doi:https://doi.org/10.1186/s12935-016-0306-5.

Aretz, P., Maciaczyk, D., Yusuf, S., Sorg, R.V., Hänggi, D., Liu, H., Liu, H., Dakal, T.C., Sharma, A., Bethanabatla, R., Neumann, S. and Maciaczyk, J. (2022). Crosstalk between β-Catenin and CCL2 Drives Migration of Monocytes towards Glioblastoma Cells. *International Journal of Molecular Sciences*, [online] 23(9), p.4562. doi:https://doi.org/10.3390/ijms23094562.

Atwater, I., Rosario, L. and Rojas, E. (1983). Properties of the Ca-activated K+ channel in pancreatic beta-cells. *Cell Calcium*, [online] 4(5-6), pp.451–461. doi:https://doi.org/10.1016/0143-4160(83)90021-0.

Aydogan Gokturk, P., Sujanani, R., Qian, J., Wang, Y., Katz, L.E., Freeman, B.D. and Crumlin, E.J. (2022). The Donnan potential revealed. *Nature Communications*, [online] 13(1). doi:https://doi.org/10.1038/s41467-022-33592-3.

Bady, P., Diserens, A.-C. ., Castella, V., Kalt, S., Heinimann, K., Hamou, M.-F. ., Delorenzi, M. and Hegi, M.E. (2012). DNA fingerprinting of glioma cell lines and considerations on similarity measurements. *Neuro-Oncology*, [online] 14(6), pp.701–711. doi:https://doi.org/10.1093/neuonc/nos072.

Basrai, D., Kraft, R., Bollensdorff, C., Liebmann, L., Benndorf, K. and Patt, S. (2002). BK channel blockers inhibit potassium-induced proliferation of human astrocytoma cells. *Neuroreport*, [online] 13(4), pp.403–407. doi:https://doi.org/10.1097/00001756-200203250-00008.

Bax, D.A., Little, S.E., Gaspar, N., Perryman, L., Marshall, L., Viana-Pereira, M., Jones, T.A., Williams, R.D., Grigoriadis, A., Vassal, G., Workman, P., Sheer, D., Reis, R.M., Pearson, A.D.J., Hargrave, D. and Jones, C. (2009). Molecular and Phenotypic Characterisation of Paediatric Glioma Cell Lines as Models for Preclinical Drug Development. *PLoS ONE*, [online] 4(4), p.e5209. doi:https://doi.org/10.1371/journal.pone.0005209.

Behrens, R., Nolting, A., Reimann, F., Schwarz, M., Waldschütz, R. and Pongs, O. (2000). hKCNMB3 and hKCNMB4, cloning and characterization of two members of the large-conductance calcium-activated potassium channel beta subunit family. *FEBS letters*, [online] 474(1), pp.99–106. doi:https://doi.org/10.1016/s0014-5793(00)01584-2.

Belle, M.D.C., Diekman, C.O., Forger, D.B. and Piggins, H.D. (2009). Daily Electrical Silencing in the Mammalian Circadian Clock. *Science*, [online] 326(5950), pp.281–284. doi:https://doi.org/10.1126/science.1169657.

Benoit, C., Renaudon, B., Salvail, D. and Rousseau, E. (2001). EETs relax airway smooth muscle via an EpDHF effect: BK(Ca) channel activation and hyperpolarization. *American journal of physiology. Lung cellular and molecular physiology*, [online] 280 5. doi:https://doi.org/10.1152/AJPLUNG.2001.280.5.L965.

Bentley, D.C., Pulbutr, P., Chan, S. and Smith, P.A. (2014). Etiology of the membrane potential of rat white fat adipocytes. *American Journal of Physiology-Endocrinology and Metabolism*, 307(2), pp.E161–E175. doi:https://doi.org/10.1152/ajpendo.00446.2013.

Bernèche, S. and Roux, B. (2003). A microscopic view of ion conduction through the K+ channel. *Proceedings of the National Academy of Sciences*, [online] 100(15), pp.8644–8648. doi:https://doi.org/10.1073/pnas.1431750100.

Bernèche, S. and Roux, B. (2005). A Gate in the Selectivity Filter of Potassium Channels. *Structure*, [online] 13(4), pp.591–600. doi:https://doi.org/10.1016/j.str.2004.12.019.

Berzingi, S., Newman, M. and Yu, H.-G. (2016). Altering bioelectricity on inhibition of human breast cancer cells. *Cancer Cell International*, [online] 16(1). doi:https://doi.org/10.1186/s12935-016-0348-8.

Binggeli , R. and Weinstein, R.C. (1986). Membrane potentials and sodium channels: Hypotheses for growth regulation and cancer formation based on changes in sodium channels and gap junctions. *Journal of Theoretical Biology*, [online] 123(4), pp.377–401. doi:https://doi.org/10.1016/S0022-5193(86)80209-0.

Binggeli, R. and Cameron, I.L. (1980). Cellular potentials of normal and cancerous fibroblasts and hepatocytes. *Cancer Research*, [online] 40(6), pp.1830–1835. Available at: https://pubmed.ncbi.nlm.nih.gov/7371014/ [Accessed 30 Jul. 2023].

Binggeli, R. and Weinstein, R.C. (1985). Deficits in elevating membrane potential of rat fibrosarcoma cells after cell contact. *Cancer Research*, [online] 45(1), pp.235–241. Available at: https://pubmed.ncbi.nlm.nih.gov/3965134/ [Accessed 30 Jul. 2023].

Bjerke, L., Mackay, A., Nandhabalan, M., Burford, A., Jury, A., Popov, S., Bax, D.A., Carvalho, D., Taylor, K.R., Vinci, M., Bajrami, I., McGonnell, I.M., Lord, C.J., Reis, R.M., Hargrave, D., Ashworth, A., Workman, P. and Jones, C. (2013). Histone H3.3. mutations drive pediatric glioblastoma through upregulation of MYCN. *Cancer Discovery*, [online] 3(5), pp.512–519. doi:https://doi.org/10.1158/2159-8290.CD-12-0426.

Bokvist, K., Rorsman, P. and Smith, P.A. (1990). Block of ATP-regulated and Ca2(+)-activated K+ channels in mouse pancreatic beta-cells by external tetraethylammonium and quinine. *The Journal of Physiology*, [online] 423, pp.327–342. Available at: https://www.ncbi.nlm.nih.gov/pmc/articles/PMC1189760/ [Accessed 1 Sep. 2023].

Bordey, A., Sontheimer, H. and Trouslard, J. (2000). Muscarinic Activation of BK Channels Induces Membrane Oscillations in Glioma Cells and Leads to Inhibition of Cell Migration. *The Journal of Membrane Biology*, [online] 176(1), pp.31–40. doi:https://doi.org/10.1007/s00232001073.

Bordey, A. and Spencer, D.D. (2003). Chemokine modulation of high-conductance Ca(2+)-sensitive K(+) currents in microglia from human hippocampi. *The European Journal of Neuroscience*, [online] 18(10), pp.2893–2898. doi:https://doi.org/10.1111/j.1460-9568.2003.03021.x.

Brandalise, F., Ramieri, M., Pastorelli, E., Priori, E.C., Ratto, D., Venuti, M.T., Roda, E., Talpo, F. and Rossi, P. (2023). Role of Na+/Ca2+ Exchanger (NCX) in Glioblastoma Cell Migration (In Vitro). *International Journal of Molecular Sciences*, [online] 24(16), p.12673. doi:https://doi.org/10.3390/ijms241612673.

Branter, J., Estevez-Cebrero, M., Diksin, M., Griffin, M., Castellanos-Uribe, M., May, S., Rahman, R., Grundy, R.G., Basu, S. and Smith, S. (2022). Genome-Wide Expression and Anti-Proliferative Effects of Electric Field Therapy on Pediatric and Adult Brain Tumors. *International Journal of Molecular Sciences*, 23(4), pp.1982–1982. doi:https://doi.org/10.3390/ijms23041982.

Braun, M., Ramracheya, R., Bengtsson, M., Zhang, Q., Karanauskaite, J., Partridge, C., Johnson, P.R. and Rorsman, P. (2008). Voltage-Gated Ion Channels in Human Pancreatic  -Cells: Electrophysiological Characterization and Role in Insulin Secretion. *Diabetes*, [online] 57(6), pp.1618–1628. doi:https://doi.org/10.2337/db07-0991.

Brenner, R., Jegla, T.J., Wickenden, A., Liu, Y. and Aldrich, R.W. (2000a). Cloning and Functional Characterization of Novel Large Conductance Calcium-activated Potassium Channel β Subunits, hKCNMB3 and hKCNMB4. *Journal of Biological Chemistry*, [online] 275(9), pp.6453–6461. doi:https://doi.org/10.1074/jbc.275.9.6453.

Brenner, R., Peréz, G.J., Bonev, A.D., Eckman, D.M., Kosek, J.C., Wiler, S.W., Patterson, A.J., Nelson, M.T. and Aldrich, R.W. (2000b). Vasoregulation by the beta1 subunit of the calcium-activated

potassium channel. *Nature*, [online] 407(6806), pp.870–876. doi:https://doi.org/10.1038/35038011.

Bringmann, A., Francke, M., Pannicke, T., Biedermann, B., Faude, F., Enzmann, V., Wiedemann, P., Reichelt, W. and Reichenbach, A. (1999). Human Müller glial cells: altered potassium channel activity in proliferative vitreoretinopathy. *Investigative Ophthalmology & Visual Science*, [online] 40(13), pp.3316–3323. Available at: https://pubmed.ncbi.nlm.nih.gov/10586958/ [Accessed 4 Jan. 2023].

Butler, A.E., Janson, J., Bonner-Weir, S., Ritzel, R., Rizza, R.A. and Butler, P.C. (2003). -Cell Deficit and Increased  -Cell Apoptosis in Humans With Type 2 Diabetes. *Diabetes*, [online] 52(1), pp.102–110. doi:https://doi.org/10.2337/diabetes.52.1.102.

Cantor, E.L., Shen, F., Jiang, G., Tan, Z., Cunningham, G.M., Wu, X., Philips, S. and Schneider, B.P. (2022). Passage number affects differentiation of sensory neurons from human induced pluripotent stem cells. *Scientific Reports*, [online] 12, p.15869. doi:https://doi.org/10.1038/s41598-022-19018-6.

Catacuzzeno, L., Aiello, F., Fioretti, B., Sforna, L., Castigli, E., Ruggieri, P., Tata, A.M., Calogero, A. and Franciolini, F. (2011). Serum-activated K and Cl currents underlay U87-MG glioblastoma cell migration. *Journal of Cellular Physiology*, [online] 226(7), pp.1926–1933. doi:https://doi.org/10.1002/jcp.22523.

Catacuzzeno, L., Caramia, M., Sforna, L., Belia, S., Guglielmi, L., D'Adamo, M.C., Pessia, M. and Franciolini, F. (2015). Reconciling the discrepancies on the involvement of large-conductance Ca2+-activated K channels in glioblastoma cell migration. *Frontiers in Cellular Neuroscience*, [online] 9. doi:https://doi.org/10.3389/fncel.2015.00152.

Chay, T.R. (1986). On the effect of the intracellular calcium-sensitive K+ channel in the bursting pancreatic beta-cell. *Biophysical Journal*, [online] 50(5), pp.765–777. doi:https://doi.org/10.1016/s0006-3495(86)83517-2.

Chen, K.-Y., Bush, K., Klein, R.H., Cervantes, V., Lewis, N., Naqvi, A., Carcaboso, A.M., Lechpammer, M. and Knoepfler, P.S. (2020). Reciprocal H3.3 gene editing identifies K27M and G34R mechanisms

in pediatric glioma including NOTCH signaling. *Communications Biology*, [online] 3(1). doi:https://doi.org/10.1038/s42003-020-1076-0.

Chen, L., Becker, T.M., Koch, U. and Stauber, T. (2019). The LRRC8/VRAC anion channel facilitates myogenic differentiation of murine myoblasts by promoting membrane hyperpolarization. *The Journal of Biological Chemistry*, [online] 294(39), pp.14279–14288. doi:https://doi.org/10.1074/jbc.RA119.008840.

Chen, L., Tian, L., MacDonald, S.H.-F. ., McClafferty, H., Hammond, M.S.L., Huibant, J.-M., Ruth, P., Knaus, H.-G. and Shipston, M.J. (2005). Functionally diverse complement of large conductance calcium- and voltage-activated potassium channel (BK) alpha-subunits generated from a single site of splicing. *The Journal of Biological Chemistry*, [online] 280(39), pp.33599–33609. doi:https://doi.org/10.1074/jbc.M505383200.

Chen, Q., Tao, J., Hei, H., Li, F., Wang, Y., Peng, W. and Zhang, X. (2015). Up-Regulatory Effects of Curcumin on Large Conductance Ca2+-Activated K+ Channels. *PLOS ONE*, 10(12), p.e0144800. doi:https://doi.org/10.1371/journal.pone.0144800.

Choe, S. (2002). Potassium channel structures. *Nature Reviews Neuroscience*, [online] 3(2), pp.115–121. doi:https://doi.org/10.1038/nrn727.

Chrysafides, S.M., Bordes, S.J. and Sharma, S. (2019). *Physiology, Resting Potential*. [online] Nih.gov. Available at: https://www.ncbi.nlm.nih.gov/books/NBK538338/ [Accessed 23 Dec. 2022].

Cockle, J.V., Brüning-Richardson, A., Scott, K.J., Thompson, J., Kottke, T., Morrison, E., Ismail, A., Carcaboso, A.M., Rose, A., Selby, P., Conner, J., Picton, S., Short, S., Vile, R., Melcher, A. and Ilett, E. (2017). Oncolytic Herpes Simplex Virus Inhibits Pediatric Brain Tumor Migration and Invasion. *Molecular Therapy - Oncolytics*, [online] 5, pp.75–86. doi:https://doi.org/10.1016/j.omto.2017.04.002.

Cockle, J.V., Picton, S., Levesley, J., Ilett, E., Carcaboso, A.M., Short, S., Steel, L.P., Melcher, A., Lawler, S.E. and Brüning-Richardson, A. (2015). Cell migration in paediatric glioma; characterisation and potential therapeutic targeting. *British Journal of Cancer*, [online] 112(4), pp.693–703. doi:https://doi.org/10.1038/bjc.2015.16.

Cone, C.D. and Cone, C.M. (1976). Induction of Mitosis in Mature Neurons in Central Nervous System by Sustained Depolarization. *Science*, [online] 192(4235), pp.155–158. doi:https://doi.org/10.1126/science.56781.

Cone, C.D. and Tongier, M. (1973). Contact inhibition of division: Involvement of the electrical transmembrane potential. *Journal of Cellular Physiology*, [online] 82(3), pp.373–386. doi:https://doi.org/10.1002/jcp.1040820307.

Corsi, L., Mescola, A. and Alessandrini, A. (2019). Glutamate Receptors and Glioblastoma Multiforme: An Old 'Route' for New Perspectives. *International Journal of Molecular Sciences*, [online] 20(7), p.1796. doi:https://doi.org/10.3390/ijms20071796.

Cota, G. (1986). Calcium channel currents in pars intermedia cells of the rat pituitary gland. Kinetic properties and washout during intracellular dialysis. *The Journal of General Physiology*, 88(1), pp.83–105. doi:https://doi.org/10.1085/jgp.88.1.83.

Cox, D.H. and Aldrich, R.W. (2000). Role of the β1 Subunit in Large-Conductance Ca2+-Activated K+ Channel Gating Energetics. *Journal of General Physiology*, [online] 116(3), pp.411–432. doi:https://doi.org/10.1085/jgp.116.3.411.

Curtis, H.J. and Cole, K.S. (1942). Membrane resting and action potentials from the squid giant axon. *Journal of Cellular and Comparative Physiology*, [online] 19(2), pp.135–144. doi:https://doi.org/10.1002/jcp.1030190202.

Davis, M. (2016). Glioblastoma: Overview of Disease and Treatment. *Clinical Journal of Oncology Nursing*, [online] 20(5), pp.S2–S8. doi:https://doi.org/10.1188/16.cjon.s1.2-8.

De Wet, H., Allen, M., Holmes, C., Stobbart, M., Lippiat, J.D., De Wet, H., Allen, M., Holmes, C., Stobbart, M., Lippiat, J.D. and Callaghan, R. (2006). Modulation of the BK channel by estrogens: examination at single channel level. *Molecular Membrane Biology*, 23(5), pp.420–429. doi:https://doi.org/10.1080/09687860600802803.

Dean, P.M. and Mathews, E.K. (1968). Electrical Activity in Pancreatic Islet Cells. *Nature*, [online] 219(5152), pp.389–390. doi:https://doi.org/10.1038/219389a0.

Dorte Strøbæk, Christophersen, P., Holm, N.R., P. Moldt, Ahring, P.K., Johansen, T.E. and Olesen, S.-P. (1996). Modulation of the Ca 2+ -dependent K + Channel, hslo , by the Substituted Diphenylurea NS 1608, Paxilline and Internal Ca 2+. *Neuropharmacology*, 35(7), pp.903–914. doi:https://doi.org/10.1016/0028-3908(96)00096-2.

Doyle, D.A., Cabral, J.M., Pfuetzner, R.A., Kuo, A., Gulbis, J.M., Cohen, S.L., Chait, B.T. and MacKinnon, R. (1998). The Structure of the Potassium Channel: Molecular Basis of K+ Conduction and Selectivity. *Science*, 280(5360), pp.69–77. doi:https://doi.org/10.1126/science.280.5360.69.

Du, W., Bautista, J.F., Yang, H., Diez-Sampedro, A., You, S.-A., Wang, L., Kotagal, P., Lüders, H.O., Shi, J., Cui, J., Richerson, G.B. and Wang, Q.K. (2005). Calcium-sensitive potassium channelopathy in human epilepsy and paroxysmal movement disorder. *Nature Genetics*, 37(7), pp.733–738. doi:https://doi.org/10.1038/ng1585.

Du, X., Carvalho-de-Souza, J.L., Wei, C., Carrasquel-Ursulaez, W., Lorenzo, Y., Gonzalez, N., Kubota, T., Staisch, J., Hain, T., Petrossian, N., Xu, M., Latorre, R., Bezanilla, F. and Gomez, C.M. (2020). Loss-of-function BK channel mutation causes impaired mitochondria and progressive cerebellar ataxia. *Proceedings of the National Academy of Sciences*, [online] 117(11), pp.6023–6034. doi:https://doi.org/10.1073/pnas.1920008117.

Düfer, M., Neye, Y., Hörth, K., Krippeit-Drews, P., Hennige, A., Widmer, H., McClafferty, H., Shipston, M.J., Häring, H.-U. ., Ruth, P. and Drews, G. (2010). BK channels affect glucose homeostasis and cell viability of murine pancreatic beta cells. *Diabetologia*, [online] 54(2), pp.423–432. doi:https://doi.org/10.1007/s00125-010-1936-0.

Dworetzky, S.I., Boissard, C.G., Lum-Ragan, J.T., McKay, M.C., Post-Munson, D.J., Trojnacki, J.T., Chang, C.-P. and Gribkoff, V.K. (1996). Phenotypic Alteration of a Human BK (***hSlo***) Channel by***hSloβ***Subunit Coexpression: Changes in Blocker Sensitivity, Activation/Relaxation and Inactivation Kinetics, and Protein Kinase A Modulation. *The Journal of Neuroscience*, [online] 16(15), pp.4543–4550. doi:https://doi.org/10.1523/jneurosci.16-15-04543.1996.

Edalat, L., Stegen, B., Klumpp, L., Haehl, E., Schilbach, K., Lukowski, R., Kühnle, M., Bernhardt, G., Buschauer, A., Zips, D., Ruth, P. and Huber, S.M. (2016). BK K+ channel blockade inhibits radiation-

induced migration/brain infiltration of glioblastoma cells. *Oncotarget*, [online] 7(12), pp.14259–14278. doi:https://doi.org/10.18632/oncotarget.7423.

Egbivwie, N., Cockle, J.V., Humphries, M.P., Ismail, A., Esteves, F., Taylor, C., Karakoula, K., Morton, R., Warr, T., Short, S. and Anke Brüning-Richardson (2019). FGFR1 Expression and Role in Migration in Low and High Grade Pediatric Gliomas. *Frontiers in Oncology* , [online] 9. doi:https://doi.org/10.3389/fonc.2019.00103.

Erxleben, C., Everhart, A.L., Romeo, C., Florance, H., Bauer, M.B., Alcorta, D.A., Rossie, S., Shipston, M.J. and Armstrong, D.L. (2002). Interacting effects of N-terminal variation and strex exon splicing on slo potassium channel regulation by calcium, phosphorylation, and oxidation. *The Journal of Biological Chemistry*, [online] 277(30), pp.27045–27052. doi:https://doi.org/10.1074/jbc.M203087200.

Faber, E.S.L. and Sah, P. (2003). Calcium-Activated Potassium Channels: Multiple Contributions to Neuronal Function. *The Neuroscientist*, [online] 9(3), pp.181–194. doi:https://doi.org/10.1177/1073858403009003011.

Fang, J., Huang, Y., Mao, G., Yang, S., Rennert, G., Gu, L., Li, H. and Li, G.-M. (2018). Cancer-driving H3G34V/R/D mutations block H3K36 methylation and H3K36me3–MutSα interaction. *Proceedings of the National Academy of Sciences*, [online] 115(38), pp.9598–9603. doi:https://doi.org/10.1073/pnas.1806355115.

Filosa, J.A., Bonev, A.D., Straub, S.V., Meredith, A.L., Wilkerson, M.K., Aldrich, R.W. and Nelson, M.T. (2006). Local potassium signaling couples neuronal activity to vasodilation in the brain. *Nature Neuroscience*, [online] 9(11), pp.1397–1403. doi:https://doi.org/10.1038/nn1779.

Findlay, I. (1984). A patch-clamp study of potassium channels and whole-cell currents in acinar cells of the mouse lacrimal gland. *The Journal of Physiology*, [online] 350(1), pp.179–195. doi:https://doi.org/10.1113/jphysiol.1984.sp015195.

Findlay, I., Dunne, M.J., Ullrich, S., Wollheim, C.B. and Petersen, O.H. (1985). Quinine inhibits Ca2+ -independent K+ channels whereas tetraethylammonium inhibits Ca2+ -activated K+ channels in insulin-secreting cells. *FEBS Letters*, 185(1), pp.4–8. doi:https://doi.org/10.1016/0014-5793(85)80729-8.

Fodor, A.A. and Aldrich, R.W. (2009). Convergent Evolution of Alternative Splices at Domain Boundaries of the BK Channel. *Annual Review of Physiology*, [online] 71(1), pp.19–36. doi:https://doi.org/10.1146/annurev.physiol.010908.163124.

Franciolini, F., Hogg, R., Catacuzzeno, L., Petris, A., Trequattrini, C. and Adams, D.J. (2001). Large-conductance calcium-activated potassium channels in neonatal rat intracardiac ganglion neurons. *Pflugers Archiv: European Journal of Physiology*, [online] 441(5), pp.629–638. doi:https://doi.org/10.1007/s004240000471.

Fraser, S.P., Grimes, J.A. and Djamgoz, M.B.A. (2000). Effects of voltage-gated ion channel modulators on rat prostatic cancer cell proliferation: Comparison of strongly and weakly metastatic cell lines. *The Prostate*, [online] 44(1), pp.61–76. doi:https://doi.org/10.1002/1097-0045(20000615)44:1%3C61::aid-pros9%3E3.0.co;2-3.

Fricker, D., Verheugen, J.A.H. and Miles, R. (1999). Cell-attached measurements of the firing threshold of rat hippocampal neurones. *The Journal of Physiology*, [online] 517(3), pp.791–804. doi:https://doi.org/10.1111/j.1469-7793.1999.0791s.x.

Fridlyand, L.E., Tamarina, N. and Philipson, L.H. (2010). Bursting and calcium oscillations in pancreatic β-cells: specific pacemakers for specific mechanisms. *American Journal of Physiology - Endocrinology and Metabolism*, [online] 299(4), pp.E517–E532. doi:https://doi.org/10.1152/ajpendo.00177.2010.

Fu, Z., Gilbert, E.R. and Liu, D. (2013). Regulation of Insulin Synthesis and Secretion and Pancreatic Beta-Cell Dysfunction in Diabetes. *Current diabetes reviews*, [online] 9(1), pp.25–53. Available at: https://www.ncbi.nlm.nih.gov/pmc/articles/PMC3934755/#S4title [Accessed 31 Dec. 2022].

Gallacher, D.V. and Morris, A.P. (1986). A patch-clamp study of potassium currents in resting and acetylcholine-stimulated mouse submandibular acinar cells. *The Journal of Physiology*, [online] 373(1), pp.379–395. doi:https://doi.org/10.1113/jphysiol.1986.sp016054.

Ge, L., Hoa, N.T., Cornforth, A.N., Bota, D.A., Mai, A., Kim, D.I., Chiou, S.-K., Hickey, M.J., Kruse, C.A. and Jadus, M.R. (2012). Glioma Big Potassium Channel Expression in Human Cancers and Possible T Cell Epitopes for Their Immunotherapy. *The Journal of Immunology*, 189(5), pp.2625–2634. doi:https://doi.org/10.4049/jimmunol.1102965.

Ge, L., Hoa, N.T., Wilson, Z., Arismendi-Morillo, G., Kong, X.-T., Tajhya, R.B., Beeton, C. and Jadus, M.R. (2014). Big Potassium (BK) ion channels in biology, disease and possible targets for cancer immunotherapy. *International Immunopharmacology*, [online] 22(2), pp.427–443. doi:https://doi.org/10.1016/j.intimp.2014.06.040.

Gerlach, J.H., Kartner, N., Bell, D.R. and Ling, V. (1986). Multidrug resistance. *Cancer Surveys*, [online] 5(1), pp.25–46. Available at: https://pubmed.ncbi.nlm.nih.gov/2885085/ [Accessed 9 Sep. 2023].

Gilard, V., Tebani, A., Dabaj, I., Laquerrière, A., Fontanilles, M., Derrey, S., Marret, S. and Bekri, S. (2021). Diagnosis and Management of Glioblastoma: A Comprehensive Perspective. *Journal of Personalized Medicine*, [online] 11(4), p.258. doi:https://doi.org/10.3390/jpm11040258.

Glavinović, M.I. and Trifaró, J.M. (1988). Quinine blockade of currents through Ca2+-activated K+ channels in bovine chromaffin cells. *The Journal of Physiology*, [online] 399, pp.139–152. Available at: https://www.ncbi.nlm.nih.gov/pmc/articles/PMC1191656/ [Accessed 1 Sep. 2023].

Gloy, J., Greger, R., Schollmeyer, P., Huber, M. and Pavenstädt, H. (1994). Influence of cell culture conditions and passage number on the response of membrane voltage to ATP and angiotensin II in rat mesangial cells. *Renal Physiology and Biochemistry*, [online] 17(2), pp.62–72. doi:https://doi.org/10.1159/000173789.

Golding, N.L., Jung, H., Mickus, T. and Spruston, N. (1999). Dendritic Calcium Spike Initiation and Repolarization Are Controlled by Distinct Potassium Channel Subtypes in CA1 Pyramidal Neurons. *The Journal of Neuroscience*, [online] 19(20), pp.8789–8798. doi:https://doi.org/10.1523/jneurosci.19-20-08789.1999.

Gong, L.W., Gao, T.M., Huang, H. and Tong, Z. (2001). Properties of large conductance calcium-activated potassium channels in pyramidal neurons from the hippocampal CA1 region of adult rats. *The Japanese Journal of Physiology*, [online] 51(6), pp.725–731. doi:https://doi.org/10.2170/jjphysiol.51.725.

González, C., Baez-Nieto, D., Valencia, I., Oyarzún, I., Rojas, P., Naranjo, D. and Latorre, R. (2012). K(+) channels: function-structural overview. *Comprehensive Physiology*, [online] 2(3), pp.2087–2149. doi:https://doi.org/10.1002/cphy.c110047.

Griguoli, M., Sgritta, M. and Cherubini, E. (2016). Presynaptic BK channels control transmitter release: physiological relevance and potential therapeutic implications. *The Journal of Physiology*, [online] 594(13), pp.3489–3500. doi:https://doi.org/10.1113/jp271841.

Grossman, R., Tyler, B., Brem, H., Eberhart, C.G., Wang, S., Fu, D., Wen, Z. and Zhou, J. (2012). Growth properties of SF188/V+ human glioma in rats in vivo observed by magnetic resonance imaging. *Journal of Neuro-Oncology* , [online] 110(3), pp.315–323. doi:https://doi.org/10.1007/s11060-012-0974-5.

Grunnet, M. and Kaufmann, W.A. (2004). Coassembly of Big Conductance Ca2+-activated K+ Channels and L-type Voltage-gated Ca2+ Channels in Rat Brain. *Journal of Biological Chemistry*, [online] 279(35), pp.36445–36453. doi:https://doi.org/10.1074/jbc.m402254200.

Gu, N., Vervaeke, K. and Storm, J.F. (2007). BK potassium channels facilitate high-frequency firing and cause early spike frequency adaptation in rat CA1 hippocampal pyramidal cells. *The Journal of Physiology*, [online] 580(3), pp.859–882. doi:https://doi.org/10.1113/jphysiol.2006.126367.

Haas-Kogan, D., Shalev, N., Wong, M., Mills, G., Yount, G. and Stokoe, D. (1998). Protein kinase B (PKB/Akt) activity is elevated in glioblastoma cells due to mutation of the tumor suppressor PTEN/MMAC. *Current Biology*, 8(21), pp.1195-S1. doi:https://doi.org/10.1016/s0960-9822(07)00493-9.

Hammond, C. (2015). The voltage-gated channels of Na+ action potentials. *Cellular and Molecular Neurophysiology*, [online] pp.55–91. doi:https://doi.org/10.1016/b978-0-12-397032-9.00004-2.

Hanif, F., Muzaffar, K., Perveen, K., Malhi, S.M. and Simjee, S.U. (2019). Glioblastoma Multiforme: A Review of its Epidemiology and Pathogenesis through Clinical Presentation and Treatment. *Asian Pacific journal of cancer prevention : APJCP*, [online] 18(1), pp.3–9. doi:https://doi.org/10.22034/APJCP.2017.18.1.3.

Harberts, J., Kusch, M., O'Sullivan, J., Zierold, R. and Blick, R.H. (2020). A Temperature-Controlled Patch Clamp Platform Demonstrated on Jurkat T Lymphocytes and Human Induced Pluripotent Stem Cell-Derived Neurons. *Bioengineering*, [online] 7(2), p.46. doi:https://doi.org/10.3390/bioengineering7020046.

Hartmann, J. and Verkhratsky, A. (1998). Relations between intracellular Ca2+stores and store-operated Ca2+entry in primary cultured human glioblastoma cells. *The Journal of Physiology*, 513(2), pp.411–424. doi:https://doi.org/10.1111/j.1469-7793.1998.411bb.x.

Häusser, M. (2000). The Hodgkin-Huxley theory of the action potential. *Nature Neuroscience*, [online] 3(11), pp.1165–1165. doi:https://doi.org/10.1038/81426.

Hayashi, Y., Kawaji, K., Sun, L., Zhang, X., Koyano, K., Yokoyama, T., Kohsaka, S., Inoue, K. and Nakanishi, H. (2011). Microglial Ca2+-Activated K+ Channels Are Possible Molecular Targets for the Analgesic Effects of S-Ketamine on Neuropathic Pain. *Journal of Neuroscience*, [online] 31(48), pp.17370–17382. doi:https://doi.org/10.1523/jneurosci.4152-11.2011.

He, Y., Lin, Y., He, F., Shao, L., Ma, W. and He, F. (2021). Role for calcium-activated potassium channels (BK) in migration control of human hepatocellular carcinoma cells. *Journal of Cellular and Molecular Medicine*, [online] 25(20), pp.9685–9696. doi:https://doi.org/10.1111/jcmm.16918.

Henney, N.C., Li, B., Elford, C., P Reviriego, Campbell, A.K., Wann, K.T. and James, A. (2009). A large-conductance (BK) potassium channel subtype affects both growth and mineralization of human osteoblasts. *American Journal of Physiology-cell Physiology*, [online] 297(6), pp.C1397–C1408. doi:https://doi.org/10.1152/ajpcell.00311.2009.

Herrera, G.M. and Nelson, M.T. (2002). Differential regulation of SK and BK channels by Ca2+signals from Ca2+channels and ryanodine receptors in guinea-pig urinary bladder myocytes. *The Journal of Physiology*, [online] 541(2), pp.483–492. doi:https://doi.org/10.1113/jphysiol.2002.017707.

Herrington, J., Zhou, Y.-P., Bugianesi, R.M., Dulski, P.M., Feng, Y., Warren, V.A., Smith, M.M., Kohler, M.G., Garsky, V.M., Sanchez, M., Wagner, M., Raphaelli, K., Banerjee, P., Ahaghotu, C., Wunderler, D., Priest, B.T., Mehl, J.T., Garcia, M.L., McManus, O.B. and Kaczorowski, G.J. (2006). Blockers of the delayed-rectifier potassium current in pancreatic beta-cells enhance glucose-dependent insulin secretion. *Diabetes*, [online] 55(4), pp.1034–1042. doi:https://doi.org/10.2337/diabetes.55.04.06.db05-0788.

Hill, C.L. and Stephens, G.J. (2020). An Introduction to Patch Clamp Recording. *Patch Clamp Electrophysiology*, [online] pp.1–19. doi:https://doi.org/10.1007/978-1-0716-0818-0_1.

Hirano, J., Nakamura, K., Itazawa, S., Sohma, Y., Kubota, T. and Kubokawa, M. (2002). Modulation of the Ca2+-Activated Large Conductance K+ Channel by Intracellular pH in Human Renal Proximal Tubule Cells. *The Japanese Journal of Physiology*, [online] 52(3), pp.267–276. doi:https://doi.org/10.2170/jjphysiol.52.267.

Hoa, N.T., Zhang, J.G., Delgado, C.L., Myers, M.P., Callahan, L.L., Vandeusen, G., Schiltz, P.M., Wepsic, H.T. and Jadus, M.R. (2007). Human monocytes kill M-CSF-expressing glioma cells by BK channel activation. *Laboratory Investigation*, [online] 87(2), pp.115–129. doi:https://doi.org/10.1038/labinvest.3700506.

Höber, R. (1905). Über den Einfluss der Salze auf den Ruhestrom des Froschmuskels. *Pflüger, Archiv für die Gesammte Physiologie des Menschen und der Thiere*, [online] 106-106(10-12), pp.599–635. doi:https://doi.org/10.1007/bf01679564.

Hodgkin, A.L. and Huxley, A.F. (1952). The components of membrane conductance in the giant axon of Loligo. *The Journal of Physiology*, [online] 116(4), pp.473–496. Available at: https://www.ncbi.nlm.nih.gov/pmc/articles/PMC1392209/ [Accessed 23 Dec. 2022].

Hooper, S.L., Thuma, J.B., Guschlbauer, C., Schmidt, J. and Büschges, A. (2015). Cell dialysis by sharp electrodes can cause nonphysiological changes in neuron properties. *Journal of Neurophysiology*, [online] 114(2), pp.1255–1271. doi:https://doi.org/10.1152/jn.01010.2014.

Houamed, K.M., Sweet, I.R. and Satin, L.S. (2010). BK channels mediate a novel ionic mechanism that regulates glucose-dependent electrical activity and insulin secretion in mouse pancreatic β-cells. *The Journal of Physiology*, [online] 588(18), pp.3511–3523. doi:https://doi.org/10.1113/jphysiol.2009.184341.

Hu, H., Shao, L.-R., Chavoshy, S., Gu, N., Trieb, M., Behrens, R., Laake, P., Pongs, O., Knaus, H.G., Ottersen, O.P. and Storm, J.F. (2001). Presynaptic Ca2+-Activated K+Channels in Glutamatergic Hippocampal Terminals and Their Role in Spike Repolarization and Regulation of Transmitter Release. *The Journal of Neuroscience*, [online] 21(24), pp.9585–9597. doi:https://doi.org/10.1523/jneurosci.21-24-09585.2001.

Hu, H.-J., Wang, S., Wang, Y., Liu, Y., Feng, X., Shen, Y., Zhu, L., Chen, H. and Song, M. (2019). Blockade of the forward $Na^{+}/Ca^{2+}$ exchanger suppresses the growth of glioblastoma cells through

Ca $^{2+}$ -mediated cell death. *British Journal of Pharmacology*, 176(15), pp.2691–2707. doi:https://doi.org/10.1111/bph.14692.

Hurley, B., Preiksaitis, H.G. and Sims, S.M. (1999). Characterization and regulation of Ca2+-dependent K+ channels in human esophageal smooth muscle. *American Journal of Physiology-gastrointestinal and Liver Physiology*. doi:https://doi.org/10.1152/ajpgi.1999.276.4.g843.

Imlach, W.L., Finch, S.C., Dunlop, J., Meredith, A.L., Aldrich, R.W. and Dalziel, J.E. (2008). The Molecular Mechanism of 'Ryegrass Staggers,' a Neurological Disorder of K+ Channels. *Journal of Pharmacology and Experimental Therapeutics*, [online] 327(3), pp.657–664. doi:https://doi.org/10.1124/jpet.108.143933.

Islam, M.S., Gaston, J.P. and Baker, M.A.B. (2021). Fluorescence Approaches for Characterizing Ion Channels in Synthetic Bilayers. *Membranes*, [online] 11(11), p.857. doi:https://doi.org/10.3390/membranes11110857.

J.R. Lymangrover, A. Frances Pearlmutter, Franco-Saenz, R. and Saffran, M. (1975). Transmembrane Potentials and Steroidogenesis in Normal and Neoplastic Human Adrenocortical Tissue. *The Journal of Clinical Endocrinology & Metabolism*, [online] 41(4), pp.697–706. doi:https://doi.org/10.1210/jcem-41-4-697.

Jacobson, D.A. and Philipson, L.H. (2007). Action potentials and insulin secretion: new insights into the role of Kv channels. *Diabetes, Obesity and Metabolism*, [online] 9(s2), pp.89–98. doi:https://doi.org/10.1111/j.1463-1326.2007.00784.x.

Jessen, K.R. (2004). Cells in Focus Glial Cells. *The International Journal of Biochemistry & Cell Biology*, [online] 36(10), pp.1861–1867. doi:https://doi.org/10.1016/j.biocel.2004.02.023.

JOHNSTONE, B.M. (1959). Micro-Electrode Penetration of Ascites Tumour Cells. *Nature*, [online] 183(4658), pp.411–411. doi:https://doi.org/10.1038/183411a0.

Jos A. H. Verheugen, Fricker, D. and Miles, R. (1999). Noninvasive Measurements of the Membrane Potential and GABAergic Action in Hippocampal Interneurons. *The Journal of Neuroscience*, [online] 19(7), pp.2546–2555. doi:https://doi.org/10.1523/jneurosci.19-07-02546.1999.

Jospin, M., Mariol, M.-C., Ségalat, L. and Allard, B. (2002). Characterization of K+currents using anin situpatch clamp technique in body wall muscle cells fromCaenorhabditis elegans. *The Journal of Physiology*, [online] 544(2), pp.373–384. doi:https://doi.org/10.1113/jphysiol.2002.022293.

Kanderi, T. and Gupta, V. (2022). *Glioblastoma Multiforme*. [online] PubMed. Available at: https://pubmed.ncbi.nlm.nih.gov/32644380/ [Accessed 6 Jan. 2023].

Kehl, S.J. and Wong, K. (1996). Large-conductance Calcium-activated Potassium Channels of Cultured Rat Melanotrophs. *Journal of Membrane Biology*, [online] 150(3), pp.219–230. doi:https://doi.org/10.1007/s002329900046.

Khadria, A. (2022). Tools to measure membrane potential of neurons. *Biomedical Journal*, [online] 45(5), pp.749–762. doi:https://doi.org/10.1016/j.bj.2022.05.007.

Kim, D.M. and Nimigean, C.M. (2016). Voltage-Gated Potassium Channels: A Structural Examination of Selectivity and Gating. *Cold Spring Harbor Perspectives in Biology*, [online] 8(5), p.a029231. doi:https://doi.org/10.1101/cshperspect.a029231.

Klec, C., Ziomek, G., Pichler, M., Malli, R. and Graier, W.F. (2019). Calcium Signaling in ß-cell Physiology and Pathology: A Revisit. *International journal of molecular sciences*, [online] 20(24), p.6110. doi:https://doi.org/10.3390/ijms20246110.

Ko, E.A., Burg, E.D., Oleksandr Platoshyn, Msefya, J., Firth, A.L. and Jason X.-J. Yuan (2007). Functional characterization of voltage-gated $K^+$ channels in mouse pulmonary artery smooth muscle cells. *American Journal of Physiology-cell Physiology*, 293(3), pp.C928–C937. doi:https://doi.org/10.1152/ajpcell.00101.2007.

Konig, S., Hinard, V., Arnaudeau, S., Holzer, N., Potter, G., Bader, C. and Bernheim, L. (2004). Membrane Hyperpolarization Triggers Myogenin and Myocyte Enhancer Factor-2 Expression during Human Myoblast Differentiation. *Journal of Biological Chemistry*, 279(27), pp.28187–28196. doi:https://doi.org/10.1074/jbc.m313932200.

Kopec, W., Rothberg, B.S. and de Groot, B.L. (2019). Molecular mechanism of a potassium channel gating through activation gate-selectivity filter coupling. *Nature Communications*, [online] 10(1). doi:https://doi.org/10.1038/s41467-019-13227-w.

Kraft, R., Krause, P., Jung, S., Basrai, D., Liebmann, L., Bolz, J. and Patt, S. (2003). BK channel openers inhibit migration of human glioma cells. *Pflugers Archiv: European Journal of Physiology*, [online] 446(2), pp.248–255. doi:https://doi.org/10.1007/s00424-003-1012-4.

Kryshtal', D.O., Nesin, V.V. and Shuba, M.F. (2007). [Effect of paxilline on Ca(2+)-dependent K+ current in smooth muscle cells isolated from rat vas deferens]. *Fiziolohichnyi Zhurnal (Kiev, Ukraine: 1994)*, [online] 53(5), pp.67–74. Available at: https://pubmed.ncbi.nlm.nih.gov/18080495/ [Accessed 3 Sep. 2023].

Kuang, Q., Purhonen, P. and Hebert, H. (2015). Structure of potassium channels. *Cellular and Molecular Life Sciences*, [online] 72(19), pp.3677–3693. doi:https://doi.org/10.1007/s00018-015-1948-5.

Kuhn, S., Müller, U., Hanisch, U.-K., Christian, Schoenwald, I., Brodhun, M., Hartwig Kosmehl, Ewald, C., Kalff, R. and Reichart, R. (2009). Glioblastoma cells express functional cell membrane receptors activated by daily used medical drugs. *Journal of Cancer Research and Clinical Oncology*, 135(12), pp.1729–1745. doi:https://doi.org/10.1007/s00432-009-0620-6.

Kukuljan, M., Goncalves, A.A. and Atwater, I. (1991). Charybdotoxin-sensitive K(Ca) channel is not involved in glucose-induced electrical activity in pancreatic beta-cells. *The Journal of Membrane Biology*, [online] 119(2), pp.187–195. doi:https://doi.org/10.1007/BF01871418.

Kyle, B.D., Hurst, S., Swayze, R.D., Sheng, J. and Braun, A.P. (2013). Specific phosphorylation sites underlie the stimulation of a large conductance, Ca2+-activated K+channel by cGMP-dependent protein kinase. *The FASEB Journal*, [online] 27(5), pp.2027–2038. doi:https://doi.org/10.1096/fj.12-223669.

Lange, F., Hörnschemeyer, J. and Kirschstein, T. (2021). Glutamatergic Mechanisms in Glioblastoma and Tumor-Associated Epilepsy. *Cells*, 10(5), p.1226. doi:https://doi.org/10.3390/cells10051226.

Lara, J., Acevedo, J.J. and Onetti, C.G. (1999). Large-Conductance Ca2+-Activated Potassium Channels in Secretory Neurons. *Journal of Neurophysiology*, [online] 82(3), pp.1317–1325. doi:https://doi.org/10.1152/jn.1999.82.3.1317.

Laumonnier, F., Roger, S., Guérin, P., Molinari, F., M'rad, R., Cahard, D., Belhadj, A., Halayem, M., Persico, A.M., Elia, M., Romano, V., Holbert, S., Andres, C., Chaabouni, H., Colleaux, L., Constant, J., Le Guennec, J.-Y. and Briault, S. (2006). Association of a functional deficit of the BKCa channel, a synaptic regulator of neuronal excitability, with autism and mental retardation. *The American Journal of Psychiatry*, [online] 163(9), pp.1622–1629. doi:https://doi.org/10.1176/ajp.2006.163.9.1622.

Leclerc, C., Haeich, J., Aulestia, F.J., Kilhoffer, M.-C., Miller, A.L., Néant, I., Webb, S.E., Schaeffer, E., Junier, M.-P., Chneiweiss, H. and Moreau, M. (2016). Calcium signaling orchestrates glioblastoma development: Facts and conjunctures. *Biochimica et Biophysica Acta (BBA) - Molecular Cell Research*, [online] 1863(6, Part B), pp.1447–1459. doi:https://doi.org/10.1016/j.bbamcr.2016.01.018.

Lee, U.S. and Cui, J. (2010). BK channel activation: structural and functional insights. *Trends in neurosciences*, [online] 33(9), pp.415–423. doi:https://doi.org/10.1016/j.tins.2010.06.004.

Lee, U.S., Shi, J. and Cui, J. (2010). Modulation of BK Channel Gating by the  2 Subunit Involves Both Membrane-Spanning and Cytoplasmic Domains of Slo1. *Journal of Neuroscience*, [online] 30(48), pp.16170–16179. doi:https://doi.org/10.1523/jneurosci.2323-10.2010.

Levin, M. (2014). Molecular bioelectricity: how endogenous voltage potentials control cell behavior and instruct pattern regulation in vivo. *Molecular Biology of the Cell*, [online] 25(24), pp.3835–3850. doi:https://doi.org/10.1091/mbc.e13-12-0708.

Li, A., Walling, J., Kotliarov, Y., Center, A., Steed, M.E., Ahn, S.J., Rosenblum, M., Mikkelsen, T., Zenklusen, J.C. and Fine, H.A. (2008). Genomic Changes and Gene Expression Profiles Reveal That Established Glioma Cell Lines Are Poorly Representative of Primary Human Gliomas. *Molecular Cancer Research*, [online] 6(1), pp.21–30. doi:https://doi.org/10.1158/1541-7786.mcr-07-0280.

Li, G. and Cheung, D.W. (1999). Effects of paxilline on K+ channels in rat mesenteric arterial cells. *European Journal of Pharmacology*, [online] 372(1), pp.103–107. doi:https://doi.org/10.1016/S0014-2999(99)00188-0.

Li, N., Liu, L., Li, G., Xia, M., Du, C. and Zheng, Z. (2018). The role of BKCa in endometrial cancer HEC-1-B cell proliferation and migration. *Gene*, [online] 655, pp.42–47. doi:https://doi.org/10.1016/j.gene.2018.02.055.

Li, Q. and Yan, J. (2016). Modulation of BK Channel Function by Auxiliary Beta and Gamma Subunits. *International review of neurobiology*, [online] 128, pp.51–90. doi:https://doi.org/10.1016/bs.irn.2016.03.015.

Li, W.-C. ., Soffe, S.R. and Roberts, A. (2004). A Direct Comparison of Whole Cell Patch and Sharp Electrodes by Simultaneous Recording From Single Spinal Neurons in Frog Tadpoles. *Journal of Neurophysiology*, [online] 92(1), pp.380–386. doi:https://doi.org/10.1152/jn.01238.2003.

Li, X., Spelat, R., Bartolini, A., Cesselli, D., Ius, T., Skrap, M., Caponnetto, F., Manini, I., Yang, Y. and Torre, V. (2020). Mechanisms of malignancy in glioblastoma cells are linked to MCU upregulation and higher intracellular calcium level. *Journal of Cell Science*. doi:https://doi.org/10.1242/jcs.237503.

Liang, G.H., Kim, J.A., Seol, G.H., Choi, S. and Suh, S.H. (2008). The Na+/Ca2+ exchanger inhibitor KB-R7943 activates large-conductance Ca2+-activated K+ channels in endothelial and vascular smooth muscle cells. *European Journal of Pharmacology*, [online] 582(1-3), pp.35–41. doi:https://doi.org/10.1016/j.ejphar.2007.12.021.

Lin, C.-W. ., Yan, F., Shimamura, S., Barg, S. and Shyng, S.-L. . (2005). Membrane Phosphoinositides Control Insulin Secretion Through Their Effects on ATP-Sensitive K+ Channel Activity. *Diabetes*, [online] 54(10), pp.2852–2858. doi:https://doi.org/10.2337/diabetes.54.10.2852.

Liu, X., Chang, Y., Reinhart, P.H. and Sontheimer, H. (2002). Cloning and Characterization of Glioma BK, a Novel BK Channel Isoform Highly Expressed in Human Glioma Cells. *The Journal of Neuroscience*, [online] 22(5), pp.1840–1849. doi:https://doi.org/10.1523/jneurosci.22-05-01840.2002.

Lock, J.T., Parker, I. and Smith, I.F. (2015). A comparison of fluorescent Ca2+ indicators for imaging local Ca2+ signals in cultured cells. *Cell Calcium*, [online] 58(6), pp.638–648. doi:https://doi.org/10.1016/j.ceca.2015.10.003.

Lorenz, S., Heils, A., Kasper, J.M. and Sander, T. (2006). Allelic association of a truncation mutation of theKCNMB3 gene with idiopathic generalized epilepsy. *American Journal of Medical Genetics Part B: Neuropsychiatric Genetics*, [online] 144B(1), pp.10–13. doi:https://doi.org/10.1002/ajmg.b.30369.

Ly, C., Melman, T., Barth, A.L. and Ermentrout, G.B. (2010). Phase-resetting curve determines how BK currents affect neuronal firing. *Journal of Computational Neuroscience*, [online] 30(2), pp.211–223. doi:https://doi.org/10.1007/s10827-010-0246-3.

M. Hallani, Lynch, J.W. and Barry, P.H. (1998). Characterization of Calcium-activated Chloride Channels in Patches Excised from the Dendritic Knob of Mammalian Olfactory Receptor Neurons. *The Journal of Membrane Biology*, [online] 161(2), pp.163–171. doi:https://doi.org/10.1007/s002329900323.

Ma, Z., Lou, X.J. and Horrigan, F.T. (2006). Role of Charged Residues in the S1–S4 Voltage Sensor of BK Channels. *Journal of General Physiology*, [online] 127(3), pp.309–328. doi:https://doi.org/10.1085/jgp.200509421.

Mancilla, E. and Rojas, E. (1990). Quinine blocks the high conductance, calcium-activated potassium channel in rat pancreatic β-cells. *FEBS Letters*, [online] 260(1), pp.105–108. doi:https://doi.org/10.1016/0014-5793(90)80078-w.

Marchetti, P., Bugliani, M., De Tata, V., Suleiman, M. and Marselli, L. (2017). Pancreatic Beta Cell Identity in Humans and the Role of Type 2 Diabetes. *Frontiers in Cell and Developmental Biology*, [online] 5(55). doi:https://doi.org/10.3389/fcell.2017.00055.

Marino, A.A., Morris, D.M., Schwalke, M.A., Iliev, I.G. and Rogers, S. (1994). Electrical potential measurements in human breast cancer and benign lesions. *Tumour Biology: The Journal of the International Society for Oncodevelopmental Biology and Medicine*, [online] 15(3), pp.147–152. doi:https://doi.org/10.1159/000217885.

Martinez-Espinosa, P.L., Yang, C., Gonzalez-Perez, V., Xia, X.-M. and Lingle, C.J. (2014). Knockout of the BK β2 subunit abolishes inactivation of BK currents in mouse adrenal chromaffin cells and results in slow-wave burst activity. *Journal of General Physiology*, [online] 144(4), pp.275–295. doi:https://doi.org/10.1085/jgp.201411253.

Meister, M., Pine, J. and Baylor, D.A. (1994). Multi-neuronal signals from the retina: acquisition and analysis. *Journal of Neuroscience Methods*, [online] 51(1), pp.95–106. doi:https://doi.org/10.1016/0165-0270(94)90030-2.

MELCZER, N. and KISS, J. (1957). Electrical Method for Detection of Early Cancerous Growth of the Skin. *Nature*, [online] 179(4571), pp.1177–1179. doi:https://doi.org/10.1038/1791177b0.

Meredith, A.L., Thorneloe, K.S., Werner, M.E., Nelson, M.T. and Aldrich, R.W. (2004). Overactive Bladder and Incontinence in the Absence of the BK Large Conductance Ca2+-activated K+Channel. *Journal of Biological Chemistry*, [online] 279(35), pp.36746–36752. doi:https://doi.org/10.1074/jbc.m405621200.

Meredith, A.L., Wiler, S.W., Miller, B.H., Takahashi, J.S., Fodor, A.A., Ruby, N.F. and Aldrich, R.W. (2006). BK calcium-activated potassium channels regulate circadian behavioral rhythms and pacemaker output. *Nature Neuroscience*, [online] 9(8), pp.1041–1049. doi:https://doi.org/10.1038/nn1740.

Mobasheri, A., Lewis, R., Maxwell, J.E.J., Hill, C., Womack, M. and Barrett-Jolley, R. (2010). Characterization of a stretch-activated potassium channel in chondrocytes. *Journal of Cellular Physiology*, [online] 223(2), pp.511–518. doi:https://doi.org/10.1002/jcp.22075.

Mohammed, S., M, D. and T, A. (2022). Survival and quality of life analysis in glioblastoma multiforme with adjuvant chemoradiotherapy: a retrospective study. *Reports of Practical Oncology and Radiotherapy*, [online] 27(6), pp.1026–1036. doi:https://doi.org/10.5603/rpor.a2022.0113.

Mohr, C.J., Schroth, W., Mürdter, T.E., Gross, D., Maier, S., Stegen, B., Dragoi, A., Steudel, F.A., Stehling, S., Hoppe, R., Madden, S.F., Ruth, P., Huber, S.M., Brauch, H. and Lukowski, R. (2020). Subunits of BK channels promote breast cancer development and modulate responses to endocrine treatment in preclinical models. *British Journal of Pharmacology*, 179(12), pp.2906–2924. doi:https://doi.org/10.1111/bph.15147.

Molenaar, R.J. (2011). Ion Channels in Glioblastoma. *ISRN Neurology*, [online] 2011, pp.1–7. doi:https://doi.org/10.5402/2011/590249.

Moorhouse, A.J. (2016). Membrane Potential: Concepts. *Encyclopedia of Cell Biology*, [online] 1, pp.218–236. doi:https://doi.org/10.1016/b978-0-12-394447-4.10027-6.

Morais-Cabral, J.H., Zhou, Y. and MacKinnon, R. (2001). Energetic optimization of ion conduction rate by the K+ selectivity filter. *Nature*, [online] 414(6859), pp.37–42. doi:https://doi.org/10.1038/35102000.

Nara, M., Dhulipala, P.D., Wang, Y.X. and Kotlikoff, M.I. (1998). Reconstitution of beta-adrenergic modulation of large conductance, calcium-activated potassium (maxi-K) channels in Xenopus oocytes. Identification of the camp-dependent protein kinase phosphorylation site. *The Journal of Biological Chemistry*, [online] 273(24), pp.14920–14924. doi:https://doi.org/10.1074/jbc.273.24.14920.

NEHER, E. and SAKMANN, B. (1976). Single-channel currents recorded from membrane of denervated frog muscle fibres. *Nature*, [online] 260(5554), pp.799–802. doi:https://doi.org/10.1038/260799a0.

Nelson, M.T. and Quayle, J.M. (1995). Physiological roles and properties of potassium channels in arterial smooth muscle. *American Journal of Physiology-Cell Physiology*, [online] 268(4), pp.C799–C822. doi:https://doi.org/10.1152/ajpcell.1995.268.4.c799.

Nguyen, A., François Marie Moussallieh, Mackay, A., A. Ercument Cicek, Coca, A., Chenard, M.P., Noëlle Weingertner, Benoit Lhermitte, Letouze, E., Guérin, E., Erwan Pencreach, Jannier, S., Guenot, D., Izzie Jacques Namer, Jones, C. and Entz-Werle, N. (2017). Characterization of the transcriptional and metabolic responses of pediatric high grade gliomas to mTOR-HIF-1α axis inhibition. *Oncotarget*, [online] 8(42), pp.71597–71617. doi:https://doi.org/10.18632/oncotarget.16500.

Nilius, B. and Wohlrab, W. (1992). Potassium channels and regulation of proliferation of human melanoma cells. *The Journal of Physiology* , [online] 445(1), pp.537–548. doi:https://doi.org/10.1113/jphysiol.1992.sp018938.

Numata, T., Sato-Numata, K. and Yoshino, M. (2021). BK Channels Are Activated by Functional Coupling With L-Type Ca2+ Channels in Cricket Myocytes. *Frontiers in Insect Science*, 1. doi:https://doi.org/10.3389/finsc.2021.662414.

Oh, M.C., Kim, J.M., Safaee, M., Kaur, G., Sun, M.Z., Kaur, R., Celli, A., Mauro, T.M. and Parsa, A.T. (2012). Overexpression of Calcium-Permeable Glutamate Receptors in Glioblastoma Derived Brain Tumor Initiating Cells. *PLoS ONE*, 7(10), p.e47846. doi:https://doi.org/10.1371/journal.pone.0047846.

Olsen, M.L., Schade, S., Lyons, S.A., Amaral, M.D. and Sontheimer, H. (2003). Expression of Voltage-Gated Chloride Channels in Human Glioma Cells. *The Journal of Neuroscience*, [online] 23(13), pp.5572–5582. doi:https://doi.org/10.1523/jneurosci.23-13-05572.2003.

Orio, P. and Latorre, R. (2005). Differential Effects of β1 and β2 Subunits on BK Channel Activity. *Journal of General Physiology*, [online] 125(4), pp.395–411. doi:https://doi.org/10.1085/jgp.200409236.

Orio, P., Rojas, P., Ferreira, G. and Latorre, R. (2002). New Disguises for an Old Channel: MaxiK Channel β-Subunits. *Physiology*, [online] 17(4), pp.156–161. doi:https://doi.org/10.1152/nips.01387.2002.

Overington, J.P., Al-Lazikani, B. and Hopkins, A.L. (2006). How many drug targets are there? *Nature Reviews Drug Discovery*, [online] 5(12), pp.993–996. doi:https://doi.org/10.1038/nrd2199.

Park, J.H., Park, S.J., Chung, M.K., Jung, K.H., Choi, M.R., Kim, Y., Chai, Y.G., Kim, S.J. and Park, K.S. (2010). High expression of large-conductance Ca2+-activated K+ channel in the CD133+ subpopulation of SH-SY5Y neuroblastoma cells. *Biochemical and Biophysical Research Communications*, [online] 396(3), pp.637–642. doi:https://doi.org/10.1016/j.bbrc.2010.04.142.

Parpura, V. and Haydon, P.G. (2000). Physiological astrocytic calcium levels stimulate glutamate release to modulate adjacent neurons. *Proceedings of the National Academy of Sciences of the United States of America*, [online] 97(15), pp.8629–8634. Available at: https://www.ncbi.nlm.nih.gov/pmc/articles/PMC26999/#:~:text=Because%20the%20agonists%20glutamate%2C%20norepinephrine [Accessed 9 Sep. 2023].

Pei, Z., Lee, K.-C., Khan, A., Erisnor, G. and Wang, H.-Y. (2020). Pathway analysis of glutamate-mediated, calcium-related signaling in glioma progression. *Biochemical Pharmacology*, [online] 176, p.113814. doi:https://doi.org/10.1016/j.bcp.2020.113814.

Perkins, K.L. (2006). Cell-attached voltage-clamp and current-clamp recording and stimulation techniques in brain slices. *Journal of neuroscience methods*, [online] 154(1-2), pp.1–18. doi:https://doi.org/10.1016/j.jneumeth.2006.02.010.

Pitts, G.R., Ohta, H. and McMahon, D.G. (2006). Daily rhythmicity of large-conductance Ca2+-activated K+ currents in suprachiasmatic nucleus neurons. *Brain Research*, [online] 1071(1), pp.54–62. doi:https://doi.org/10.1016/j.brainres.2005.11.078.

Price, D.L., Ludwig, J.W., Mi, H., Schwarz, T.L. and Ellisman, M.H. (2002). Distribution of rSlo Ca2+-activated K+ channels in rat astrocyte perivascular endfeet. *Brain Research*, [online] 956(2), pp.183–193. doi:https://doi.org/10.1016/s0006-8993(02)03266-3.

Qin, T., Mullan, B., Ravindran, R., Messinger, D., Siada, R., Cummings, J.R., Harris, M., Muruganand, A., Pyaram, K., Miklja, Z., Reiber, M., Garcia, T., Tran, D., Danussi, C., Brosnan-Cashman, J., Pratt, D., Zhao, X., Rehemtulla, A., Sartor, M.A. and Venneti, S. (2022). ATRX loss in glioma results in dysregulation of cell-cycle phase transition and ATM inhibitor radio-sensitization. *Cell Reports*, [online] 38(2), p.110216. doi:https://doi.org/10.1016/j.celrep.2021.110216.

Raffaelli, G., Saviane, C., Mohajerani, M.H., Pedarzani, P. and Cherubini, E. (2004). BK potassium channels control transmitter release at CA3-CA3 synapses in the rat hippocampus. *The Journal of Physiology*, [online] 557(1), pp.147–157. doi:https://doi.org/10.1113/jphysiol.2004.062661.

Rakotomalala, A., Bailleul, Q., Savary, C., Mélanie Arcicasa, Hamadou, M., Huchedé, P., Hochart, A., Restouin, A., Castellano, R., Collette, Y., Dieny, E., Vincent, A., Angrand, P.-O., Xuefen Le Bourhis, Leblond, P., Furlan, A., Castets, M., Pasquier, E. and Meignan, S. (2021). H3.3K27M Mutation Controls Cell Growth and Resistance to Therapies in Pediatric Glioma Cell Lines. *Cancers*, [online] 13(21), pp.5551–5551. doi:https://doi.org/10.3390/cancers13215551.

Ramahi, A.A. and Ruff, R.L. (2014). Membrane Potential. *Encyclopedia of the Neurological Sciences*, [online] pp.1034–1035. doi:https://doi.org/10.1016/b978-0-12-385157-4.00062-2.

Ransom, C.B., Liu, X. and Sontheimer, H. (2002). BK channels in human glioma cells have enhanced calcium sensitivity. *Glia*, [online] 38(4), pp.281–291. doi:https://doi.org/10.1002/glia.10064.

Ransom, C.B. and Sontheimer, H. (2001). BK Channels in Human Glioma Cells. *Journal of Neurophysiology*, [online] 85(2), pp.790–803. doi:https://doi.org/10.1152/jn.2001.85.2.790.

Rorsman, P. and Ashcroft, F.M. (2018). Pancreatic β-Cell Electrical Activity and Insulin Secretion: Of Mice and Men. *Physiological Reviews*, [online] 98(1), pp.117–214. doi:https://doi.org/10.1152/physrev.00008.2017.

Rosa, P., Catacuzzeno, L., Sforna, L., Mangino, G., Carlomagno, S., Mincione, G., Petrozza, V., Ragona, G., Franciolini, F. and Calogero, A. (2018). BK channels blockage inhibits hypoxia-induced migration and chemoresistance to cisplatin in human glioblastoma cells. *Journal of Cellular Physiology*, [online] 233(9), pp.6866–6877. doi:https://doi.org/10.1002/jcp.26448.

Rosa, P., Sforna, L., Carlomagno, S., Mangino, G., Miscusi, M., Pessia, M., Franciolini, F., Calogero, A. and Catacuzzeno, L. (2017). Overexpression of Large-Conductance Calcium-Activated Potassium Channels in Human Glioblastoma Stem-Like Cells and Their Role in Cell Migration. *Journal of Cellular Physiology*, [online] 232(9), pp.2478–2488. doi:https://doi.org/10.1002/jcp.25592.

Rouzaire-Dubois, B. and Dubois, J.-M. (1991). A quantitative analysis of the role of K+ channels in mitogenesis of neuroblastoma cells. *Cellular Signalling*, [online] 3(4), pp.333–339. doi:https://doi.org/10.1016/0898-6568(91)90062-y.

Rutka, J.T., Giblin, J.R., Dougherty, D.V., Liu, H.C., McCulloch, J.R., C. David Bell, Stern, R.S., Wilson, C.B. and Rosenblum, M.L. (1987). Establishment and characterization of five cell lines derived from human malignant gliomas. *Acta Neuropathologica*, 75(1), pp.92–103. doi:https://doi.org/10.1007/bf00686798.

Saito, M., Nelson, C., Salkoff, L. and Lingle, C.J. (1997). A cysteine-rich domain defined by a novel exon in a slo variant in rat adrenal chromaffin cells and PC12 cells. *The Journal of Biological Chemistry*, [online] 272(18), pp.11710–11717. doi:https://doi.org/10.1074/jbc.272.18.11710.

Saleem, F., Rowe, I. and Shipston, M. (2009). Characterization of BK channel splice variants using membrane potential dyes. *British Journal of Pharmacology*, [online] 156(1), pp.143–152. doi:https://doi.org/10.1111/j.1476-5381.2008.00011.x.

Sancho, M. and Kyle, B.D. (2021). The Large-Conductance, Calcium-Activated Potassium Channel: A Big Key Regulator of Cell Physiology. *Frontiers in Physiology*, 12. doi:https://doi.org/10.3389/fphys.2021.750615.

Sausbier, M., Arntz, C., Bucurenciu, I., Zhao, H., Zhou, X.-B., Sausbier, U., Feil, S., Kamm, S., Essin, K., Sailer, C.A., Abdullah, U., Krippeit-Drews, P., Feil, R., Hofmann, F., Knaus, H.-G., Kenyon, C., Shipston, M.J., Storm, J.F., Neuhuber, W. and Korth, M. (2005). Elevated Blood Pressure Linked to Primary Hyperaldosteronism and Impaired Vasodilation in BK Channel–Deficient Mice. *Circulation*, [online] 112(1), pp.60–68. doi:https://doi.org/10.1161/01.cir.0000156448.74296.fe.

Sausbier, M., Hu, H., Arntz, C., Feil, S., Kamm, S., Adelsberger, H., Sausbier, U., Sailer, C.A., Feil, R., Hofmann, F., Korth, M., Shipston, M.J., Knaus, H.-G. ., Wolfer, D.P., Pedroarena, C.M., Storm, J.F. and Ruth, P. (2004). Cerebellar ataxia and Purkinje cell dysfunction caused by $Ca^{2+}$ -activated $K^{+}$ channel deficiency. *Proceedings of the National Academy of Sciences*, [online] 101(25), pp.9474–9478. doi:https://doi.org/10.1073/pnas.0401702101.

Schickling, B.M., England, S.K., Nukhet Aykin-Burns, Norian, L.A., Leslie, K.K. and Frieden-Korovkina, V.P. (2014). BKCa channel inhibitor modulates the tumorigenic ability of hormone-independent breast cancer cells via the Wnt pathway. *Oncology Reports*, 33(2), pp.533–538. doi:https://doi.org/10.3892/or.2014.3617.

Sempou, E., Kostiuk, V., Zhu, J., Cecilia Guerra, M., Tyan, L., Hwang, W., Camacho-Aguilar, E., Caplan, M.J., Zenisek, D., Warmflash, A., Owens, N.D.L. and Khokha, M.K. (2022). Membrane potential drives the exit from pluripotency and cell fate commitment via calcium and mTOR. *Nature Communications*, [online] 13(1), p.6681. doi:https://doi.org/10.1038/s41467-022-34363-w.

Sherriff, J., Tamangani, J., Senthil, L., Cruickshank, G., Spooner, D., Jones, B., Brookes, C. and Sanghera, P. (2013). Patterns of relapse in glioblastoma multiforme following concomitant chemoradiotherapy with temozolomide. *The British Journal of Radiology*, [online] 86(1022). doi:https://doi.org/10.1259/bjr.20120414.

Silantyev, A., Falzone, L., Libra, M., Gurina, O., Kardashova, K., Nikolouzakis, T., Nosyrev, A., Sutton, C., Mitsias, P. and Tsatsakis, A. (2019). Current and Future Trends on Diagnosis and Prognosis of

Glioblastoma: From Molecular Biology to Proteomics. *Cells*, 8(8), p.863. doi:https://doi.org/10.3390/cells8080863.

Simon, S.M. and Schindler, M. (1994). Cell biological mechanisms of multidrug resistance in tumors. *Proceedings of the National Academy of Sciences of the United States of America*, [online] 91(9), pp.3497–3504. Available at: https://www.ncbi.nlm.nih.gov/pmc/articles/PMC43607/ [Accessed 9 Sep. 2023].

Smart, T.G. (1987). Single calcium-activated potassium channels recorded from cultured rat sympathetic neurones. *The Journal of Physiology*, [online] 389(1), pp.337–360. doi:https://doi.org/10.1113/jphysiol.1987.sp016660.

Smith, P.A., Ashcroft, F.M. and Rorsman, P. (1990). Simultaneous recordings of glucose dependent electrical activity and ATP-regulated K+ -currents in isolated mouse pancreatic β-cells. *FEBS Letters*, 261(1), pp.187–190. doi:https://doi.org/10.1016/0014-5793(90)80667-8.

Smith, P.A., Bokvist, K., Arkhammar, P., Berggren, P.O. and Rorsman, P. (1990). Delayed rectifying and calcium-activated K+ channels and their significance for action potential repolarization in mouse pancreatic beta-cells. *Journal of General Physiology*, 95(6), pp.1041–1059. doi:https://doi.org/10.1085/jgp.95.6.1041.

Soroceanu, L., Manning, T.J. and Sontheimer, H. (1999). Modulation of Glioma Cell Migration and Invasion Using Cl− and K+ Ion Channel Blockers. *Journal of Neuroscience*, [online] 19(14), pp.5942–5954. doi:https://doi.org/10.1523/JNEUROSCI.19-14-05942.1999.

Steinle, M., Palme, D., Misovic, M., Rudner, J., Dittmann, K., Lukowski, R., Ruth, P. and Huber, S.M. (2011). Ionizing radiation induces migration of glioblastoma cells by activating BK K(+) channels. *Radiotherapy and Oncology: Journal of the European Society for Therapeutic Radiology and Oncology*, [online] 101(1), pp.122–126. doi:https://doi.org/10.1016/j.radonc.2011.05.069.

Stevenson, D., Binggeli, R., Weinstein, R.C., Keck, J.G., Lai, M.C. and Tong, M.J. (1989). Relationship between cell membrane potential and natural killer cell cytolysis in human hepatocellular carcinoma cells. *Cancer Research*, [online] 49(17), pp.4842–4845. Available at: https://pubmed.ncbi.nlm.nih.gov/2547520/ [Accessed 30 Jul. 2023].

Strong, A.D., Indart, M.C., Hill, N.R. and Daniels, R.L. (2018). GL261 glioma tumor cells respond to ATP with an intracellular calcium rise and glutamate release. *Molecular and Cellular Biochemistry*, 446(1-2), pp.53–62. doi:https://doi.org/10.1007/s11010-018-3272-5.

Sun, X.-P., Schlichter, L.C. and Stanley, E.F. (1999). Single-channel properties of BK-type calcium-activated potassium channels at a cholinergic presynaptic nerve terminal. *The Journal of Physiology*, [online] 518(3), pp.639–651. doi:https://doi.org/10.1111/j.1469-7793.1999.0639p.x.

Sun, X.-P., Yazejian, B. and Grinnell, A.D. (2004). Electrophysiological properties of BK channels inXenopusmotor nerve terminals. *The Journal of Physiology*, [online] 557(1), pp.207–228. doi:https://doi.org/10.1113/jphysiol.2003.060509.

Sundelacruz, S., Levin, M. and Kaplan, D.L. (2008). Membrane Potential Controls Adipogenic and Osteogenic Differentiation of Mesenchymal Stem Cells. *PLoS ONE*, [online] 3(11), p.e3737. doi:https://doi.org/10.1371/journal.pone.0003737.

Tan, C.H. and Tan, E.H. (2012). Post-treatment Assessment of Glioblastoma Multiforme: Imaging with Fluorodeoxyglucose, Sestamibi, and Choline. *World Journal of Nuclear Medicine*, [online] 11(1), p.30. doi:https://doi.org/10.4103/1450-1147.98745.

Tews, D.S., Nissen, A., Külgen, C. and Gaumann, A.K. (2000). Drug resistance-associated factors in primary and secondary glioblastomas and their precursor tumors. *Journal of Neuro-Oncology*, [online] 50(3), pp.227–237. doi:https://doi.org/10.1023/a:1006491405010.

Tian, L., Duncan, R.R., Hammond, M.S., Coghill, L.S., Wen, H., Rusinova, R., Clark, A.G., Levitan, I.B. and Shipston, M.J. (2001). Alternative splicing switches potassium channel sensitivity to protein phosphorylation. *The Journal of Biological Chemistry*, [online] 276(11), pp.7717–7720. doi:https://doi.org/10.1074/jbc.C000741200.

Tsuchiya, W. and Okada, Y. (1982). Membrane potential changes associated with differentiation of enterocytes in the rat intestinal villi in culture. *Developmental Biology*, [online] 94(2), pp.284–290. doi:https://doi.org/10.1016/0012-1606(82)90348-7.

Typlt, M., Mirkowski, M., Azzopardi, E., Ruettiger, L., Ruth, P. and Schmid, S. (2013). Mice with Deficient BK Channel Function Show Impaired Prepulse Inhibition and Spatial Learning, but Normal

Working and Spatial Reference Memory. *PLoS ONE*, [online] 8(11), p.e81270. doi:https://doi.org/10.1371/journal.pone.0081270.

Tyzio, R., Ivanov, A., Bernard, C., Holmes, G.L., Ben-Ari, Y. and Khazipov, R. (2003). Membrane Potential of CA3 Hippocampal Pyramidal Cells During Postnatal Development. *Journal of Neurophysiology*, [online] 90(5), pp.2964–2972. doi:https://doi.org/10.1152/jn.00172.2003.

Uebele, V.N., Lagrutta, A., Wade, T., Figueroa, D.J., Liu, Y., McKenna, E., Austin, C.P., Bennett, P.B. and Swanson, R. (2000). Cloning and Functional Expression of Two Families of β-Subunits of the Large Conductance Calcium-activated K+Channel. *Journal of Biological Chemistry*, [online] 275(30), pp.23211–23218. doi:https://doi.org/10.1074/jbc.m910187199.

Verheugen, J.A., Vijverberg, H.P., Oortgiesen, M. and Cahalan, M.D. (1995). Voltage-gated and Ca(2+)-activated K+ channels in intact human T lymphocytes. Noninvasive measurements of membrane currents, membrane potential, and intracellular calcium. *The Journal of general physiology*, [online] 105(6), pp.765–794. doi:https://doi.org/10.1085/jgp.105.6.765.

VERKHRATSKY, A., ORKAND, R.K. and KETTENMANN, H. (1998). Glial Calcium: Homeostasis and Signaling Function. *Physiological Reviews*, [online] 78(1), pp.99–141. doi:https://doi.org/10.1152/physrev.1998.78.1.99.

Vigneswaran, K., Neill, S. and Hadjipanayis, C.G. (2015). Beyond the World Health Organization grading of infiltrating gliomas: advances in the molecular genetics of glioma classification. *Annals of Translational Medicine*, [online] 3(7). doi:https://doi.org/10.3978/j.issn.2305-5839.2015.03.57.

Wallner, M., Meera, P., Ottolia, M., Kaczorowski, G.J., Latorre, R., Garcia, M.L., Stefani, E. and Toro, L. (1995). Characterization of and modulation by a beta-subunit of a human maxi KCa channel cloned from myometrium. *Receptors & Channels*, [online] 3(3), pp.185–199. Available at: https://pubmed.ncbi.nlm.nih.gov/8821792/ [Accessed 29 Dec. 2022].

Wang, B., Rothberg, B.S. and Brenner, R. (2006). Mechanism of β4 Subunit Modulation of BK Channels. *Journal of General Physiology*, [online] 127(4), pp.449–465. doi:https://doi.org/10.1085/jgp.200509436.

Wang, Y., Jia, H., Walker, A.M. and Cukierman, S. (1992). K-current mediation of prolactin-induced proliferation of malignant (Nb2) lymphocytes. *Journal of Cellular Physiology*, 152(1), pp.185–189. doi:https://doi.org/10.1002/jcp.1041520123.

Wang, Y. and Mathers, D.A. (1993). Ca(2+)-dependent K+ channels of high conductance in smooth muscle cells isolated from rat cerebral arteries. *The Journal of Physiology*, [online] 462(1), pp.529–545. doi:https://doi.org/10.1113/jphysiol.1993.sp019567.

Wann, K.T. and Richards, C.D. (1994). Properties of single calcium-activated potassium channels of large conductance in rat hippocampal neurons in culture. *The European Journal of Neuroscience*, [online] 6(4), pp.607–617. doi:https://doi.org/10.1111/j.1460-9568.1994.tb00305.x.

Watkins, S. and Sontheimer, H. (2011). Hydrodynamic Cellular Volume Changes Enable Glioma Cell Invasion. *Journal of Neuroscience*, [online] 31(47), pp.17250–17259. doi:https://doi.org/10.1523/jneurosci.3938-11.2011.

Weaver, A.K., Bomben, V.C. and Sontheimer, H. (2006). Expression and function of calcium-activated potassium channels in human glioma cells. *Glia*, [online] 54(3), pp.223–233. doi:https://doi.org/10.1002/glia.20364.

Weaver, A.K., Liu, X. and Sontheimer, H. (2004). Role for calcium-activated potassium channels (BK) in growth control of human malignant glioma cells. *Journal of Neuroscience Research*, [online] 78(2), pp.224–234. doi:https://doi.org/10.1002/jnr.20240.

Wei, M.-Y., Xue, L., Tan, L., Sai, W.-B., Liu, X.-C., Jiang, Q.-J., Shen, J., Peng, Y.-B., Zhao, P., Yu, M.-F., Chen, W., Ma, L.-Q., Zhai, K., Zou, C., Guo, D., Qin, G., Zheng, Y.-M., Wang, Y.-X., Ji, G. and Liu, Q.-H. (2015). Involvement of Large-Conductance Ca2+-Activated K+ Channels in Chloroquine-Induced Force Alterations in Pre-Contracted Airway Smooth Muscle. *PLoS ONE*, [online] 10(3), p.e0121566. doi:https://doi.org/10.1371/journal.pone.0121566.

Werner, M.E., Zvara, P., Meredith, A.L., Aldrich, R.W. and Nelson, M.T. (2005). Erectile dysfunction in mice lacking the large-conductance calcium-activated potassium (BK) channel. *The Journal of Physiology*, [online] 567(2), pp.545–556. doi:https://doi.org/10.1113/jphysiol.2005.093823.

Whitt, J.P., Montgomery, J.R. and Meredith, A.L. (2016). BK channel inactivation gates daytime excitability in the circadian clock. *Nature Communications*, [online] 7(1). doi:https://doi.org/10.1038/ncomms10837.

Wiecha, J., Münz, B., Wu, Y., Noll, T., Tillmanns, H. and Waldecker, B. (1998). Blockade of Ca2+-activated K+ channels inhibits proliferation of human endothelial cells induced by basic fibroblast growth factor. *Journal of Vascular Research*, [online] 35(5), pp.363–371. doi:https://doi.org/10.1159/000025606.

Wilson, H.A. and Chused, T.M. (1985). Lymphocyte membrane potential and Ca2+-sensitive potassium channels described by oxonol dye fluorescence measurements. *Journal of Cellular Physiology*, [online] 125(1), pp.72–81. doi:https://doi.org/10.1002/jcp.1041250110.

Woehler, A., Lin, K. and Neher, E. (2014). Calcium-buffering effects of gluconate and nucleotides, as determined by a novel fluorimetric titration method. *The Journal of Physiology*, [online] 592(22), pp.4863–4875. doi:https://doi.org/10.1113/jphysiol.2014.281097.

Wondergem, R. and Bartley, J.W. (2009). Menthol increases human glioblastoma intracellular Ca2+, BK channel activity and cell migration. *Journal of Biomedical Science*, [online] 16(1), p.90. doi:https://doi.org/10.1186/1423-0127-16-90.

Wondergem, R., Ecay, T.W., Mahieu, F., Owsianik, G. and Nilius, B. (2008). HGF/SF and menthol increase human glioblastoma cell calcium and migration. *Biochemical and Biophysical Research Communications*, [online] 372(1), pp.210–215. doi:https://doi.org/10.1016/j.bbrc.2008.05.032.

Wonderlin, W.F., Woodfork, K.A. and Strobl, J.S. (1995). Changes in membrane potential during the progression of MCF-7 human mammary tumor cells through the cell cycle. *Journal of Cellular Physiology*, [online] 165(1), pp.177–185. doi:https://doi.org/10.1002/jcp.1041650121.

Woodfork, K.A., Wonderlin, W.F., Peterson, V.A. and Strobl, J.S. (1995). Inhibition of ATP-sensitive potassium channels causes reversible cell-cycle arrest of human breast cancer cells in tissue culture. *Journal of Cellular Physiology*, [online] 162(2), pp.163–171. doi:https://doi.org/10.1002/jcp.1041620202.

Woodrough, R.E., Canti, G. and Watson, B.W. (1975). Electrical potential difference between basal cell carcinoma, benign inflammatory lesions and normal tissue. *The British Journal of Dermatology*, [online] 92(1), pp.1–7. Available at: https://pubmed.ncbi.nlm.nih.gov/1156538/ [Accessed 30 Jul. 2023].

Wright, S.H. (2004). Generation of resting membrane potential. *Advances in Physiology Education*, [online] 28(4), pp.139–142. doi:https://doi.org/10.1152/advan.00029.2004.

Wu, C., V. Gopal, K., Lukas, T.J., Gross, G.W. and Moore, E.J. (2014a). Pharmacodynamics of potassium channel openers in cultured neuronal networks. *European Journal of Pharmacology*, [online] 732, pp.68–75. doi:https://doi.org/10.1016/j.ejphar.2014.03.017.

Wu, C., V. Gopal, K., Lukas, T.J., Gross, G.W. and Moore, E.J. (2014b). Pharmacodynamics of potassium channel openers in cultured neuronal networks. *European Journal of Pharmacology*, [online] 732, pp.68–75. doi:https://doi.org/10.1016/j.ejphar.2014.03.017.

Wulff, H. and Zhorov, B.S. (2008). K+ Channel Modulators for the Treatment of Neurological Disorders and Autoimmune Diseases. *Chemical Reviews*, 108(5), pp.1744–1773. doi:https://doi.org/10.1021/cr078234p.

Yu, M., Liu, S., Sun, P., Pan, H., Tian, C. and Zhang, L. (2016). Peptide toxins and small-molecule blockers of BK channels. *Acta Pharmacologica Sinica*, 37(1), pp.56–66. doi:https://doi.org/10.1038/aps.2015.139.

Yuan, P., Leonetti, M.D., Pico, A.R., Hsiung, Y. and MacKinnon, R. (2010). Structure of the Human BK Channel Ca2+-Activation Apparatus at 3.0 A Resolution. *Science*, [online] 329(5988), pp.182–186. doi:https://doi.org/10.1126/science.1190414.

Zarei, M.M., Eghbali, M., Alioua, A., Song, M., Knaus, H.-G. ., Stefani, E. and Toro, L. (2004). An endoplasmic reticulum trafficking signal prevents surface expression of a voltage- and $Ca^{2+}$-activated $K^{+}$ channel splice variant. *Proceedings of the National Academy of Sciences*, [online] 101(27), pp.10072–10077. doi:https://doi.org/10.1073/pnas.0302919101.

Zeng, X., Xia, X.-M. and Lingle, C.J. (2008). Species-specific Differences among KCNMB3 BK β3 Auxiliary Subunits: Some β3 N-terminal Variants May Be Primate-specific Subunits. *Journal of General Physiology*, [online] 132(1), pp.115–129. doi:https://doi.org/10.1085/jgp.200809969.

Zhang, L., Li, X., Zhou, R. and Xing, G. (2006). Possible role of potassium channel, big K in etiology of Schizophrenia. *Medical Hypotheses*, [online] 67(1), pp.41–43. doi:https://doi.org/10.1016/j.mehy.2005.09.055.

Zhang, X., Solaro, C.R. and Lingle, C.J. (2001). Allosteric Regulation of Bk Channel Gating by Ca2+ and Mg2+ through a Nonselective, Low Affinity Divalent Cation Site. *The Journal of General Physiology*, [online] 118(5), pp.607–636. Available at: https://www.ncbi.nlm.nih.gov/pmc/articles/PMC2233841/ [Accessed 19 Sep. 2023].

Zhao, H., Xue, Q., Li, C., Wang, Q., Han, S., Zhou, Y., Yang, T., Xie, Y., Fu, H., Lu, C., Meng, F., Zhang, M., Zhang, Y., Wu, X., Wu, S., Zhuo, M. and Xu, H. (2020). Upregulation of Beta4 subunit of BKCa channels in the anterior cingulate cortex contributes to mechanical allodynia associated anxiety-like behaviors. *Molecular Brain*, [online] 13(1). doi:https://doi.org/10.1186/s13041-020-0555-z.

Zhou, X., Wulfsen, I., Korth, M., McClafferty, H., Lukowski, R., Shipston, M.J., Ruth, P., Dobrev, D. and Wieland, T. (2012). Palmitoylation and Membrane Association of the Stress Axis Regulated Insert (STREX) Controls BK Channel Regulation by Protein Kinase C. *The Journal of Biological Chemistry*, [online] 287(38), pp.32161–32171. doi:https://doi.org/10.1074/jbc.M112.386359.

Zhou, X.-B., Ruth, P., Schlossmann, J., Hofmann, F. and Korth, M. (1996). Protein Phosphatase 2A Is Essential for the Activation of Ca2+-activated K+ Currents by cGMP-dependent Protein Kinase in Tracheal Smooth Muscle and Chinese Hamster Ovary Cells. *Journal of Biological Chemistry*, [online] 271(33), pp.19760–19767. doi:https://doi.org/10.1074/jbc.271.33.19760.

Zhou, Y. and Lingle, C.J. (2014). Paxilline inhibits BK channels by an almost exclusively closed-channel block mechanism. *Journal of General Physiology*, [online] 144(5), pp.415–440. doi:https://doi.org/10.1085/jgp.201411259.